

AN ABSTRACT OF THE DISSERTATION OF

Rebecca Ann Bader for the degree of Doctor of Philosophy in Material Science presented on December 15, 2006.

Title: Development and Characterization of Novel Hydrogels for Nucleus Pulposus Replacement.

Abstract approved: _____

Willie E. Rochefort

Hydrogels have been proposed as candidates for nucleus pulposus replacement due to their similarity in mechanical behavior to the native tissue when subjected to transient or static loading; however, given the viscoelastic nature of soft biological tissues, the lack of dynamic testing is a significant inadequacy in the studies performed to date. Our goal was to identify hydrogel systems whose viscoelastic behavior, particularly under dynamic torsional shear, mimicked that of the native tissue. Hydrogels were formed via photopolymerization of glycidyl methacrylate and 1,2-epoxy-5-hexene modified poly(vinyl alcohol) and were allowed to equilibrate in Hank's solution prior to analysis. The viscoelastic behavior of all prepared materials was compared with that of sheep nucleus pulposi. Complex shear moduli and phase shift angles were determined from dynamic frequency sweeps in torsional shear. Resistance towards hydrolysis was assessed by evaluation of the viscoelastic behavior of hydrogels submerged in Hank's solution for progressively longer periods of time. For glycidyl methacrylate-PVA hydrogels the viscoelastic parameters could be modulated by varying the molecular

weight of PVA and the concentration of polymer prior to photopolymerization. The mechanical behavior of 1,2-epoxy-5-hexene-PVA hydrogels could be regulated in a similar manner by altering the type and percentage of monomer used to induce polymerization. The phase shift angles of all hydrogels were lower than those of the nucleus pulposi; however, the complex shear moduli of both synthetic systems spanned the values observed for the natural system. Over the time frame of the experiment, no change in moduli was observed following submersion in Hank's solution. This study represents the first attempt to successfully mimic the viscoelastic nature of the nucleus pulposus exhibited under dynamic torsional loading with that of materials intended for use in tissue replacement.

© Copyright by Rebecca Ann Bader

December 15, 2006

All Rights Reserved

DEVELOPMENT AND CHARACTERIZATION OF NOVEL HYDROGELS FOR
NUCLEUS PULPOSUS REPLACEMENT

by

REBECCA ANN BADER

A DISSERTATION

submitted to

Oregon State University

in partial fulfillment of
the requirements for the
degree of

Doctor of Philosophy

Presented December 15, 2006

Commencement June 2007

Doctor of Philosophy dissertation of Rebecca Ann Bader presented on December 15, 2006.

APPROVED:



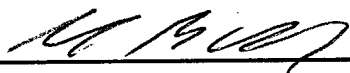
Major Professor, representing Material Science



Director of the Material Science Program

Dean of the Graduate School

I understand that my dissertation will become part of the permanent collection of Oregon State University libraries. My signature below authorizes release of my dissertation to any reader upon request.



Rebecca Ann Bader, Author

ACKNOWLEDGEMENTS

I will forever be thankful that I stumbled upon Dr. Willie E. (Skip) Rochefort in my quest for a doctoral degree. He gave me a place to work, think, and just be me when I most needed one. In the past two years under his advisement, I have become a more confident, independent research scientist. Thank you Skip.

Dr. William Warnes provided me with guidance on all written works and simply listened to me when I was down about the hardships of graduate school. Sometimes all that is needed to get through another day is to know that someone else understands. Thank you Bill for being that someone and for believing in my abilities as a scientist.

I am grateful to have such a supportive and loving family in my parents on the east coast and my surrogate parents, Bill and Michele, on the west coast. I know that they will be there for me in the future as they have always been there in the past. Thank you.

Thanks to my laboratory soul mate Sara Tracy who provided me with a reason to go into the lab when I was most discouraged. My time in the confines of the Chemical Engineering Building would not have been the same without her. I'm thankful that she appreciated the humor in leaving a chunk of sheep spine out on the bench counter as much as I. You are phenomenal Sara.

My gratitude goes to Christa Rose and Rachel Paroutka for not only helping me in the lab and listening to me when I needed to ramble about science, but for teaching me more about myself than I had known before. I could not imagine anyone having better assistants than I have had. Both of you will go far.

David Varoujean receives thanks as both my coach and my friend for providing me with some sense of order and accomplishment in my otherwise chaotic life at Oregon

State. Thank you for believing that I am capable of being great and teaching me the mantra that “there is no crying in cycling.”

Thanks to Dr. Sarah C. Petitto for being there to laugh at and with me from the very beginnings of my research career and for helping me to see the light at the end of the tunnel when I thought there was none. From the moment I accidentally swallowed a distasteful mouthful of norbornadiene and quadricyclene to the time I was rushed to the hospital for managing to explode my glass separation column into my arm she has always been there for me. Thank you Sarah.

“A friend is someone who knows the song in your heart and can sing it back to you when you have forgotten the words.”

Dr. Angela Sauers receives my most heartfelt appreciation for being my most steadfast friend, through thick and thin, who at times knew me better than I knew myself. I will never forget that fateful day at the NMR at Princeton where our friendship began. Followers of Confucianism believe that true friends are two bodies that share one mind, and we have provided ample evidence to support this philosophy. Thank you Angie.

Assistance on all chemistry related topics was provided by Dr. David Tyler and Bevin Daglen at the University of Oregon. This work was supported by funds from the John D. Erkkila, M.D. Endowment for Health and Human Performances

TABLE OF CONTENTS

	<u>Page</u>
INTRODUCTION.....	1
BACKGROUND.....	6
Biology of the Intervertebral Disc.....	6
Anatomy.....	5
Nutrition.....	7
Disc Degeneration & Back Pain.....	8
Mechanical Properties of the Nucleus Pulposus.....	10
Current Devices for Nucleus Pulposus Replacement.....	12
Introduction.....	12
PDN [®] Prosthetic Disc Nucleus (Raymedica, Inc., Bloomington, MN).....	12
Aquarelle (Stryker Spine, Allendale,NJ).....	14
NeuDisc (Replication Medical Inc.,NewBrunswick,NJ).....	15
Newcleus (Zimmer, Spine).....	17
DASCOR [™] Disc Arthoroplasty Device (Disc Dynamics,Inc., Eden Prairie, MN).....	18
Biodisc [™] Spinal Disc Repair System (Cryolife, Kennesaw, GA).....	19
Hydrogels for Biomaterials Applications.....	21
General.....	21
Poly(vinyl alcohol) Based Hydrogels.....	22
Injectable & Photopolymerizable Hydrogels.....	25
Summary.....	27
Preliminary Research with Chemically Crosslinked Poly(vinyl alcohol).....	27
MATERIALS & METHODS.....	33
Analytical Data.....	33
Reagents.....	34
Cell Culture.....	35
Intervertebral Disc Specimens.....	35

TABLE OF CONTENTS (Continued)

	<u>Page</u>
Hydrogel Preparation via Crosslinking of Poly(vinyl alcohol) with Glutaraldehyde.....	36
Hydrogel Preparation via Crosslinking of Poly(vinyl alcohol) with Epichlorohydrin.....	36
Synthesis and Characterization of Glycidyl Methacrylate Modified Poly(vinyl alcohol).....	37
Hydrogel Preparation from Glycidyl Methacrylate Modified Poly(vinyl alcohol) (Glycidyl Methacrylate-PVA).....	38
Synthesis and Characterization of 1,2-Epoxy-5-hexene Modified Poly(vinyl alcohol).....	39
Hydrogel Preparation from 1,2-Epoxy-5-hexene Modified Poly(vinyl alcohol) (1,2-Epoxy-5-hexene-PVA).....	40
Hydrogel NMR.....	41
Cytotoxicity Studies.....	41
Determination of Photopolymerization Time.....	42
Rheological Testing.....	43
Network Characterization.....	44
Dynamic Compression Testing.....	45
Degradation Studies.....	46
Statistical Analysis.....	46
RESULTS.....	47
Rheological Characterization of Glycidyl Methacrylate-PVA Hydrogels.....	47
Determination of Photopolymerization Time.....	54
Rheological Characterization of 1,2-Epoxy-5-hexene-PVA Hydrogels.....	55

TABLE OF CONTENTS (Continued)

	<u>Page</u>
Cytotoxicity Studies on 1,2-Epoxy-5-hexene-PVA Hydrogels.....	63
Dynamic Compression Testing.....	65
Degradation Studies.....	69
DISCUSSION.....	71
CONCLUSIONS.....	84
FUTURE WORK.....	77
BIBLIOGRAPHY.....	89
APPENDIX A: SPECTRA.....	98
APPENDIX B: PLOTS OF STORAGE AND LOSS MODULI.....	103

LIST OF FIGURES

<u>Figure</u>	<u>Page</u>
1. Anatomy of the intervertebral disc.....	7
2. Non-degenerate sheep intervertebral disc.....	9
3. Modification of poly(vinyl alcohol) with glycidyl acrylate, followed by photopolymerization.....	25
4. Chemical crosslinking of poly(vinyl alcohol) with glutaraldehyde.....	28
5. Comparison of complex shear moduli of hydrogel generated via crosslinking of PVA with glutaraldehyde with those of sheep nucleus pulposi.....	29
6. Percent mass loss of hydrogels generated via crosslinking of PVA with glutaraldehyde.....	30
7. Chemical crosslinking of poly(vinyl alcohol) with epichlorohydrin.....	31
8. Comparison of complex shear moduli of hydrogels prepared via crosslinking of PVA with epichlorohydrin with those of sheep nucleus pulposi.....	32
9. Modification of PVA with glycidyl methacrylate, followed by photopolymerization.....	38
10. Modification of poly(vinyl alcohol) with 1,2-epoxy-5-hexene.....	40
11. Photopolymerization of 1,2-epoxy-5-hexene modified PVA in the presence of N-vinylpyrrolidone (NVP), hydroxyethyl acrylate (HEA), N,N-dimethylacrylamide (DMAA), or acrylic acid (AA).....	41
12. Device used for determination of photopolymerization time.....	43
13. Variation in complex shear moduli (a) and phase shift angles (b) of glycidyl methacrylate-PVA hydrogels with molecular weight of PVA.....	50
14. Variation in complex shear moduli (a) and phase shift angles (b) of glycidyl methacrylate-PVA hydrogels with initial weight percent of polymer.....	51
15. Variation in storage modulus, G' , with time upon exposure of a solution of glycidyl methacrylate modified PVA to UV light for two different initial concentrations of polymer.....	55

LIST OF FIGURES (Continued)

<u>Figure</u>	<u>Page</u>
16. Variation in complex shear moduli (a) and phase shift angles (b) with monomer type for 1,2-epoxy-5-hexene-PVA hydrogels.....	58
17. Variation in complex shear moduli (a) and phase shift angles (b) with percentage (w/w) of hydroxyethyl acrylate (HEA) for 1,2-epoxy-5-hexene-PVA hydrogels.....	59
18. Variation in complex shear moduli (a) and phase shift angles (b) with percentage (w/w) of acrylic acid (AA) for 1,2-epoxy-5-hexene-PVA hydrogels.....	60
19. Light micrographs (100x) taken from an inverted light microscope showing the response of mouse fibroblasts to direct contact with hydrogels.....	64
20. Representative light micrographs (100x) taken from an inverted light microscope showing the response of mouse fibroblasts to fluid extracts taken from media surrounding hydrogel samples.....	65
21. Variation in complex compressive dynamic moduli (a) and phase shift angles (b) of glycidyl methacrylate-PVA hydrogels with molecular weight of PVA.....	67
22. Variation in complex compressive dynamic moduli (a) and phase shift angles (b) with monomer type for 1,2-epoxy-5-hexene-PVA hydrogels.....	68
23. Variation in complex shear moduli of glycidyl methacrylate-PVA hydrogels (M_w of PVA = 50-85k) with time following immersion in Hank's solution.....	69
24. Variation in complex shear moduli of hydrogels generated from photopolymerization of 1,2-epoxy-5-hexene modified PVA in the presence of 1.5% (w/w) hydroxyethyl acrylate with time following immersion in Hank's solution.....	70
25. Proposed structure resultant from the photopolymerization of 1,2-epoxy-5-hexene modified poly(vinyl alcohol) in the presence of acrylic acid (AA).....	76

LIST OF TABLES

<u>Table</u>	<u>Page</u>
1. Summary of nucleus pulposus replacements currently under investigation.....	20
2. Composition of Hank's solution.....	30
3. Conversion between δ and $\tan \delta$	44
4. Variation in viscoelastic parameters of glycidyl methacrylate-PVA hydrogels with molecular weight of PVA at 10 rad/s (1.6 Hz).....	52
5. Variation in viscoelastic parameters of glycidyl methacrylate-PVA hydrogels with initial concentration of polymer at 10 rad/s (1.6 Hz).....	52
6. Variation in crosslink density with molecular weight of PVA for glycidyl methacrylate-PVA hydrogels as calculated from rubber elasticity theory.....	53
7. Variation in crosslink density with initial concentration of polymer for glycidyl methacrylate-PVA hydrogels as calculated from rubber elasticity theory.....	53
8. Comparison between initial concentrations prior to photopolymerization and critical concentrations of entanglement for poly(vinyl alcohol).....	54
9. Variation in viscoelastic parameters of 1,2-epoxy-5-hexene-PVA hydrogels with monomer type at 10 rad/s (1.6 Hz).....	61
10. Variation in viscoelastic parameters of 1,2-epoxy-5-hexene-PVA hydrogels with percentage (w/w) of hydroxyethyl acrylate (HEA) at 10 rad/s (1.6 Hz).....	61
11. Variation in viscoelastic parameters of 1,2-epoxy-5-hexene-PVA hydrogels with percentage (w/w) of acrylic acid (AA) at 10 rad/s (1.6 Hz).....	61
12. Variation in crosslink density with type of monomer added to initiate photopolymerization of 1,2-epoxy-5-hexene modified PVA	62
13. Variation in crosslink density with percentage of hydroxyethyl acrylate (HEA) added to initiate photopolymerization of 1,2-epoxy-5-hexene modified PVA.....	62
14. Variation in crosslink density with percentage of acrylic acid (AA) added to initiate photopolymerization of 1,2-epoxy-5-hexene modified PVA.....	62
15. Comparison of complex shear moduli and phase shift angles for biological tissues and hydrogels at 10 rad/s.....	79

16. Comparison between complex dynamic compressive and shear moduli obtained for glycidyl methacrylate-PVA hydrogels with different molecular weights of PVA.....81
17. Comparison between complex dynamic compressive and shear moduli obtained for 1,2-epoxy-5-hexene-PVA hydrogels with different types of monomers..... 82

LIST OF APPENDIX FIGURES

<u>Figure</u>	<u>Page</u>
A1. TGA of the sheep nucleus pulposus.....	98
A2. ¹ H NMR of glycidyl methacrylate modified poly(vinyl alcohol).....	99
A3. ¹ H NMR of 1,2-epoxy-5-hexene modified poly(vinyl alcohol).....	99
A4. ¹³ C NMR of 1,2-epoxy-5-hexene modified poly(vinyl alcohol).....	100
A5. GPC of 1,2-epoxy-5-hexene modified poly(vinyl alcohol).....	100
A6. DSC of 1,2-epoxy-5-hexene modified poly(vinyl alcohol).....	101
A7. ¹ H NMR of 1,2-epoxy-5-hexene-PVA hydrogel.....	101
A8. ¹³ C NMR of 1,2-epoxy-5-hexene-PVA hydrogel.....	102
B1. Variation in dynamic moduli, G' and G'', of glycidyl methacrylate-PVA hydrogels with molecular weight of PVA.....	105
B2. Variation in dynamic moduli, G' and G'', of glycidyl methacrylate-PVA hydrogels with initial weight percent of polymer.....	106
B3. Variation in dynamic moduli, G' and G'', with type of monomer for 1,2-epoxy-5-hexene-PVA hydrogels.....	107
B4. Variation in dynamic moduli, G' and G'', with percentage (w/w) of hydroxyethyl acrylate (HEA) for 1,2-epoxy-5-hexene-PVA hydrogels.....	108
B5. Variation in dynamic moduli, G' and G'', with percentage (w/w) of acrylic acid (AA) for 1,2-epoxy-5-hexene-PVA hydrogels.....	109

DEDICATION

For the Oregon State University Cycling Team, my comrades, who have supported me during all of my greatest triumphs and defeats, on and off the bike.

DEVELOPMENT AND CHARACTERIZATION OF NOVEL HYDROGELS FOR NUCLEUS PULPOSUS REPLACEMENT

INTRODUCTION



“I thought of that while riding my bike.”
- **Albert Einstein**, on the theory of relativity

Currently, the two most commonly employed surgical procedures for the treatment of lower back pain, discectomy and fusion, focus upon the rapid alleviation of the symptoms, regardless as to the long-term consequences. Discectomy, whereby the innermost portion of the intervertebral disc, the nucleus pulposus, is removed, is typically recommended for patients with radicular pain resulting from direct nerve root compression. Although removal of the nucleus pulposus leads to the immediate alleviation of nerve pressure and irritation, the intervertebral disc is rendered less functional and more unstable.¹ Alternatively, fusion, or permanent immobilization of a

segment, is recommended for pain relief when other forms of more conservative treatment have failed. The procedure is successful in eliminating any motion-induced pain in the treated segment; however, degeneration of adjacent segments is accelerated as a result of increased stress.² In an attempt to avoid the future complications associated with discectomy and fusion, a number of surgeons have explored the possibility of designing a total artificial disc to restore both comfort and function. Despite some success, the surgical implantation of a total artificial disc is highly invasive, as are any subsequent revisions, and the device necessitates the removal of all remaining disc tissue, regardless of the level of degeneration.³ A potentially superior approach to the repair of intervertebral discs in the early stages of degenerative disc disease is the replacement of only the nucleus pulposus, where deterioration begins. In contrast to total disc replacement, nucleus pulposus replacement is minimally invasive and preserves healthy intervertebral disc tissue.³

In the last two decades, several researchers have suggested using hydrogels as nucleus pulposus prostheses⁴⁻¹⁴ due to their ability to retain large quantities of water and their resultant high permeability towards low molecular weight solutes, such as glucose and oxygen. The latter attribute of hydrogels is critical to the health of the remaining tissue given the avascular nature of the intervertebral disc. In a nondegenerative disc, interior cells are supplied with nutrients via diffusion from capillary networks within the vertebral body that terminate above the cartilaginous endplates.¹⁵ An argument has also been made that the mechanical properties of hydrogels are comparable to those of the native

tissue;^{16,17} however, the analyses performed have been insufficient with regards to the intended use of the material.

During static loading of the spine, the highly hydrated nucleus functions to dissipate stress isotropically to the surrounding annulus fibrosus.¹⁸ Consequently, the nucleus pulposus is often viewed as an incompressible, inviscid fluid, despite evidence from Iatridis et al.¹⁹ that the tissue exhibits a more “solid like” nature when subjected to dynamic oscillatory shear. The complex shear moduli and phase shift angles are more characteristic of those possessed by biological solids, such as articular cartilage and meniscus,¹⁹ than biological fluids, including *in vitro* mixtures of the extracellular matrix components common to the intervertebral disc.²⁰ However, at slow deformation rates, as shown with transient stress relaxation experiments, the nucleus pulposus tissue behaves in a more “fluid-like” manner.¹⁹ The large difference between static and dynamic results, in addition to a significant frequency dependence, exemplifies the viscoelastic nature of the nucleus pulposus.

The viscoelastic response of the nucleus pulposus, as described above, suggests that studies on replacement materials should encompass a variety of loading modes to better simulate the mechanical environment found *in-vivo*; however, the hydrogel based devices currently being considered have, for the most part, only been evaluated under static or transient axial loading.^{5,11} Analyses of studies that do include dynamic and/or shear testing are often inadequate.^{13, 14} The differences between viscoelastic materials, including biological tissues, and simple liquids or solids are more noticeable in shear than

in axial loading.²¹ Therefore, torsional shear testing can be used as a benchmark method for comparing the mechanical properties of engineered tissue to those of native tissue.

Although the hydrogel based devices currently in clinical trials are purportedly for long term replacement, the nature of the crosslinks suggests that erosion may become a problem in the future. Within the three dimensional networks, portions of the polymer chains are organized into insoluble, microcrystalline regions that serve as physical crosslinks.^{5, 8} Relative to covalent, chemical crosslinks, physical crosslinks possess similar mechanical strength and avoid the use of potentially toxic chemical reagents, but are less resistant towards erosion under physiological conditions²² and problems with wear resistance have been encountered in other applications.²³ Chemical crosslinks will alleviate problems with erosion in the short term; however, many conventional crosslinking agents contain hydrolysable bonds. In the long term, scission of the latter bonds will lead to polymer degradation, the principal process of erosion. The rate of hydrolysis can be altered by changing the type of bond prevalent within the crosslinks.²⁴ For hydrogels to serve as plausible nucleus pulposus replacements, a composition must be found that has mechanical behavior comparable to that of the native system and that is relatively non-degradable under physiological conditions.

The primary goal of our research was to identify hydrogels for potential use in nucleus pulposus replacement through comparison of the mechanical behavior of the natural and synthetic systems. Additionally, a novel hydrogel composition was sought that was biocompatible and non-degradable within the time frame of the application. Specifically, our aims were:

- (1) To provide rational guidelines for the mechanical evaluation of hydrogels for use in nucleus pulposus replacement
- (2) To identify a hydrogel system whose viscoelastic behavior mimics that of the nucleus pulposus.
- (3) To create a new hydrogel system whose viscoelastic behavior mimics that of the nucleus pulposus and that possesses long term physiological stability.

BACKGROUND



“At the beginning stages, it is definitely the total physical development that is important. Later on you develop more mental concentration, mental preparation to maintain the physical capacity. Next you develop the spiritual.”

-Eddy Merckx

Biology of the Intervertebral Disc

Anatomy

The intervertebral discs are flexible spacers between the 24 vertebrae of the human spine that function in motion, stability and load distribution. Moving caudally, the discs, in addition to the vertebral bodies, gradually increase in size in response to the larger load imposed by the upper body. As a result, most clinical and experimental research, including the present study, focus upon the lumbar region of the spine.²⁵

As depicted in Figure 1, the intervertebral disc can be divided into two primary regions, the outer annulus fibrosus and the inner nucleus pulposus, that differ in cellularity and, consequently, the composition of the extracellular matrix.²⁶ The annulus

fibrosus consists largely of inelastic type I cartilage arranged in distinct layers of lamellae that attach to the vertebral body at 30° angles and alternate in orientation relative to the longitudinal axis of the spine. Approaching the nucleus pulposus, the lamellae become less distinct as the concentration of type I collagen decreases, and that of type II collagen and hydrophilic proteoglycans increases.²⁷ The transition in the disc matrix composition is reflected in the change from fibroblast-like cells within the annulus fibrosus to chondrocyte-like cells in the nucleus pulposus.²⁶ The cellular and molecular components are indicators of the mechanical roles played by each section.

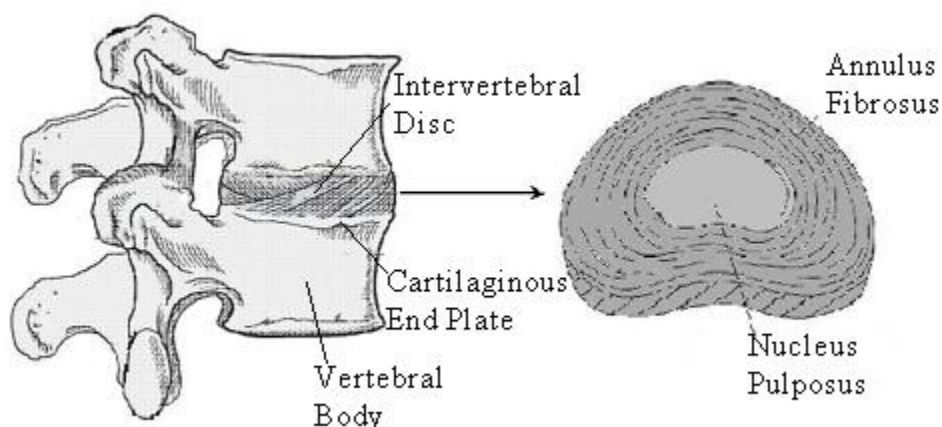


Figure 1. Anatomy of the intervertebral disc.

Nutrition

The intervertebral discs constitute the largest avascular structure in the body.²⁷ As such, cells of the nucleus pulposus and annulus fibrosus are supplied with nutrients via diffusion from capillary networks at the margins of the disc. Outer annular cells readily receive nutrients from the immediate, surrounding soft tissue; however, cells of the inner annulus and nucleus pulposus may be up to 8mm from the nearest blood supply.

Nutrients essential for energy metabolism and protein synthesis are provided by a capillary network that penetrates the vertebral body and terminates above the cartilaginous end plate. The nutrients must diffuse across the endplate and through the extracellular matrix to reach the interior disc cells.¹⁵ A number of researchers have suggested that fluid flow as a result of cyclic loading is also critical to nutrient delivery; however, for small solutes, such as O₂, glucose, amino acids, and CO₂, the fraction transported by convection is insignificant compared to the fraction that permeates the disc by diffusion.²⁸⁻³⁰ Transport of larger molecules, for instance hormones and enzymes, with higher diffusion coefficients may be affected by fluid flow.²⁸ In an analogous manner, metabolic byproducts, particularly lactic acid, are transported out of the intervertebral disc via diffusion through the end plates.³¹ Alterations in metabolite and nutrient transport, especially in the nucleus pulposus where the concentration gradients are steepest, are thought to play a critical role in disc degeneration.¹⁵

Disc Degeneration & Back Pain

The onset of intervertebral disc degeneration is marked by fragmentation of proteoglycan aggregates and reduction in aggrecan size within the nucleus pulposus.³² The ability of the disc to retain water is directly proportional to the number of proteoglycans; therefore, as degeneration progresses, the water content, and, consequently, the swelling pressure, is reduced. Stress on the surrounding annulus is increased, the lamellae become irregular, and fissures and cracks begin to form throughout the disc.³³ In contrast to the non-degenerate disc shown in Figure 2, the nucleus becomes less distinct from the annulus as the concentration of collagen fibers

risks with the reduction in hydration.²⁵ Additionally, the nucleus becomes hard and opaque, rather than soft and translucent.³³ The number of viable cells in all regions of the disc declines^{15, 33, 34} and the remaining cells appear to be surrounded by granular, noncollagenous protein. Severely degenerate discs have lost a significant amount of height and large fissures and clefts are prominent.³³ The gross morphological alterations that occur during degeneration are thought to contribute to spinal instability.

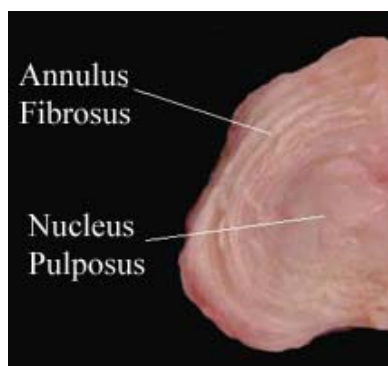


Figure 2. Non-degenerate sheep intervertebral disc. The annular lamellae encapsulating the soft nucleus pulposus are distinct.

Changes in endplate permeability, in addition to a reduction in the number of blood vessels at the periphery of the annulus, are presumably the leading causes of disc degeneration. Over time, the endplate is calcified and the transport of small solutes, particularly nutrients and metabolic waste, via diffusion becomes more limited.³⁵ Due to a low oxygen supply, cells undergo anaerobic metabolism and lactic acid accumulates in the nucleus pulposus.^{36, 37} The resultant rise in pH promotes the degenerative process by compromising the production of extracellular matrix, especially proteoglycans,³⁷ and inducing cell death.³³ As noted above, a reduction in the number of proteoglycans leads to a decrease in hydration, which further limits the ability of solutes to diffuse through the

matrix.³³ Additionally, the bulky proteoglycans act to control the flow of nutrients into and the movement of enzymes and cytokines out of the disc.³⁵ Therefore, an alteration in the production of proteoglycans will impact solute transport properties through multiple routes. The nutritional problems that play a large role in disc degeneration act as barriers to intervertebral disc repair.

Not all individuals with signs of disc degeneration experience back pain. The morphological changes noted above do not cause symptoms in and of themselves. Even in the case of intervertebral disc prolapse (i.e. herniation) where a bulge in the annulus presses directly onto the nerve root, only 30% of people present with pain. Purportedly, in some instances, cytokines are released by the disc cells that sensitize the nerve roots.^{39,40} Other inflammatory cells are believed to induce vascular and nerve ingrowth into annular defects.⁴¹ The free nerve endings may then be more susceptible towards mechanical irritation.³⁸ Disc alterations can also lead to misalignments of other structures along the spinal column, including the vertebral bodies, spinal ligaments and muscles, and facet joints. The resultant, abnormal mechanical and physiological environment may further contribute to back pain.³⁴ The ultimate goal of all treatment methods for degenerative disc disease is to eliminate pain; therefore, the absence of an identifiable pain source is a severe deficit in knowledge.

Mechanical Properties of the Nucleus Pulposus

As suggested by the different extracellular matrix compositions, the nucleus pulposus and annulus fibrosus have distinct mechanical roles. During static compressive loading, the healthy nucleus pulposus dissipates the applied stress isotropically to the surrounding

tissue.^{25, 27} Based upon transducer measurements, the hydrostatic pressure ranges from 0.1-0.3 MPa without an externally applied load and up to 3.0 MPa when subjected to various loading conditions.⁶ Under compression, the intradiscal pressure is approximately 1.5 times the applied load per unit area.²⁷ Constant load forces water out of the nucleus over time and leads to a reduction in disc height. The internal pressure of the nucleus pulposus causes the annulus fibrosus to bulge laterally, and the resultant tensile stress is sustained by the inelastic type I collagen fibers.²⁵ Due to the “fluid-like” behavior exhibited under static, axial loading, the nucleus pulposus is often inappropriately modeled as an incompressible, inviscid fluid.

Iatridis et. al. has extensively studied the viscoelastic behavior of the nucleus pulposus under torsional shear. The differences between viscoelastic materials, including soft biological tissues, and simple liquids or solids are more noticeable in shear than in axial loading.²² Nucleus pulposus samples were subjected to dynamic oscillatory shear and transient stress relaxation experiments. The complex shear moduli and phase shift angles found under dynamic loading were more characteristic of those possessed by biological solids, such as articular cartilage and meniscus,⁶ than biological fluids, including *in vitro* mixtures of collagen and proteoglycans.⁷ However, at slow shear deformation rates, i.e. with transient loading, the tissue behaved in a more “fluid-like” manner, as indicated by rapid relaxation to stress values near zero.⁶ The large difference in results obtained with transient versus dynamic stress application illustrates the viscoelastic nature of the nucleus pulposus. Materials for nucleus pulposus replacement should mimic this behavior as closely as possible.

Current Devices for Nucleus Pulposus Replacement

Introduction

Despite considerable research towards the development of nucleus pulposus replacements in the past decade, no nucleus prostheses are commercially available in the United States. The devices that have received the most attention are summarized in Table 1, at the conclusion of this section, and are described in more detail below. Although the utility of hydrogels in biomedical applications is explained further in the following section, they are a popular choice for nucleus pulposus replacement due to their ability to absorb water up to a percentage comparable to that of the natural tissue. All prosthetic devices aim to restore the physiological and mechanical functions of the nucleus pulposus to prevent further degeneration, but none of the implants described fully meet this requirement. The efforts made to ensure that the replacements have a mechanical environment analogous to that of the native tissue are particularly inadequate.

PDN[®] Prosthetic Disc Nucleus (Raymedica, Inc., Bloomington, MN)

The most extensive studies have been conducted on the PDN[®] Prosthetic Disc Nucleus. The device is composed of a non-covalently crosslinked poly(acrylamide)/poly(acrylonitrile) hydrogel core contained within a poly(ethylene) semi-permeable membrane. The ratio of poly(acrylamide) to poly(acrylonitrile) can be used to control the ability of the hydrogel to absorb water, while the outside jacket limits the amount of swelling.⁸ In 1996, initial clinical trials in Wiesbaden, Germany were conducted with two rectangular-shaped prosthetic units implanted within each enucleated cavity. Despite a reported 83% success rate, changes were made in the device shape to

conform better to the concave endplates, and the water content was increased from 68% to 80% by altering the hydrogel composition. Clinical trials conducted immediately following the alterations gave lower success rates than those originally observed; however, the success rate has risen to over 90% in more recent trials.⁴² The latter result is potentially a consequence of more selective criteria for patient eligibility for nucleus pulposus replacement.

Device migration and extrusion are the foremost problems associated with the Prosthetic Disc Nucleus. The sizes of the prostheses can be minimized by dehydration or compression prior to implantation; however, the bulkiness of the enclosures still necessitate that large incisions be made in the annulus fibrosus. The potential for extrusion is increased further by failure of the implant to properly match the size and shape of the nucleus cavity.⁸ Regardless of the changes made to the PDN[®] to account for the curvature of the endplates, the device still does not properly accommodate for the irregularity of nucleus pulposus cavities. Such an ill fitting device does not present a considerable advantage over traditional discectomy.

The hydrogel core is purported to mimic the natural nucleus pulposus in regards to mechanical strength, yet no evidence has been provided to substantiate this claim. Thus far, only one biomechanical study has been performed in addition to fatigue tests. The ranges of motion (ROM), neutral zones (NZ), and disc heights of intact, post-discectomy, and implanted discs of cadavers were compared. Although the ROM and disc heights of the implanted and intact specimens were comparable, the results are not necessarily meaningful given that the device was tested in the dehydrated state, which only exists for

a short period of time while under true physiological conditions. Additionally, despite the authors' claim that the NZ values of the implanted and intact specimens were similar, significantly greater values were actually observed for spinal segments containing the nucleus pulposus replacement.⁴³ NZ measurements are often used as a general reflection of spinal instability;⁴⁴ therefore, the PDN device in fact rendered the intervertebral disc less stable.

A claim is also made indicating that the hydrogel absorbs and releases nutrients via cyclic loading, in a manner similar to the natural nucleus pulposus.⁸ The latter claim is somewhat irrelevant considering the abundance of evidence demonstrating that nutrient transport does not occur as a result of cyclic loading, but instead through simple molecular diffusion, as described above.^{15, 28-30} In addition, the physical crosslinks within the network, which are generated by the organization of polymer chains into insoluble, microcrystalline regions,⁵ affect the permeation of biological molecules via a size exclusion phenomenon.⁴⁵ A replacement device with significant size exclusion characteristics is not desirable when looking for a replacement that will mimic the nucleus pulposus' ability to transport nutrients.

Aquarelle (Stryker Spine, Allendale, NJ)

Aquarelle nucleus replacement has received wide spread attention, but has yet to reach clinical trials. The device is centered upon a poly(vinyl alcohol) based hydrogel with physical crosslinks which resemble those described for the PDN[®].⁹ Relative to covalent chemical crosslinks, physical crosslinks possess similar mechanical strength and avoid the use of potentially toxic chemical reagents, but are less resistant towards erosion under

physiological conditions.⁴⁵ The PVA hydrogel used in Aquarelle was previously shown to have problems with wear resistance in the development of artificial articular cartilage.⁴⁶ In accord with the latter observation, during a recent study conducted *in vivo* using non-human primate models, an inflammatory response of macrophages and giant cells due to particles of fragmented PVA was identified in three out of twenty male baboons.¹⁰ The crystalline crosslinks also lead to problems with the diffusion of nutrients through a size exclusion effect, as described above.⁴⁵

A claim is again made that the hydrogel is analogous to the natural nucleus in terms of strength; however, the mechanical behavior of the implant is only analyzed in static compression.⁵ As was the case above, the most predominant problem observed in the *in vivo* animal study was migration and extrusion of the device. In 6 out of 20 baboons, the implant extruded posteriorly into the spinal canal or the soft tissue surrounding the intervertebral disc. Although the extruded device was relatively well tolerated by most of the animals, in one instance, the baboon was killed shortly after surgery due to compression of the nerve root. All of the implants were found to be smaller than the disc cavity into which they were implanted, and the improper fit was thought to contribute significantly to the high rate of extrusion. The most discouraging results were the formation of osteophytes, or bone spurs, in animals that received implants, indicative of continued disc degeneration.¹⁰

NeuDisc (Replication Medical Inc., New Brunswick, NJ)

NeuDisc addresses the issue of implant extrusion through annular defects by swelling in an anisotropic manner when submerged in physiological solution. The device contains

alternate layers of soft hydrolyzed poly(acrylonitrile) (Aquacryl) based hydrogel and rigid hydrogel created by reinforcing the Aquacryl with Dacron fibers. The Dacron functions to restrict expansion in the radial direction; therefore, axial deformation is favored and disc height is restored. Purportedly, by minimizing radial bulging, the chances of herniation through weakened areas of the annulus fibrosus, including the incision created for device insertion, are significantly reduced. Furthermore, the prosthesis can be inserted into the enucleated cavity in a dehydrated state, thereby minimizing the size of the annular defect through which expulsion could occur.⁴⁷

Results from clinical trials are not yet available, but the device has undergone extensive mechanical testing relative to other devices designed for nucleus pulposus replacement. Confined compression tests in physiological solution revealed that a lifting force equivalent to that found in the natural tissue could be obtained by controlling the water content of the device. The bulk modulus, as well as the level of hydration, was not impacted by fatigue testing for 10 million cycles. Cadaver studies revealed that failure in compression, flexion, and lateral bending all occurred primarily through either endplate fracture or rupture of the spinal ligaments; however, expulsion did occur in several instances.⁴⁸

Although NeuDisc does seem to offer a slight advantage over other devices in terms of implant extrusion, there are still some concerns. By minimizing radial bulging, further degeneration of the annulus fibrosus could be promoted, rather than hindered. The mechanical role played by the annulus, as discussed above, relies upon swelling pressure from the nucleus pulposus.^{25, 27} Studies have shown that in the absence of adequate

pressure from the nucleus, the annulus will begin to bulge inwards instead of outwards, thereby encouraging the formation of annular fissures and tears.⁴⁹ Long term *in vivo* testing will be necessary to determine whether the loss of swelling pressure experienced by the annulus will have a detrimental effect on the intervertebral disc. Additionally, adhesion between the Aquacryl layers is reliant upon weak physical crosslinks that may be susceptible to breakage if uneven radial swelling occurs.⁴⁷ If the stacked arrangement of hydrogels begins to fall apart, the lifting force will be altered, and the device will no longer be able to function properly.

Newcleus (Zimmer, Spine)

Newcleus consists of proprietary poly(carbonate) urethane elastomer (Sulene PCUTM) in the form of a memory coiling spiral. The polymer is inserted through the annulus in a rectilinear conformation, but within the nuclear space, the implant begins to return to a spiral shape.^{50, 51} Thus far, clinical testing has been attempted on only five patients. Although expulsion and device migration have not occurred, as confirmed by MRI, definitive conclusions are not possible with such a small sample number. The MRI scans did show changes in the adjacent vertebral bodies, potentially resulting from an incorrect distribution of load between the vertebrae and the device.⁵¹ The implant has been shown to absorb only 35 wt. % water *in vitro*,⁴⁹ which almost certainly will hinder the diffusion of nutrients to the inner annulus fibrosus from above the cartilaginous end plates. In the long term, the intervertebral disc may in fact degenerate further as a result of the latter inadequacy.

Aside from fatigue tests that showed no wear up to 50 million cycles, mechanical testing of Newcleus has been insufficient. A study was conducted to determine the difference in segmental motion between an intact disc, a disc that has undergone discectomy, and a disc containing a nucleus replacement; however, a small sample size, with a large variation in results, prevented determination of statistical significance and trends were not clear. Furthermore, the researchers note that failure does not occur under compression, but do not specify the applied load, thereby reducing the importance of the test.⁵¹ Based upon the changes observed in the MRI studies, the relatively hard plastic may be too stiff to function properly as a nucleus pulposus replacement, but no moduli have been determined for direct comparison. Studies have shown that load applied in posterior shear to an intervertebral disc containing a Newcleus replacement produces endplate strains that exceed those of an intact disc,⁵² thereby lending more support to the notion that the mechanical properties of the implant and the natural tissue are not analogous.

DASCORTM Disc Arthoroplasty Device (Disc Dynamics, Inc., Eden Prairie, MN)

DASCORTM is introduced to the nuclear space after discectomy by a minimally invasive technique utilizing an *in situ* curable polymer.⁹ A prepolymer mix is prepared at the time of surgery by combining a diol terminated poly(urethane) with a diisocyanate crosslinking agent. Following insertion of a poly(urethane) balloon into the nucleus cavity, the prepolymer mix is injected via cannula and curing is completed *in vivo*. Damage to the annulus is minimized by the arthroscopic technique and the chances of expulsion are further reduced by the ability of the device to conform to the shape of each

individual enucleated cavity.⁵³ However, the delivery of nutrients to the surrounding annular tissue via diffusion through the cartilaginous endplates is effectively blocked by plastic. Degeneration of the inner annulus fibrosus, and consequently the entire intervertebral disc, will presumably occur in the future.

Biodisc™ Spinal Disc Repair System (Cryolife, Kennesaw, GA)

BioDisc™ is another nucleus replacement system that can be cured *in situ*, thereby minimizing the surgical defect created in the annulus and providing a means for the implant to conform correctly to the nuclear cavity. Results from animal studies have not been released, but clinical studies on humans were recently begun in the United Kingdom.⁵⁴ The system is based upon human or animal proteins, preferably serum albumins, which are crosslinked via dialdehydes, such as glutaraldehyde, in aqueous solution immediately prior to or during injection into the intervertebral disc.⁵⁵ The protein backbone is susceptible to enzymatic degradation and the acetal based crosslinks have been shown to degrade rapidly under physiological conditions;²⁴ therefore, the longevity of the device is questionable. Additionally, the efficacy of *in vivo* polymerization of the BioDisc™ system can be disputed given the known toxicity of glutaraldehyde, even at low concentrations.⁵⁶

Table 1. Summary of nucleus pulposus replacements currently under investigation

Device	Material	Studies	Advantages	Disadvantages
PDN[®]	Poly(acrylonitrile)/poly(acrylamide) hydrogel pellet encased in a poly(ethylene) jacket	<ul style="list-style-type: none"> Commercially available outside of the US and Canada Clinical study being conducted in Canada 	Restores disc height	<ul style="list-style-type: none"> Improper fit leads to migration and extrusion Physical crosslinks prevent diffusion of nutrients via size exclusion
Aquarelle	Poly(vinyl alcohol)	Animal studies with 20 baboons	High water content	High percentage of extrusion in animal studies
NeuDisc	Hydrolyzed poly(acrylonitrile) (Aquacryl) enclosed in a Dacron mesh	Clinical study being conducted in Europe	<ul style="list-style-type: none"> Restores disc height Few problems with extrusion 	<ul style="list-style-type: none"> The mechanical environment of the annulus fibrosus is altered Concern over adhesion of the Aquacryl layers
Newcleus	Poly(carbonate) urethane (PCU) elastomer	Clinical study being conducted in Europe (5 patients)	Few problems with implant extrusion	<ul style="list-style-type: none"> Low water content (35%) may limit nutrient diffusion Incorrect load distribution
DASCOR[™]	Curable poly(urethane) within an expandable poly(urethane) balloon	Clinical study being conducted in Europe (16 patients)	<ul style="list-style-type: none"> Minimally invasive Reduced risk of extrusion 	Concern over nutrient transport through the poly(urethane) balloon
BioDisc[™]	Protein hydrogel; purified bovine albumin (45%) and glutaraldehyde (10%)	Clinical study being conducted in Europe (10 patients)	<ul style="list-style-type: none"> Minimally invasive Reduced risk of extrusion 	Concern over longevity of the device

Hydrogels for Biomaterial Applications

General

Since the early 1960s, hydrogels have been viewed as attractive materials for biomedical applications due to their ability to retain water and generally good biocompatibility.⁵⁷⁻⁶⁰ Hydrogels are hydrophilic, three dimensional networks generated via either chemical or physical crosslinking of polymer chains. Physical crosslinks are formed via non-covalent interactions; such as van der Waals forces, hydrogen bonding, ionic complexation, or molecular entanglements, which are reversible and can be readily disrupted by a change in the surrounding environment, including application of load. Chemical crosslinks are generated from covalent, chemical bridges between monomers and are, consequently, more resistant towards dissolution and degradation.⁵⁹ However, chemical crosslink formation often necessitates the use of reagents that are potentially toxic within the body. As a result, despite shortfalls in mechanical stability and longevity, physically crosslinked hydrogels are often favored for *in vivo* use.⁵⁸

Hydrogels have found application as space-filling devices, vehicles for drug delivery, and scaffolds for tissue engineering. As space-filling devices, poly(ethylene glycol) based hydrogels have been used in the prevention of post-operative adhesion. Alternatively, through the use of biopolymers and the attachment of biologically active molecules to synthetic polymers, hydrogels have been applied as bioadhesives to seal wounds and to augment the efficacy of wound dressings. Hydrogels have also been explored for use as vocal cord replacements and as bulking materials to treat conditions such as urinary incontinence and vesicoureteral reflux.⁶⁰ In pharmaceutical applications,

drugs or proteins encapsulated within a gel matrix have been released by mechanical stimulation, diffusion, and polymer degradation.^{57,60} Bioactive molecules can thereby be delivered directly to a specific location and be released in a controlled manner, a significant advantage over oral and intravenous delivery. Hydrogels are currently being explored for use in the engineering of tissues, including articular cartilage, bone, muscle, adipose, and neurons. The highly hydrated matrix provides an ideal environment for the cultivation of cells.⁶⁰ In sum, as a result of their highly desirable properties, hydrogels will likely have a continued impact on the field of biomedical engineering.

Poly(vinyl alcohol) Based Hydrogels

Poly(vinyl alcohol) (PVA) based hydrogels, in particular, have received wide spread attention as a result of excellent biocompatibility, high elasticity, an inherently low toxicity, and a propensity to swell considerably when submerged in water.^{45,61-63} PVA can be crosslinked in a number of different manners⁴⁵ and combined with biological macromolecules, including collagen,^{56,65,65} dextran,⁶⁶⁻⁶⁸ chitosan,^{67,68} and hyaluronic acid,⁶⁹ to give materials with a wide variety of physical properties. Additional changes can be brought about by varying the polymer molecular weight and degree of hydrolysis.⁴⁵ PVA, therefore, has utility in a variety of biomedical and pharmaceutical applications.

Difunctional reagents, including succinyl chloride, adipoyl chloride, sebacoyl chloride,⁷⁰ epichlorohydrin,⁷¹ and glutaraldehyde,^{56,72,73} can be used to directly crosslink PVA chains. However, there are concerns over the possible entrapment of residual amounts of the potentially toxic chemicals within the hydrogel network. Extraction

processes are often time consuming and there is no way to assure that all traces of the reagent have been removed.⁴⁵ In order to minimize the likelihood of negative side effects from excess aqueous glutaraldehyde, crosslinking has been conducted in the presence of gaseous glutaraldehyde.^{56,68} Unfortunately, this change has not eliminated the problems. A recent study on the comparison of the biocompatibility of PVA-collagen hydrogels crosslinked physically and with gaseous glutaraldehyde, showed an increased percentage of cell death for gels prepared in the presence of glutaraldehyde.⁵⁶ Given the problems with safety, hydrogels generated from covalent, chemical crosslinking are not typically acceptable for biomedical applications.

Recent research has focused upon the freeze-thaw method of hydrogel preparation whereby an aqueous solution of PVA is frozen and thawed repeatedly.^{45,61,74,75} The properties of the resultant gel can be altered by adjusting the molecular weight of the polymer, the initial concentration of polymer in solution, and the number of freeze-thaw cycles. Crosslinks consist of crystalline regions that become increasingly stable following each freeze-thaw cycle. Although the network does initially show a strength and elasticity that is analogous to that of covalently crosslinked hydrogels, with time, dissolution of the PVA chains occurs and some of the crystallites begin to 'melt' out.⁷⁵ Hydrogels prepared via the freeze-thaw method may be suitable as vehicles for controlled drug release; however, their inherent instability precludes their use in any long-term devices, such as those for tissue replacement. As mentioned above in regards to the Aquarelle nucleus pulposus replacement, physically crosslinked PVA has shown signs of

wear *in vivo*.^{10,46} Although appealing due to the lack of toxicity, all physically linked hydrogels, including those based upon PVA, lack in mechanical strength and stability.

PVA can also be modified with a group that is susceptible towards radical attack and subsequently crosslinked via photopolymerization.⁷⁶ Networks based upon covalent bonds can thereby be generated without the use of potentially toxic crosslinking agents. For example, PVA has been coupled with glycidyl acrylate and photopolymerized upon exposure to UV radiation in the presence of an initiator (Figure 3).^{62,63} The resultant network is highly biocompatible, as illustrated by research that has shown that the viability of chondrocytes can be maintained upon encapsulation.⁷⁷ Although photopolymerized materials presumably have strength and long term stability analogous to or greater than that of covalently crosslinked gels, thus far, mechanical characterization, as well as degradation studies, have been incomplete.

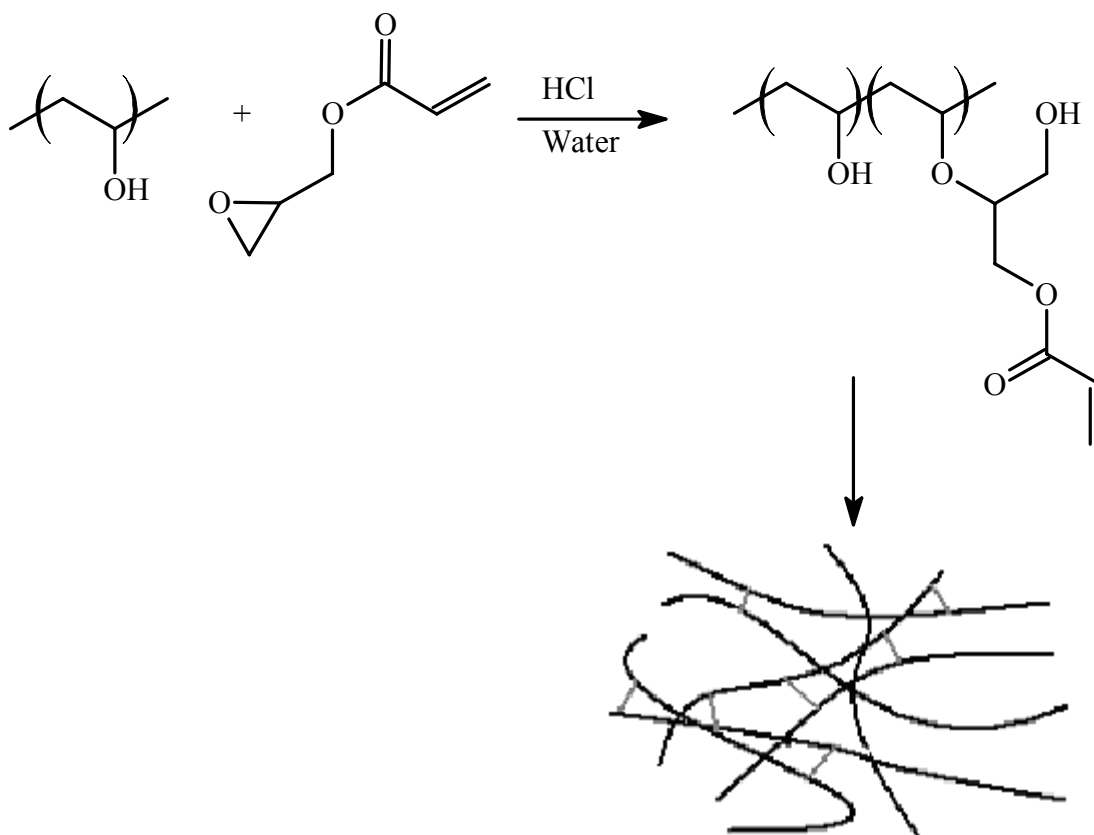


Figure 3. Modification of poly(vinyl alcohol) with glycidyl acrylate, followed by photopolymerization.

Injectable & Photopolymerizable Hydrogels

A great amount of attention is currently being given to injectable hydrogels that can be solidified *in vivo*.^{78,79} These materials offer a number of advantages over pre-formed matrices. Traditionally, implantation of hydrogels requires an aggressive surgical approach and prior knowledge of the size and conformation of the cavity to be filled. Injectable materials provide a means to deliver space-filling devices and regenerative scaffolds that perfectly conform to the shape of all defects in a minimally invasive fashion. Additionally, for tissue engineering applications, a cell suspension can be co-

injected with the hydrogel components to give a more homogeneous distribution of cells throughout the network upon solidification.⁷⁹ Injectable hydrogels are currently being investigated for a variety of applications, particularly bone repair and regeneration of articular cartilage.⁷⁸

A number of criteria must be met for an injectable hydrogel to be suitable for *in vivo* formation. Components of the injection solution, as well as degradation products from the resultant hydrogel, must be sterile and nontoxic, such that changes in cell viability and function do not occur. Additionally, the conditions necessary for solidification should be mild in order to avoid damage to the surrounding tissue. High temperatures, organic solvents, and drastic changes in pH must be avoided. Typically, solidification can be induced by chemical crosslinking, thermal gelation, ionic crosslinking, or photochemically initiated radical polymerization. The resultant hydrogel should have a mechanical strength analogous to that of the natural tissue and must be able to maintain this strength after scaffold degradation and tissue ingrowth have begun.⁷⁹ Hydrogel precursors must be carefully selected for each application in order for success.

Photopolymerization is suitable for the *in vivo* generation of hydrogels and offers an attractive alternative to chemical crosslinking, which is often avoided due to the potential toxicity of the reagents.⁷⁶ As with any covalently linked network, hydrogels generated via photopolymerization are stronger and more stable than those formed from physical crosslinks. UV or visible light induces light sensitive compounds, i.e. photoinitiators, to generate free radicals that initiate polymerization. In order to avoid the hazards of free monomers, hydrogel precursors are typically water soluble polymers with

two or more reactive groups on each chain to allow for crosslinking. The low requisite light intensity, short duration of irradiation, and minor increase in temperature allow for photopolymerization to be conducted in the presence of cells and tissues. Light can be introduced by arthroscopic techniques, catheters, or with transdermal illumination.

Photocurable materials have been used extensively in dentistry for sealants and restorations and are being explored for use in other biomedical applications, including adhesion barriers, drug delivery vehicles, and scaffolds for tissue regeneration.⁷⁶

Summary

The mechanical and physiological functions of intervertebral discs in the early stages of intervertebral disc disease can potentially be restored through nucleus pulposus replacement, where deterioration begins. Thus far, the devices designed for implantation have been lacking in a number of respects. In addition to problems with wear, extrusion, and nutrient delivery, none of the prostheses have been sufficiently tested to ensure that the viscoelastic behavior mimics that of the native tissue. Based upon strength, stability, and water content, biocompatible, covalently crosslinked hydrogel networks could serve as nucleus pulposus replacements. Poly(vinyl alcohol) is a logical starting material for the development of a device that properly mimics the native tissue given the ease with which the properties of the resultant gel can be modified through variations in the method of crosslinking.

Preliminary Research with Chemically Crosslinked Poly(vinyl alcohol)

Two commonly used crosslinking reagents were initially used to form PVA hydrogels. Poly(vinyl alcohol) was first crosslinked by intermolecular acetalization of the hydroxyl

groups with glutaraldehyde (Figure 4). In general, although a water content analogous to that of the nucleus pulposus was obtained, the hydrogels were weaker than the natural tissue (Figure 5) and degraded quickly when submerged in Hank's solution (Figure 6). As given in Table 2, the latter is a physiological solution that more closely replicates the conditions found *in vivo* than simple phosphate buffer solution.⁶⁹ The degradation study was conducted by measuring the mass of the water swollen hydrogel at regular increments. Further study demonstrated that reversal of acetal formation was accelerated by the presence of magnesium (results not shown) within Hank's solution. Additionally, as noted above, glutaraldehyde has been shown to be toxic at even low concentrations.⁵⁶ Although the mechanical properties of the hydrogel could presumably be controlled by varying the concentration of both glutaraldehyde and PVA in solution to obtain materials that more closely mimic the natural tissue, further studies were not conducted due to the high susceptibility of the crosslinks to hydrolysis under physiological conditions and the potential toxicity of the crosslinking agent.

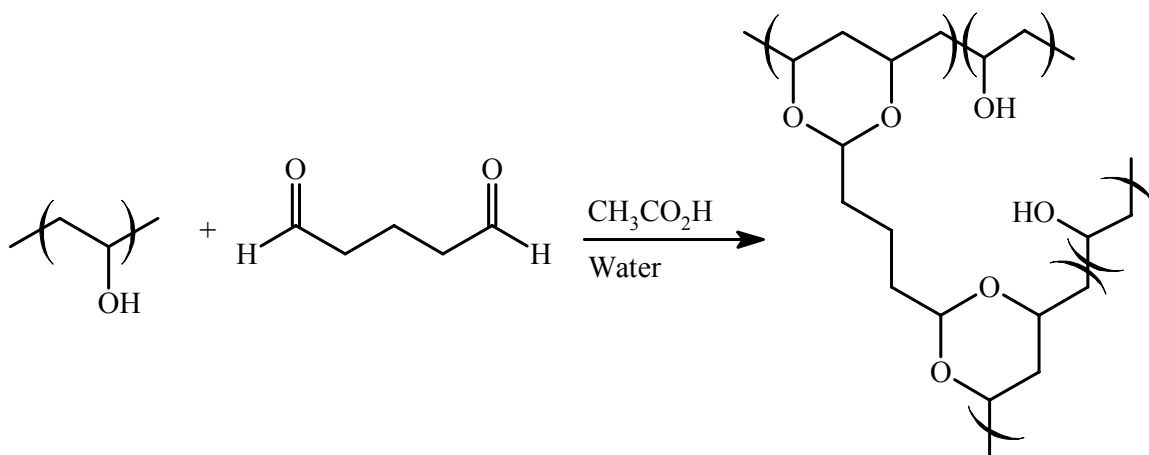


Figure 4. Chemical crosslinking of poly(vinyl alcohol) with glutaraldehyde.

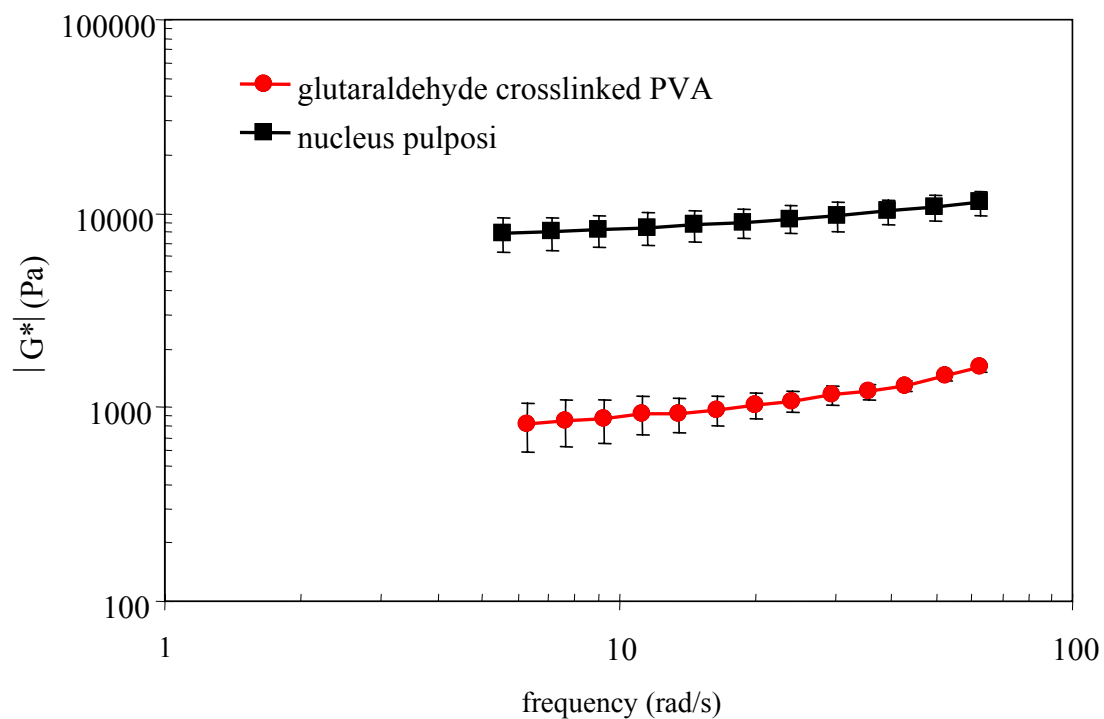


Figure 5. Comparison of complex shear moduli of hydrogels generated via crosslinking of PVA with glutaraldehyde with those of sheep nucleus pulposi. All hydrogels were prepared from an aqueous solution of 10 wt. % polymer and 2.5 wt. % crosslinking agent. Data points are shown as average values with 90% confidence intervals derived from Student's t-distributions.

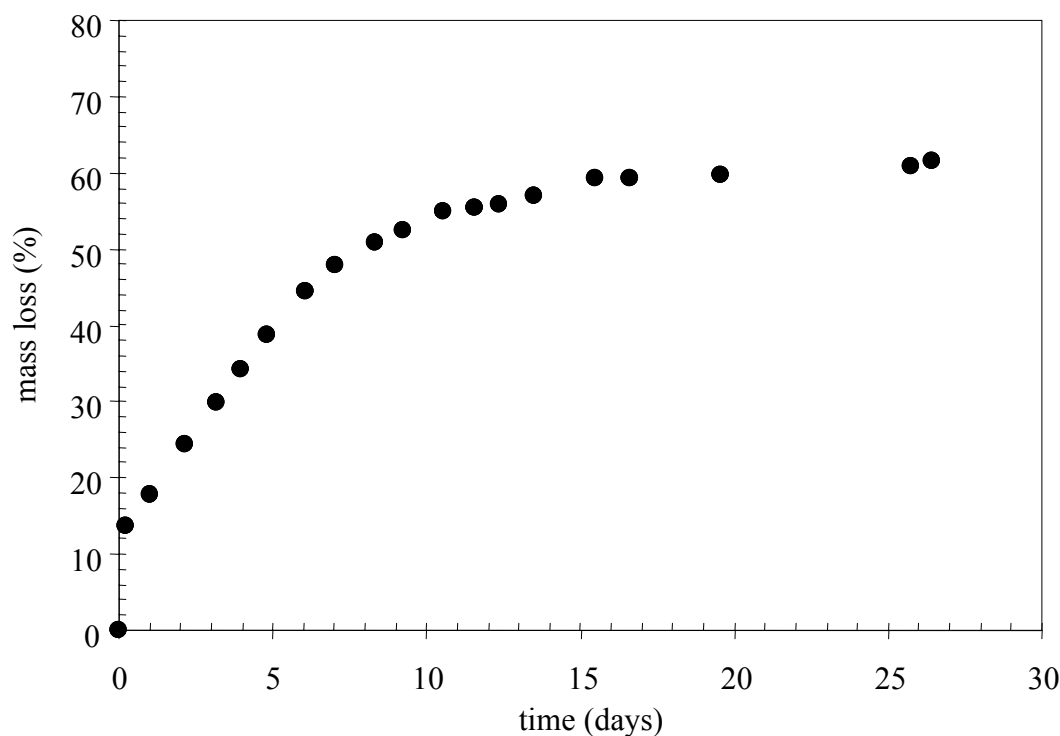


Figure 6. Percent mass loss of hydrogels generated via crosslinking of PVA with glutaraldehyde.

Table 2. Composition of Hank's solution

Composition	Concentration (mg/ml)
NaCl	8.00
Glucose	1.00
KCl	0.40
NaHCO ₃	0.35
CaCl ₂	0.14
MgCl ₂ *6H ₂ O	0.10
Na ₂ HPO ₄ *2H ₂ O	0.06
KH ₂ PO ₄	0.06
MgSO ₄ *7H ₂ O	0.06

Epichlorohydrin proved to be a superior crosslinking reagent than glutaraldehyde in terms of hydrogel longevity (Figure 7). When a ratio of epichlorohydrin to hydroxyl groups of approximately 0.5 was used, the rheological data was similar to that obtained with glutaraldehyde; however, after 30 days, no degradation had occurred. The

rheological properties could be varied in a predictable manner by varying the amount of crosslinking reagent used relative to the number of hydroxyl groups (Figure 8). The known carcinogenicity of the crosslinking reagent precluded its use in further research. However, the epichlorohydrin study did demonstrate that, based upon longevity, poly(vinyl alcohol) hydrogels with ether linkages have strong potential for use as nucleus pulposus replacements.

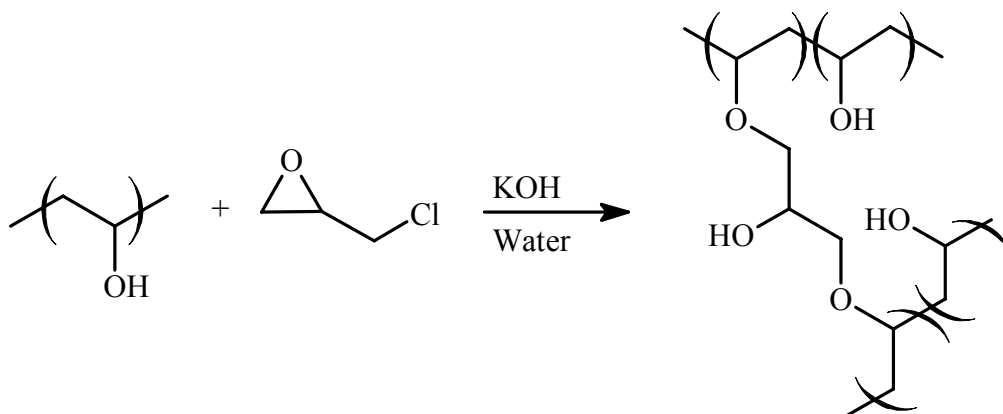


Figure 7. Chemical crosslinking of poly(vinyl alcohol) with epichlorohydrin.

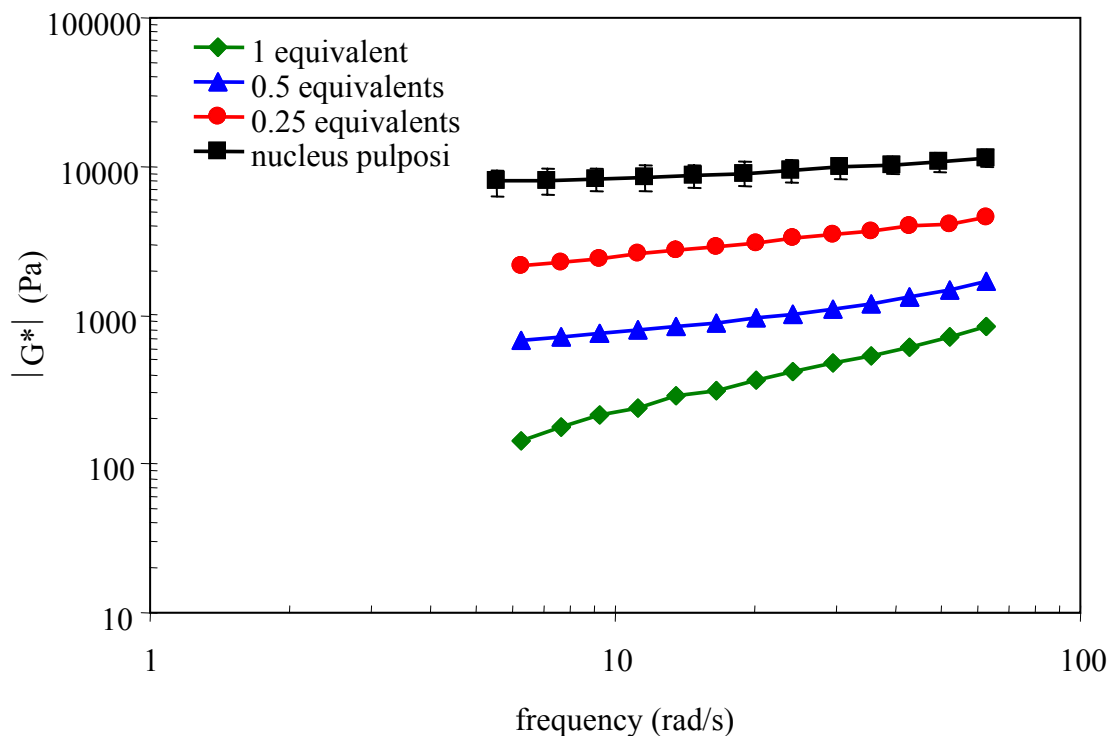


Figure 8. Comparison of complex shear moduli of hydrogels prepared via crosslinking of PVA with epichlorohydrin with those of sheep nucleus pulposi. Equivalents of epichlorohydrin are given relative to the moles of repeating units (i.e. vinyl alcohol).

Preliminary research demonstrated that covalent crosslinks could be used to generate hydrogel networks whose viscoelastic behavior approached that of the natural tissue; however, conventional crosslinking methods can not be used due to the toxicity of the reagents and problems with hydrolytic susceptibility under physiological conditions. Therefore, less traditional methods towards the formation of stable crosslinks were pursued. The applicability of a known photopolymerizable hydrogel system was investigated and a new system based upon relatively non-degradable ether crosslinks was created.

MATERIALS & METHODS



“The interactions of body, mind, muscles, terrain, gravity, air and bicycle are so complex that they defy mathematical solutions. The feel and handling of a bike borders on art. Like the violin, it’s been largely designed by touch, inspiration, and experimentation.”

-Chester Kyle

Analytical Data

Nuclear magnetic resonance (NMR) spectroscopy was used for structural characterization of all hydrogel precursors. Proton (^1H) NMR spectra were recorded with a Bruker 400 (400 MHz) or a Bruker 300 (300 MHz) at Oregon State University. Proton (^1H) chemical shifts, reported in parts per million (ppm), were referenced using internal D_2O . Coupling constants (J) are reported in Hertz (Hz). The following abbreviations for multiplicities are used: singlet, s; doublet, d; triplet, t; doublet of doublets, dd; multiplet, m. Carbon (^{13}C) NMR spectra were recorded on a Varian (500 MHz) at the University of Oregon with the assistance of Michael Strain. Carbon (^{13}C) chemical shifts, reported in parts per million (ppm), were referenced to external DMSO.

Gel permeation chromatography (GPC) was used to determine the molecular weights of new materials. Separation was carried out with two PL aquagel-OH MIXED 8 μ m columns in series, using a Wyatt differential refractometer as a detector. Millipore filtered DI water was used as the eluent at a flow rate of 1 mL/min. Molecular weights were estimated from a calibration curve constructed from poly(ethylene oxide) standards. All samples for GPC analysis were prepared at a concentration of 1 mg/mL in millipore filtered DI water and were passed through a 0.45 micron filter prior to injection.

Glass transition temperatures (T_g) and melting points (M_p) were examined via modulated differential scanning calorimetry (MDSC) (TA Instruments, Inc. New Castle, DE). MDSC was chosen over traditional DSC to remove the impact of residual water and to increase the sensitivity of the instrument to weak signals. Samples of approximately 10 mg in sealed aluminum pans were subjected to a ramp of 2°C/min from 0° to 340°C with modulation $\pm 1.70^\circ\text{C}$ every 80 seconds. An empty, crimped aluminum pan was used as a reference. Modulation was accomplished through the use of liquid nitrogen.

Water content of all hydrogels and natural tissue reported herein were determined via thermogravimetric analysis (TGA) (TA Instruments, Inc., New Castle, DE). Samples were heated up to 200°C at a rate of 10°C/min under nitrogen flow.

Sample spectra can be found in Appendix A.

Reagents

Poly(vinylalcohol) (PVA) with 98-88% hydrolysis and molecular weight ranges of 13-23 K, 30-51 K, 50-85 K, 85-124 K, 146-186 K was purchased from Aldrich Chemical

Company and used without further purification. Glycidyl methacrylate was obtained from TCI America. Monomethyl ether hydroquinone (MEHQ) inhibitor was removed from the latter reagent by washing sequentially with aqueous sodium hydroxide and water. The uninhibited monomer was dried over anhydrous magnesium sulfate and filtered. N-vinylpyrrolidone, 2-hydroxyethyl acrylate, N,N-dimethylacrylamide, and acrylic acid were obtained from Aldrich Chemical Company and purified by passing through a column of neutral alumina. All monomers were either used immediately following purification or stored in an amber glass bottle at 4°C to prevent spontaneous polymerization. Photoinitiator 2-hydroxy-1-[4-(2-hydroxyethoxy)phenyl]-2-methyl-1-propanone (Irgacure 2959, I2959) was provided by Ciba Specialty Chemicals. All other commercial reagents were purchased from Aldrich Chemical Company and used as received.

Cell Culture

Christine Kelly and Erin Rieke from the Department of Chemical Engineering at Oregon State University kindly provided assistance, facilities, and materials for mammalian cell culture. NIH 3T3 mouse embryonic fibroblast cell line was obtained from American Type Culture Collection (ATCC). Cells were cultured on fibronectin-coated T-flasks in Dulbecco's Modified Eagle's Medium (DMEM) containing phenol red and supplemented with 10% calve bovine serum and 100 µg/mL penicillin:streptomycin. Fibroblasts were grown in a 5% CO₂ atmosphere at 37°C and were used after 4 passages.

Intervertebral Disc Specimens

Sheep lumbar spines were donated by the College of Veterinary Medicine at Oregon

State University immediately following euthanasia. Spines were wrapped in plastic and frozen to prevent changes in the water content. While frozen, intervertebral discs were isolated and dissected to obtain the nucleus pulposus. The specimens were thawed at room temperature prior to analysis. The water content of the tissue was established via TGA.

Hydrogel Preparation via Crosslinking of Poly(vinyl alcohol) with Glutaraldehyde

All glutaraldehyde crosslinked hydrogels were prepared in 5 mL disposable syringes to allow for easy transfer to dialysis tubes following solidification. Acetic acid was added dropwise to a solution of PVA (0.25 g) and glutaraldehyde (.0125 g) in 4.625 mL of water until a pH of approximately 4 was reached. The reaction was allowed to proceed at room temperature until gelation was visually complete (24-48 hours). The gel was pushed directly out of the syringe into a dialysis bag and dialyzed in DI water for 48 hours, changing the water at 24 hours. Hydrogel characterization was performed after the gel was removed from the dialysis membrane and blotted to remove any excess water.

Hydrogel Preparation via Crosslinking of Poly(vinyl alcohol) with Epichlorohydrin

Epichlorohydrin-PVA hydrogels were prepared as described in the literature.⁷¹ In a typical procedure, epichlorohydrin (2.10 g, 22.7 mmol) was added to poly(vinyl alcohol) (1.0 g, 22.7 mmol) in 10 mL of water. A solution of KOH (1.66 g, 29.5 mmol) in 2 mL of water was slowly added via syringe with vigorous stirring. After becoming clear and homogeneous, the reaction mixture was transferred to a petri dish and covered. Crosslinking was allowed to proceed for 24 hours. The gel was removed from the dish and excess reagents were removed by boiling in a hot water bath for 4-5 hours, changing

the water periodically until the pH of the water became neutral.

Synthesis and Characterization of Glycidyl Methacrylate Modified Poly(vinyl alcohol)

PVA was modified with glycidyl methacrylate as described elsewhere.^{62,63} Briefly, glycidyl methacrylate (12.9 g, 90.8 mmol) was added to PVA (2g, 45.4 mmol repeating units) in 18 mL of water. Concentrated HCl was added drop-wise until a pH of approximately 1.5 was reached, and the reaction mixture was stirred at 40°C for 24 hours. A white, powder precipitate was obtained upon slow addition of the solution to acetone. The polymer was collected by filtration, washed repeatedly with acetone, and dried at 40°C for 24 hours in vacuo. The coupling of glycidyl methacrylate to PVA via epoxide ring-opening is illustrated in Figure 9. ¹HNMR (D₂O): δ 6.06(s, 1H), δ 5.64 (s, 1H), δ 4.50 (dd, J=12.0 Hz, 3.0 Hz, 0.2H), δ 4.18 (m, 1H), δ 4.08 (dd, J=11.7 Hz, 6.0 Hz, 0.8H), δ 3.93 (m, 9.1H), δ 3.70 (m, 0.8H), δ 3.56 (m, 1.6H), δ 3.35 (m, 0.2H), 2.95 (t, J=3.6 Hz, 0.2H), δ 2.82 (t, J= 3.6 Hz, 0.2H), δ 1.88 (s, 3H), δ 1.58 (m, 17.8H) . 10-20% of PVA hydroxyl groups reacted with glycidyl methacrylate based upon the relative amounts of vinyl protons (δ 6.06 and δ 5.64) to CH₂ (δ 1.58) backbone protons.

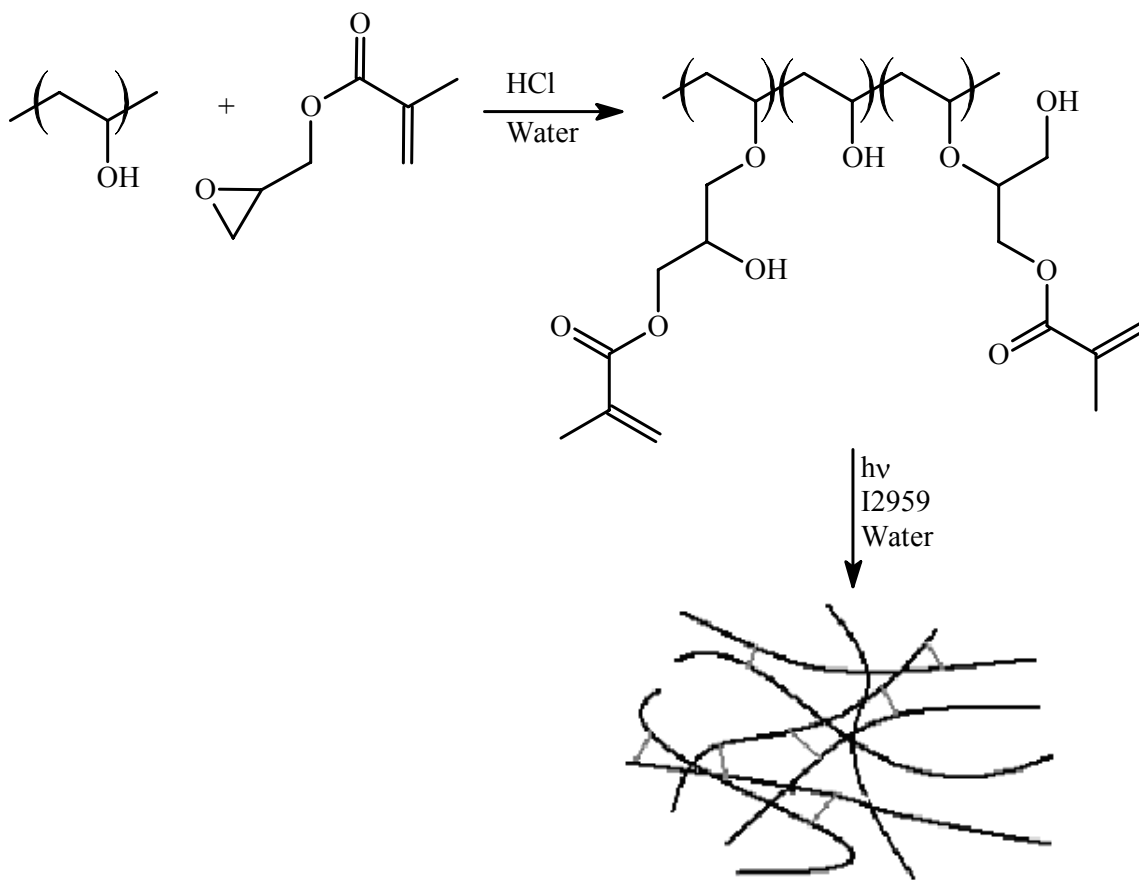


Figure 9. Modification of PVA with glycidyl methacrylate, followed by photopolymerization.

Hydrogel Preparation from Glycidyl Methacrylate Modified PVA (Glycidyl Methacrylate-PVA)

Glycidyl methacrylate modified PVA was dissolved in water at 80°C to the desired concentration. 1.0% (w/w) I2959 was added and stirring was continued for 10 minutes. The solution was transferred to a Teflon mold (disc, 15mm diameter, 1.0mm thick), covered with a glass slide, and photopolymerized using a Blak-Ray B-100A longwave UV lamp for ≤ 5 minutes. A representation of the photopolymerization process is shown in Figure 9. Hydrogel samples were immersed in Hank's solution and allowed to swell at

room temperature for 48 hours. Water content of the polymer solution prior to photopolymerization, as well as the water content of the gels following equilibration, was assessed via TGA.

Synthesis and Characterization of 1,2-Epoxy-5-hexene Modified Poly(vinyl alcohol)

1,2-Epoxy-5-hexene (6.68 g, 68.1 mmol) was added to 85-124k PVA (3g, 68.1 mmol repeating units) in 18 mL of water. Glacial acetic acid was added drop-wise until a pH of approximately 3.0 was reached, and the reaction mixture was stirred at 40°C for 48 hours. A white, powder precipitate was obtained upon slow addition of the solution to acetone. The polymer was collected by filtration, washed repeatedly with acetone, and dried at 40°C for 24 hours in vacuo. The coupling of 1,2-epoxy-5-hexene to PVA is illustrated in Figure 10. T_g (DSC): 124-131°C. M_p (DSC): 219-220°C. ^1H NMR (D_2O): δ 5.79 (m, 1H), δ 4.98 (d, $J=17.4$ Hz, 1H, d), δ 4.91 (d, $J=9.9$ Hz, 1H), δ 3.92 (5H, m), δ 3.6 (1H, m), δ 3.49 (dd, $J=11.4$ Hz, 3.6 Hz, 1H), δ 3.37 (dd, $J=11.4$ Hz, 6.6 Hz, 1H), δ 2.02 (2H, m), δ 1.48 (12H, m). ^{13}C NMR (D_2O): δ 139.11, δ 114.95, δ 71.44, δ 67.92, δ 65.57, δ 44.37, δ 31.68, δ 29.28. 10-20% of PVA hydroxyl groups reacted with 1,2-epoxy-5-hexene based upon the relative amounts of vinyl protons (δ 5.79 and δ 4.98) to CH (δ 3.92) backbone protons. The latter result was confirmed by GPC, which showed a molecular weight increase corresponding to 10-20% modification of the polymer side chains.

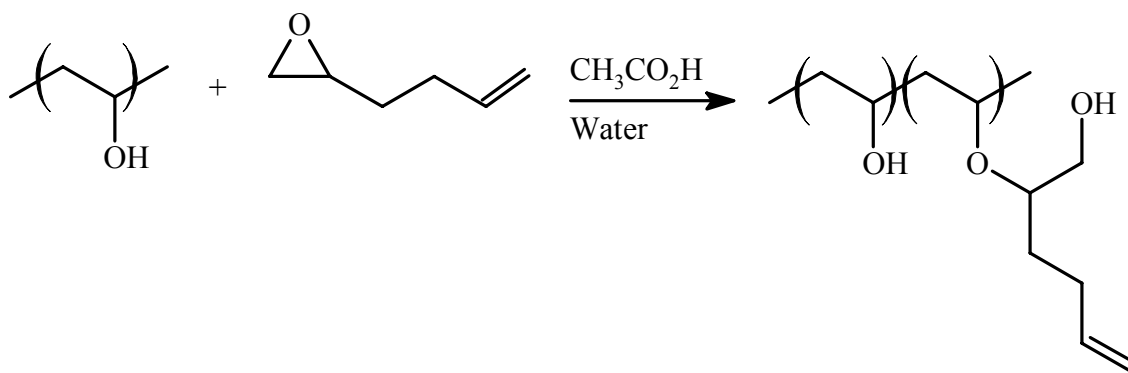


Figure 10. Modification of poly(vinyl alcohol) with 1,2-epoxy-5-hexene.

Hydrogel Preparation from 1,2-Epoxy-5-hexene Modified PVA (1,2-Epoxy-5-hexene-PVA)

0.40 g of 1,2-epoxy-5-hexene modified PVA were dissolved in 1.2 mL of water (25 wt. %) at 80°C. 1.5, 5, or 10% monomer and 1.0% (w/w) I2959 were added and stirring was continued for 10 minutes. Monomers used to promote photopolymerization were N-vinylpyrrolidone (NVP), hydroxyethyl acrylate (HEA), N,N-dimethylacrylamide (DMAA), and acrylic acid (AA). The solution was transferred to a Teflon mold (disc, 15mm diameter, 1.0mm thick), covered with a glass slide, and photopolymerized using a Blak-Ray B-100A longwave UV lamp for ≤ 5 minutes. A representation of the photopolymerization process is shown in Figure 11. Hydrogel samples were immersed in Hank's solution and allowed to swell at room temperature for 48 hours. Water content of the polymer solution prior to photopolymerization, as well as the water content of the gels following equilibration, was assessed via TGA.

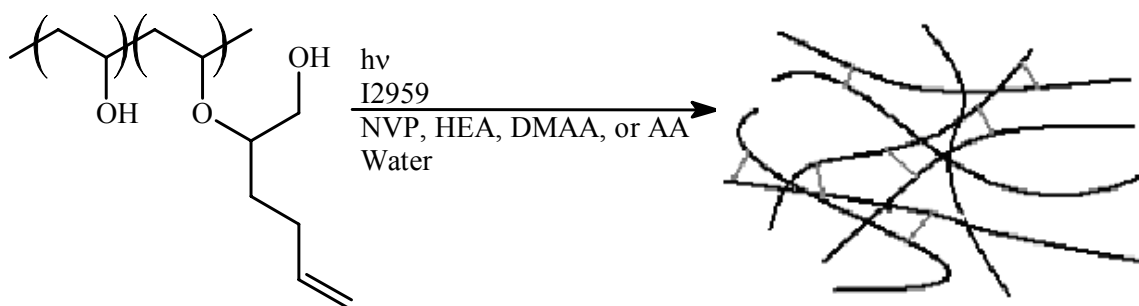


Figure 11. Photopolymerization of 1,2-epoxy-5-hexene modified PVA in the presence of N-vinylpyrrolidone (NVP), hydroxyethyl acrylate (HEA), N,N-dimethylacrylamide (DMAA), or acrylic acid (AA).

Hydrogel NMR

1,2-Epoxy-5-hexene modified PVA in D₂O was photopolymerized in the presence of acrylic acid within a 10mm NMR tube and spectra were obtained directly on the hydrogel. Resolution of the ¹H NMR spectra was not possible. Hydrogel formation was confirmed through ¹³C NMR (see Appendix A). The significance of hydrogel formation from 1,2-epoxy-5-hexene modified PVA will be discussed further in the following two chapters.

Cytotoxicity Studies

Cytotoxicity of hydrogels prepared via photopolymerization of 1,2-epoxy-5-hexene modified PVA in the presence of acrylic acid was evaluated according to ISO standards through direct contact assays and elution tests.⁵⁷ All experiments were performed in triplicate. Before either test was administered, cells were passaged into 24 well plates and grown until a monolayer was achieved. Hydrogels prepared via photopolymerization of glycidyl methacrylate modified PVA were used as controls. Samples were purified by

extraction of lower molecular weight impurities with ethanol, followed by phosphate buffer pH 7.4. Hydrogel plugs with 6 mm diameters were obtained through the use of a biopsy punch.

To perform the direct contact assays, hydrogels were placed on top of the cell monolayers and covered with media. Following 24 hours of incubation, the impact of the gels upon cells directly beneath and surrounding the samples was observed using an inverted microscope (Leica Microsystems, Inc. Wetzlar, Germany) with Image-Pro Plus software (Media Cybernetics, Inc. Salt Springs, MD).

For elution tests, hydrogels were incubated in media under a 5% CO₂ atmosphere at 37°C for 72 hours. The media for cultured-cell monolayers was replaced with fluid extracts from the media surrounding the experimental and control materials. After incubation at 37°C in 5% CO₂ atmosphere for 24 hours, the cells were microscopically examined for changes in size, appearance, and configuration.

Determination of Photopolymerization Time

To ensure that hydrogel formation was complete, a device was constructed with the assistance of Nick Wannamacher, as depicted below in Figure 12, that allowed for the measurement of rheological properties while the polymer solution was exposed to UV radiation and polymerization occurred. The bottom plate was replaced by a piece of glass that did not absorb light of the wavelength necessary to initiate polymerization. The UV lamp was shone upon a mirror located at a 45° angle to the glass plate, and the light was reflected onto the polymer solution. The photopolymerization time was determined by

measuring the change in the storage modulus, G' , with time at a frequency of 10 Hz.

Crosslinking was complete when no further variation in G' was observed.



Figure 12. Device used for determination of photopolymerization time. The bottom plate was replaced by a glass plate with a mirror attached at a 45° angle underneath.

Rheological Testing

The mechanical behavior of the hydrogels, in addition to the sheep nucleus pulposi, was assessed under dynamic torsional shear with a Bohlin controlled stress rheometer (Bohlin Rheometer CS, Malvern Instruments, Inc., Southborough, MA) in parallel plate configuration. A compressive strain of approximately 10% was applied prior to analysis to ensure contact and prevent slip. A sinusoidal angular displacement (θ) was applied to each sample, and dynamic frequency sweep experiments were performed with a shear strain amplitude $\gamma = 0.05$ rad over the range $0.1 \leq f \leq 10$ Hz ($0.628 \leq \omega \leq 62.8$ rad/s). Shear strain was related to the angular displacement by $\gamma = \theta \cdot r/h$, where r and h refer to the sample radius and thickness respectively, while shear stress (σ) was calculated from

the measured torque (T) through $\sigma = T \cdot r / J$, where J is the polar moment of inertia ($J = \pi \cdot r^4 / 2$). The storage (elastic) and loss (viscous) moduli, G' and G'' respectively, were determined as functions of frequency. The latter properties were more conveniently expressed as the magnitude of the complex shear modulus, $|G^*|$, and the phase shift angle, δ .

$$|G^*| = \sqrt{G'^2 + G''^2} \quad \tan \delta = \left(\frac{G''}{G'} \right)$$

$|G^*|$ provides a measure of stiffness under dynamic conditions, while δ is an indicator of internal dissipation. For purely elastic solids, the stress is in phase with the strain, i.e. $\delta = 0$, while for ideally viscous fluids, the stress is 90° out of phase with the strain, i.e. $\delta = 90$. A material with $\delta < 45^\circ$, or $0 < \tan \delta < 1$, is usually described as exhibiting more “solid-like” behavior.¹⁹ Table 3 is provided below for conversion between $\tan \delta$ and δ .

Table 3. Conversion between δ and $\tan \delta$

δ	$\tan \delta$
0	0
15	0.267
30	0.577
45	1
60	1.732
75	3.732
89	57.28996

Network Characterization

Network characteristics were related to rheological behavior through the equilibrium modulus, G_e , or the plateau value of the storage modulus, G' . Over the range of frequencies examined, G' was relatively constant; therefore, an average G' value from

0.1 Hz, 1 Hz, and 10 Hz was used to represent G_e . The molecular weight between crosslinks, M_e , was calculated as⁸⁰

$$M_e = \left(\frac{c}{\rho} \right)^2 \left(\frac{\rho RT}{G'} \right)$$

where c is the concentration (g/mL) and ρ is the density (g/cm³). From M_e , the number of junction points per molecule, E , and the crosslink density, ν , were determined.⁸⁰

$$E = \frac{M}{M_e} - 1 \quad \nu = \frac{c}{M_e}$$

M , the polymer molecular weight, was estimated from the known molecular weight of poly(vinyl alcohol) and a percentage of modification with glycidyl methacrylate or 1,2-epoxy-5-hexene of 20% based upon (¹H) NMR.

In order to evaluate the impact of entanglements upon the crosslink density and other network properties, the critical concentration, c^* , at which overlap of macromolecular chains begins, was approximated from the intrinsic viscosity, $[\eta]$.⁸⁰

$$c^* = \frac{0.77}{[\eta]}$$

$[\eta]$ was determined using the known Mark-Houwink-Sakurada equation for the relationship between poly(vinyl alcohol) molecular weight and intrinsic viscosity.⁸¹

$$[\eta] = 66.6 \times 10^{-5} M^{0.64}$$

Dynamic Compression Testing

Dynamic compression tests were performed on hydrogel discs ($d = 15\text{mm}$, $t = 1\text{mm}$) with a Rheometrics Solids Analyzer RSA II (Rheometrics, Inc., Piscataway, NJ) in parallel plate configuration. Logarithmic frequency sweeps were run from 0.1 to 100

rad/s at a strain of 0.1% and a temperature of 25°C. Samples were subjected to a preload of 0.196 N and a preconditioning of 1 cycle. A static force 10% greater than the previously measured dynamic force was set to ensure that loss of contact with the sample did not occur. The complex compressive dynamic modulus, $|K^*|$, and the phase shift angle, δ , were determined from the resultant data as functions of frequency and were used as general measures of stiffness and as gauges of internal energy dissipation respectively.

Degradation Studies

A series of hydrogel discs were submerged in Hank's solution in separate Petri dishes at room temperature. At regular intervals, one of the specimens was removed and the rheological behavior was evaluated as described above. Separate hydrogel samples were maintained such that the results were not impacted by repeated stress application.

Statistical Analysis

Statistical analysis of the network characterization data was performed using one-way ANOVA followed by post-hoc least significant difference (LSD) tests with a significance level of $p < 0.05$. All values are reported as averages with 90% confidence intervals derived from Student's t-distribution ($n = 3-7$). Similarly, unless otherwise noted, all graphical data points are shown as means with error bars that represent 90% confidence limits.

RESULTS



“In the last seven years, I’ve had four months that I felt good. And in those four months I won two Tours de France and the world championships. But in the rest of those years I’ve just been struggling.”

-Greg LeMond

Rheological Characterization of Glycidyl Methacrylate-PVA Hydrogels

As shown in Figure 13, the complex shear moduli of photopolymerized hydrogels were directly proportional to the molecular weight of PVA that was modified with glycidyl methacrylate over all frequencies. In contrast, the phase shift angles were independent of PVA molecular weight. The latter results can also be viewed in Table 4 where the viscoelastic parameters, G' , G'' , $|G^*|$, and $\tan \delta$, are given as functions of molecular weight at a frequency of 10 rad/s. $|G^*|$, G' , and G'' rose with increasing molecular weight and, consequently, $\tan \delta$ remained relatively constant. Following the graphical results, calculations from rubber elasticity theory showed a decrease in molecular weight between crosslinks (17.6-5.59 kPa) with a corresponding increase in

crosslink density (8.25-27.7 mol/cm³) and, consequently, the number of junction points per molecule (0.707-44.6) with increasing molecular weight (Table 6). Statistically significant differences (LSD, $p < 0.05$) were seen between all groups, with the exception of hydrogels generated from 31-50k PVA. The network characteristics of the latter showed some overlap with hydrogels generated from adjacent molecular weight ranges (13-23k and 50-85k).

The complex shear moduli of the hydrogels could be varied in a manner similar to that due to molecular weight by altering the polymer concentration prior to photopolymerization. As illustrated in Figure 14(a), higher polymer concentrations gave rise to larger complex moduli. The phase shift angles were relatively constant among concentration ranges [Figure 14(b)]. The graphical results are reinforced by Table 5, which shows that G' , G'' , and $|G^*|$ were directly proportional to the initial polymer concentration at 10 rad/s, while $\tan \delta$ was independent. Rubber elasticity theory showed a decrease in molecular weight between crosslinks (32.9-10.2 kPa), as well as an increase in both crosslink density (2.13-23.8 mol/cm³) and the number of junction points per molecule (2.60-9.50), with increasing polymer concentration (Table 7). Statistically significant differences in the crosslink density were obtained between all concentration ranges; however, the values obtained for M_e and the number of junction points per molecule showed some overlap between groups.

$|G^*|$ for the sheep nucleus pulposi ranged from 7-11 kPa over the series of frequencies examined. Hydrogels with complex shear moduli that approached the latter values could be obtained through both the modulation of the PVA molecular weight and

the polymer concentration prior to photopolymerization. The complex shear moduli of hydrogels generated from PVA of $M_w = 85\text{-}124\text{k}$ or $M_w = 124\text{-}186\text{k}$ at 25% initial polymer concentration and PVA of $M_w = 50\text{-}85\text{k}$ at 35% initial polymer concentration were comparable to those of the sheep nucleus pulposi. The phase shift angles of all hydrogels were significantly different than those obtained for the natural tissue. δ of the sheep nucleus pulposi decreased from 26 to 18 degrees with increasing frequency, while δ of the hydrogels were between 5 and 11 degrees and showed no frequency dependence.

The estimated critical concentration at which polymer entanglement begins to occur was less than the concentration of hydrogel precursor in solution prior to photocrosslinking for all molecular weights of PVA (Table 8). c^* ranged from 0.022 for PVA of $M_w = 13\text{-}23\text{k}$ to 0.0055 for PVA of $M_w = 124\text{-}186\text{k}$.

Figures 13 and 14 are presented as the storage modulus, G' , and the loss modulus, G'' , rather than $|G^*|$ and δ , in Appendix B (Figures B1 & B2). .

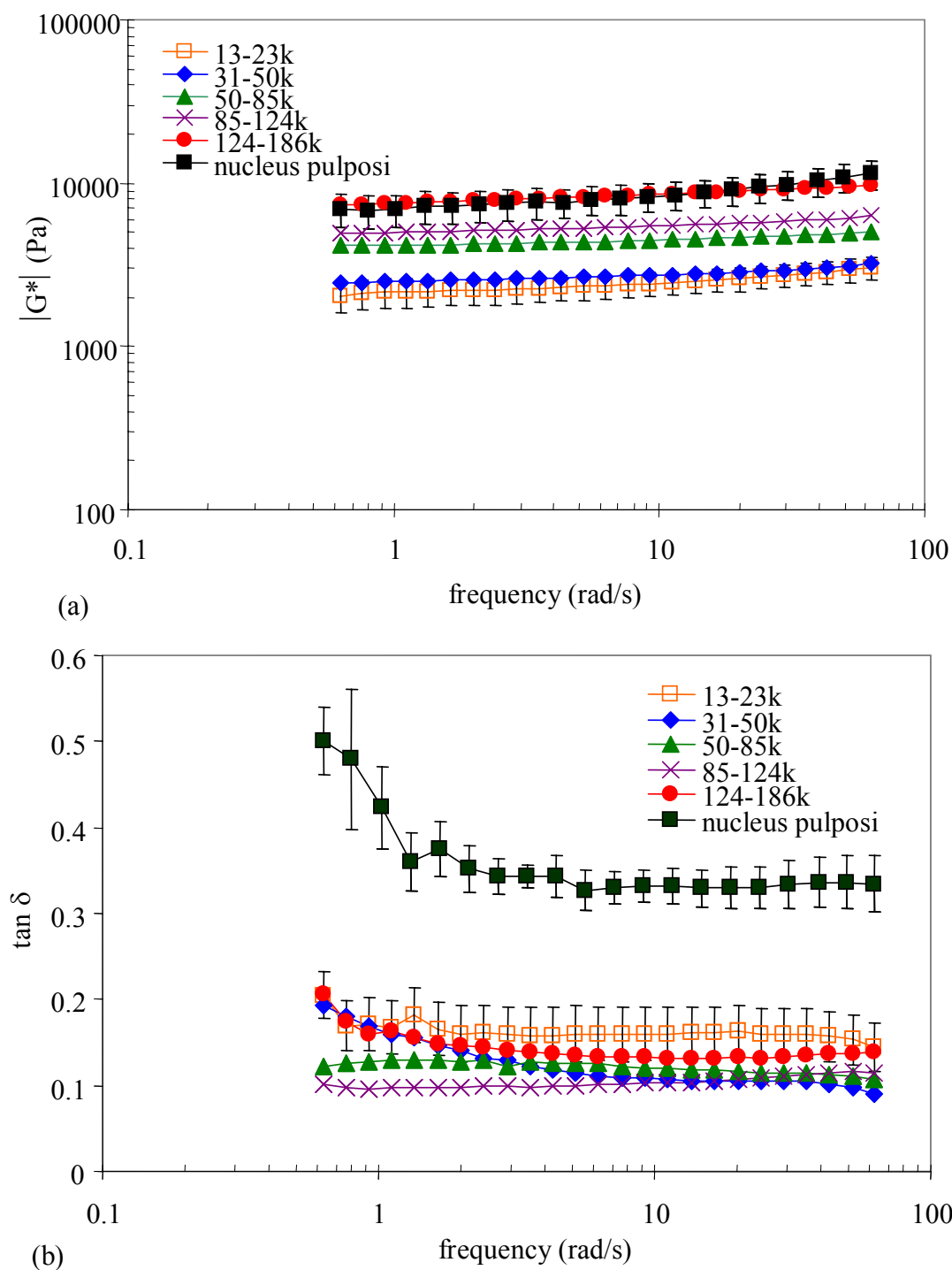


Figure 13. Variation in complex shear moduli (a) and phase shift angles (b) of glycidyl methacrylate-PVA hydrogels with molecular weight of PVA. For visual clarity, only representative sets of error bars are shown for data obtained from the hydrogels.

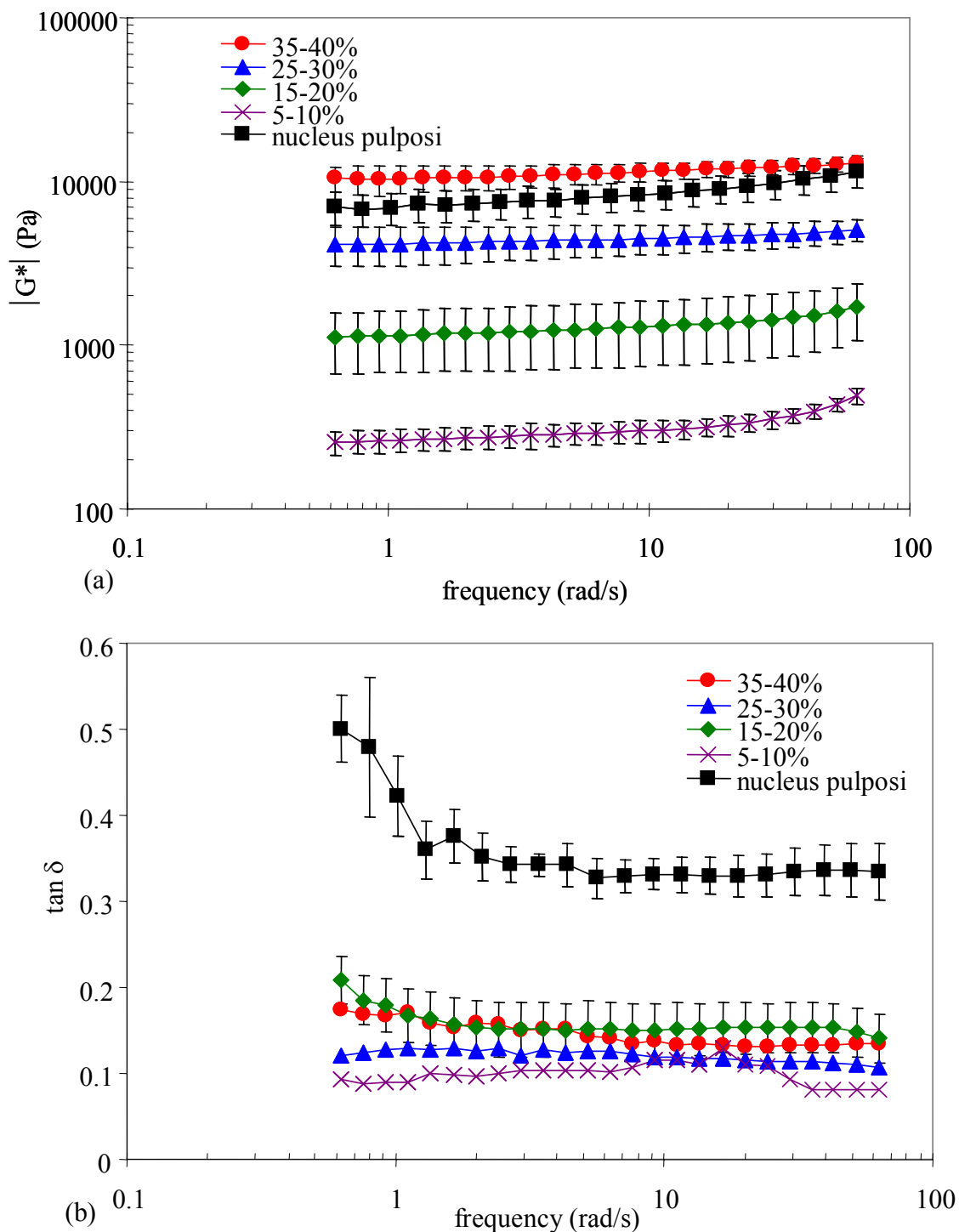


Figure 14. Variation in complex shear moduli (a) and phase shift angles (b) of glycidyl methacrylate-PVA hydrogels with initial weight percent of polymer. For visual clarity, only a representative set of error bars was shown for phase shift angles (b) of the hydrogels.⁹

Table 4. Variation in viscoelastic parameters of glycidyl methacrylate-PVA hydrogels with molecular weight of PVA at 10 rad/s (1.6 Hz)

M _w of PVA (kg/mol)	G' (Pa)	G'' (Pa)	G* (Pa)	tan δ	δ (°)
13-23	2380 ± 560	480 ± 600	2430 ± 600	0.200 ± 0.150	11.31 ± 8.55
31-50	2330 ± 370	230 ± 60	2340 ± 370	0.100 ± 0.040	5.73 ± 2.32
50-85	4450 ± 930	490 ± 290	4470 ± 960	0.111 ± 0.089	6.33 ± 5.07
85-124	5450 ± 400	550 ± 170	5480 ± 420	0.101 ± 0.038	5.79 ± 2.18
124-186	8480 ± 270	1110 ± 280	8550 ± 300	0.131 ± 0.037	7.46 ± 2.11
Nucleus Pulposi	7920 ± 1550	2669 ± 580	8350 ± 1660	0.336 ± 0.139	18.56 ± 7.94

The above experiments were performed at an initial polymer concentration of 25-30%.

Table 5. Variation in viscoelastic parameters of glycidyl methacrylate-PVA hydrogels with initial concentration of polymer at 10 rad/s (1.6 Hz)

Initial Concentration (wt. %)	G' (Pa)	G'' (Pa)	G* (Pa)	tan δ	δ (°)
5-10%	230 ±	30 ± 10	240 ± 50	0.110 ± 0.055	6.27 ± 3.12
15-20%	2890 ± 290	510 ± 230	2930 ± 1120	0.176 ± 0.146	10.01 ± 8.33
25-30%	4450 ± 930	490 ± 290	4470 ± 960	0.111 ± 0.089	6.33 ± 5.07
35-40%	11400 ± 1600	1470 ± 1110	11500 ± 1700	0.129 ± 0.115	7.35 ± 6.58
Nucleus Pulposi	7920 ± 1550	2669 ± 580	8350 ± 1660	0.336 ± 0.139	18.56 ± 7.94

The above experiments were performed with PVA of M_w = 50-85k.

Table 6. Variation in crosslink density with molecular weight of PVA for glycidyl methacrylate-PVA hydrogels as calculated from rubber elasticity theory

M_w of PVA (kg/mol)	Water Content (wt. %)	M_e (kg/mol)	Junction points/ molecule	ν (mol/cm ³)
13-23	87.4 ± 0.1	17.6 ± 2.7	0.707 ± 0.258	8.25 ± 1.05
31-50	88.3 ± 2.2	16.9 ± 7.4	3.89 ± 1.75	9.09 ± 2.38
50-85	86.2 ± 1.7	12.8 ± 2.8	8.33 ± 1.73	13.3 ± 2.0
85-124	86.0 ± 2.8	10.1 ± 2.3	17.1 ± 2.4	17.6 ± 4.7
124-186	86.6 ± 0.3	5.59 ± 0.15	44.6 ± 0.9	27.7 ± 1.3

The above experiments were performed at an initial polymer concentration of 25-30%.

Table 7. Variation in crosslink density with initial concentration of polymer for glycidyl methacrylate-PVA hydrogels as calculated from rubber elasticity theory

Initial Concentration (wt. %)	Water Content (wt. %)	M_e (kg/mol)	Junction points/ molecule	ν (mol/cm ³)
35-40	80.6 ± 1.1	10.2 ± 1.5	9.50 ± 2.02	23.8 ± 3.4
25-30	86.2 ± 1.7	13.0 ± 2.8	8.33 ± 1.73	13.3 ± 2.0
15-20	88.2 ± 2.1	14.0 ± 6.3	8.21 ± 5.06	10.7 ± 4.6
5-10	93.8 ± 0.3	32.9 ± 6.5	2.60 ± 0.66	2.13 ± 0.39

The above experiments were performed with PVA of $M_w = 50-85k$.

Table 8. Comparison between initial concentrations prior to photopolymerization and critical concentrations of entanglement for poly(vinyl alcohol)

M _w of PVA	Initial Concentration (wt. %)	Initial Concentration (g/mL)	[η] (dL/g)	c* (g/mL)
50-85	35-40	0.54-0.67	0.821	0.0094
50-85	25-30	0.33-0.43	0.821	0.0094
50-85	15-20	0.18-0.25	0.821	0.0094
50-85	5-10	0.056-0.11	0.821	0.0094
13-23	25-30	0.33	0.352	0.022
31-50	25-30	0.33	0.592	0.013
85-124	25-30	0.33	1.09	0.0071
124-186	25-30	0.33	1.40	0.0055

Determination of Photopolymerization Time

Photopolymerization time was initially estimated to be ≤ 5 minutes based upon visual observation. As shown in figure 15, the estimated photopolymerization time was confirmed by rheological studies that measured the storage modulus, G' , as a function of time at a frequency of 10 Hz upon exposure of glycidyl methacrylate modified PVA to UV light. For initial polymer concentrations of 10-15% and 20-25%, no further change in the rheological properties occurred after 4-5 minutes, indicating that crosslinking was complete. The photopolymerization time was assumed to be similar for all other polymerization conditions.

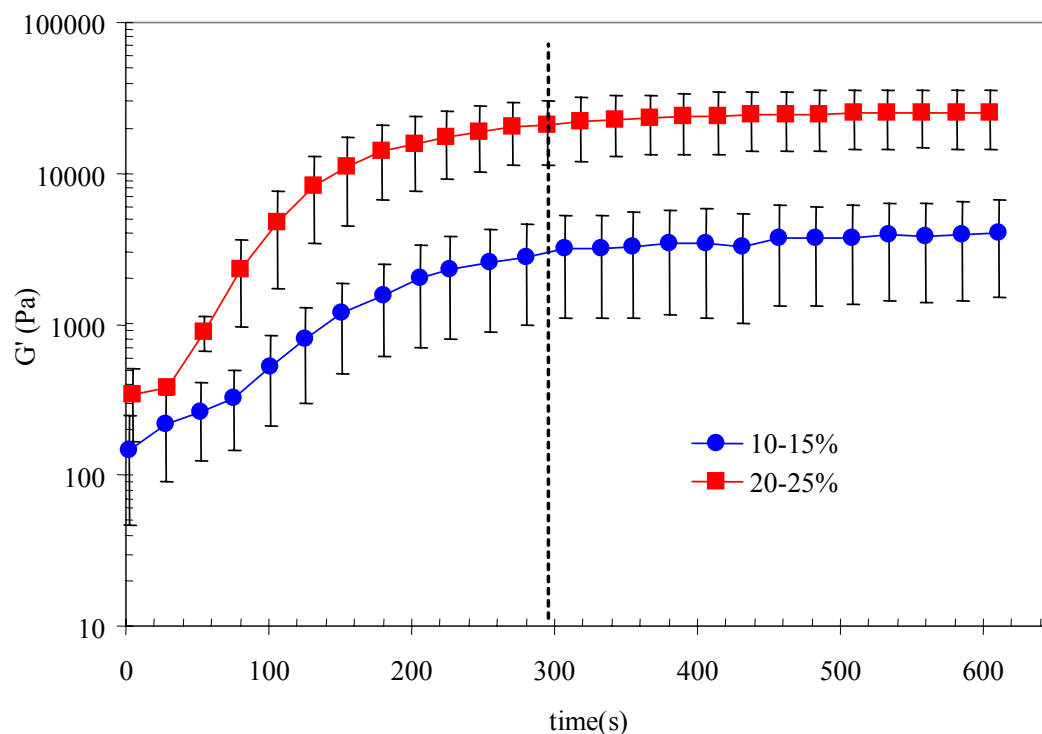


Figure 15. Variation in storage modulus, G' , with time upon exposure of a solution of glycidyl methacrylate modified PVA to UV light for two different initial concentrations of polymer. A dashed line was used to highlight the previously estimated photopolymerization time.

Rheological Characterization of 1,2-Epoxy-5-hexene-PVA Hydrogels

As shown in Figure 16(a), the complex shear moduli of hydrogels generated from 1,2-epoxy-5-hexene modified PVA could be varied by altering the type of monomer used to induce photocrosslinking. In contrast, the phase shift angles were not impacted by changes in the monomer [Figure 16(b)]. Table 9 further shows that G' , G'' , and $|G^*|$ could all be varied through the use of different monomers, while $\tan \delta$ remained unaffected. Calculations from rubber elasticity theory demonstrated that the hydrogels possessed a wide range of network characteristics (Table 12). Molecular weight between crosslinks varied from 8.0 kg/mol for dimethylacrylamide (DMAA) to 36.0

kg/mol for hydroxyethyl acrylate (HEA), crosslink density spanned values of 1.58 mol/cm³ for HEA to 15.2 mol/cm³ for acrylic acid (AA), and the number of junction points per molecule ranged from 3.32 for HEA to 17.9 for DMAA. The crosslink density of hydrogels generated in the presence of AA was significantly greater than that found for all other monomers (LSD, $p < 0.05$). The values obtained for M_e and the number of junction points per molecule showed overlap between groups.

To some extent, the complex shear moduli could be controlled by altering the weight percent of monomer incorporated into the solution prior to photopolymerization. 10% HEA gave higher values of $|G^*|$ at all frequencies than those observed for 1.5% and 5% [Figure 17(a), Table 10]. However, none of the network characteristics determined from rubber elasticity theory were significantly different between groups (Table 13). The phase shift angles were similar for all percentages of HEA [Figure 17(b), Table 10]. Using AA as the monomer, the complex shear moduli increased as the concentration was raised from 1.5% to 10% [Figure 18(a), Table 11]. Rubber elasticity theory showed a corresponding increase in crosslink density (10.8-34.6 mol/cm³). Additionally, the molecular weight between crosslinks of hydrogels prepared with 10% AA (4.99 kg/mol) was significantly less than those generated with 1.5% and 5% AA, while the number of junction points per molecule was significantly greater (30.4) (Table 14). The phase shift angles did not show a dependence upon AA concentration [Figure 18(b), Table 11].

Complex shear moduli that approached the values obtained for sheep nucleus pulposi (7-11 kPa) were obtained from hydrogels prepared from photopolymerization of 1,2-epoxy-5-hexene modified PVA in the presence of 5 and 10% AA. The phase shift angles

of the hydrogels (1.4-14 degrees) were frequency independent and significantly less than those obtained for the natural tissue (18-26 degrees).

Figures 16-18 are presented as the storage modulus, G' , and the loss modulus, G'' , rather than $|G^*|$ and δ , in Appendix B (Figures B3-B5).

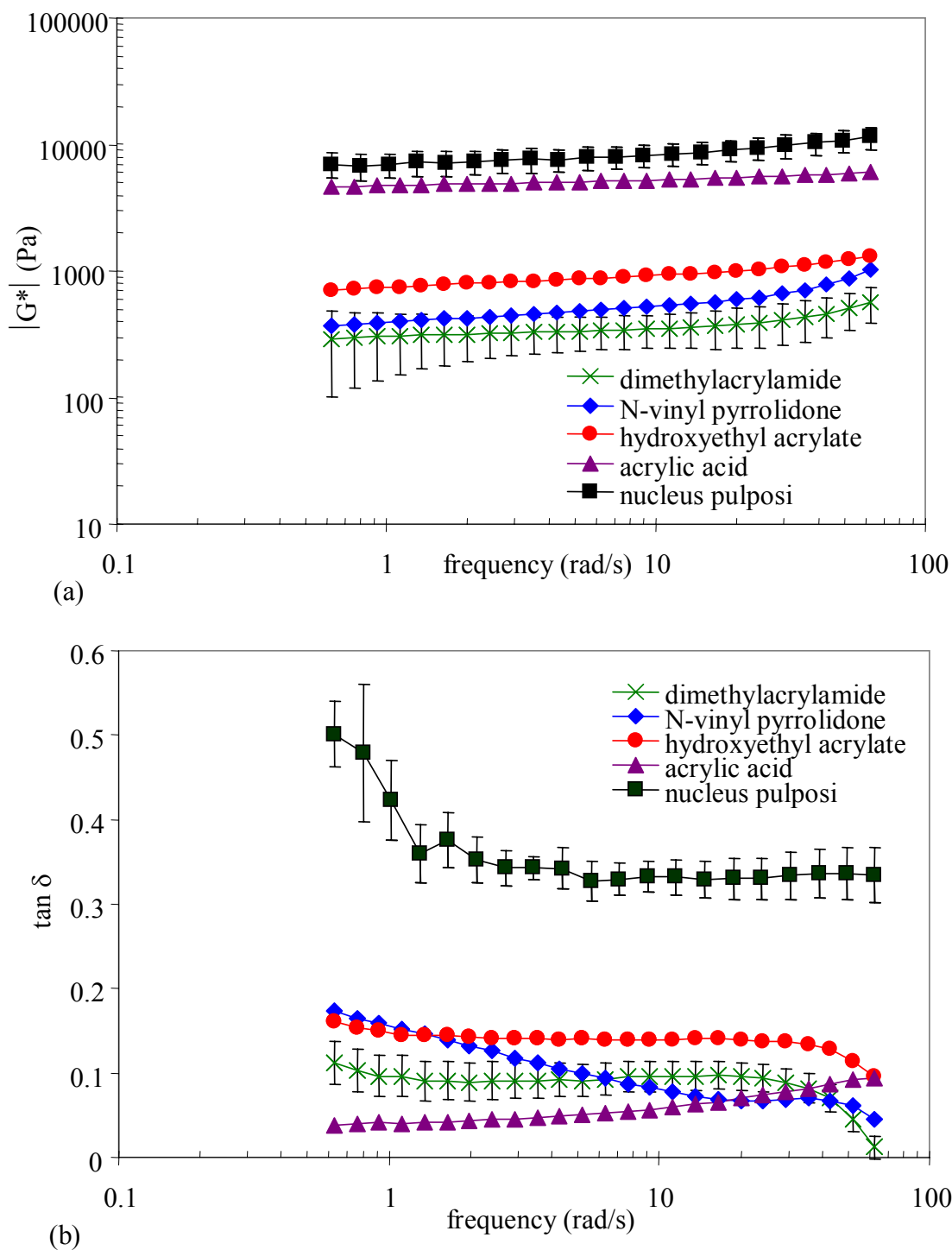


Figure 16. Variation in complex shear moduli (a) and phase shift angles (b) with monomer type for 1,2-epoxy-5-hexene-PVA hydrogels. Monomers were included at a concentration of 5 wt. %. For visual clarity, only representative sets of error bars are shown for data obtained from the hydrogels.

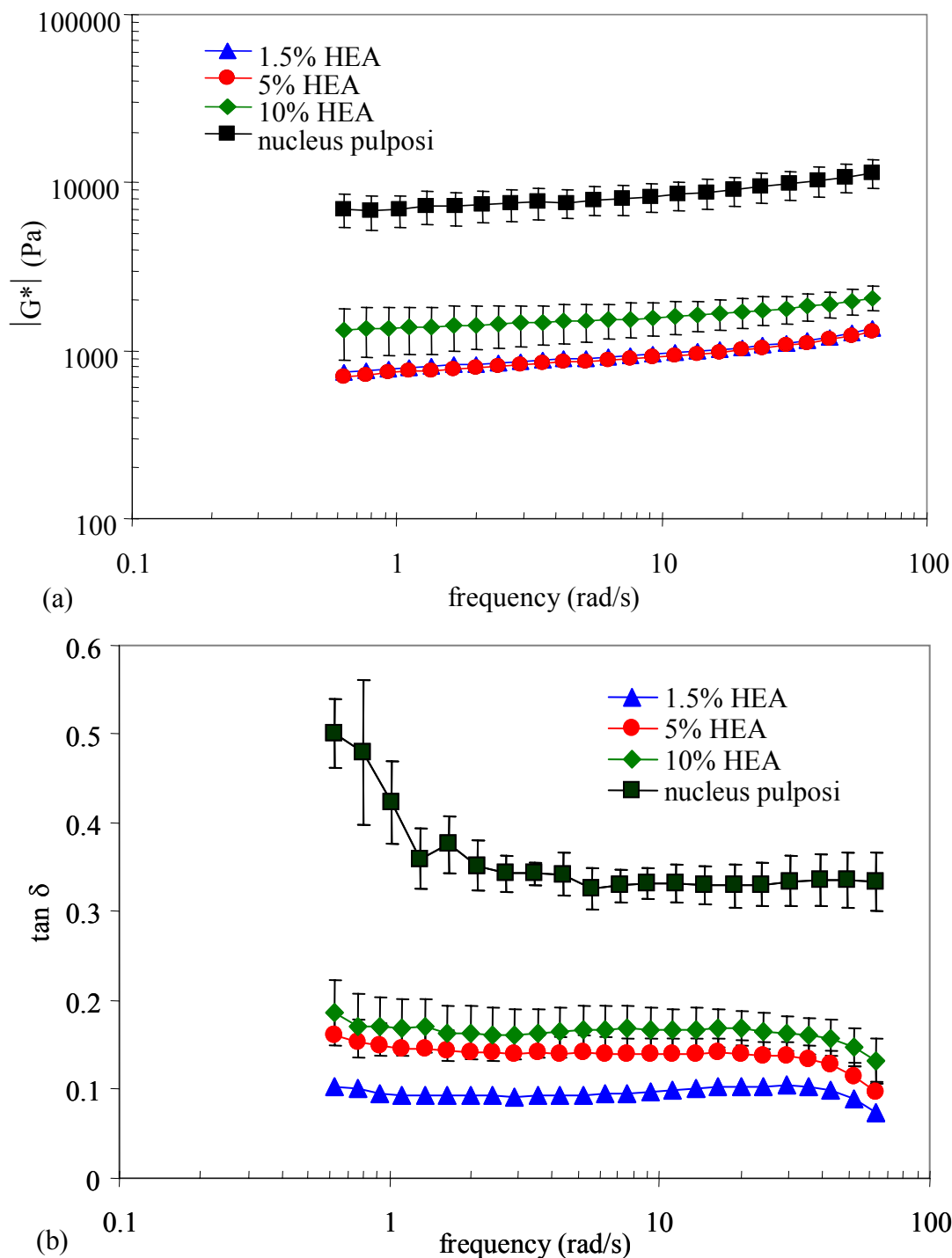


Figure 17. Variation in complex shear moduli (a) and phase shift angles (b) with percentage (w/w) of hydroxyethyl acrylate (HEA) for 1,2-epoxy-5-hexene-PVA hydrogels. For visual clarity, only representative sets of error bars are shown for data obtained from the hydrogels.

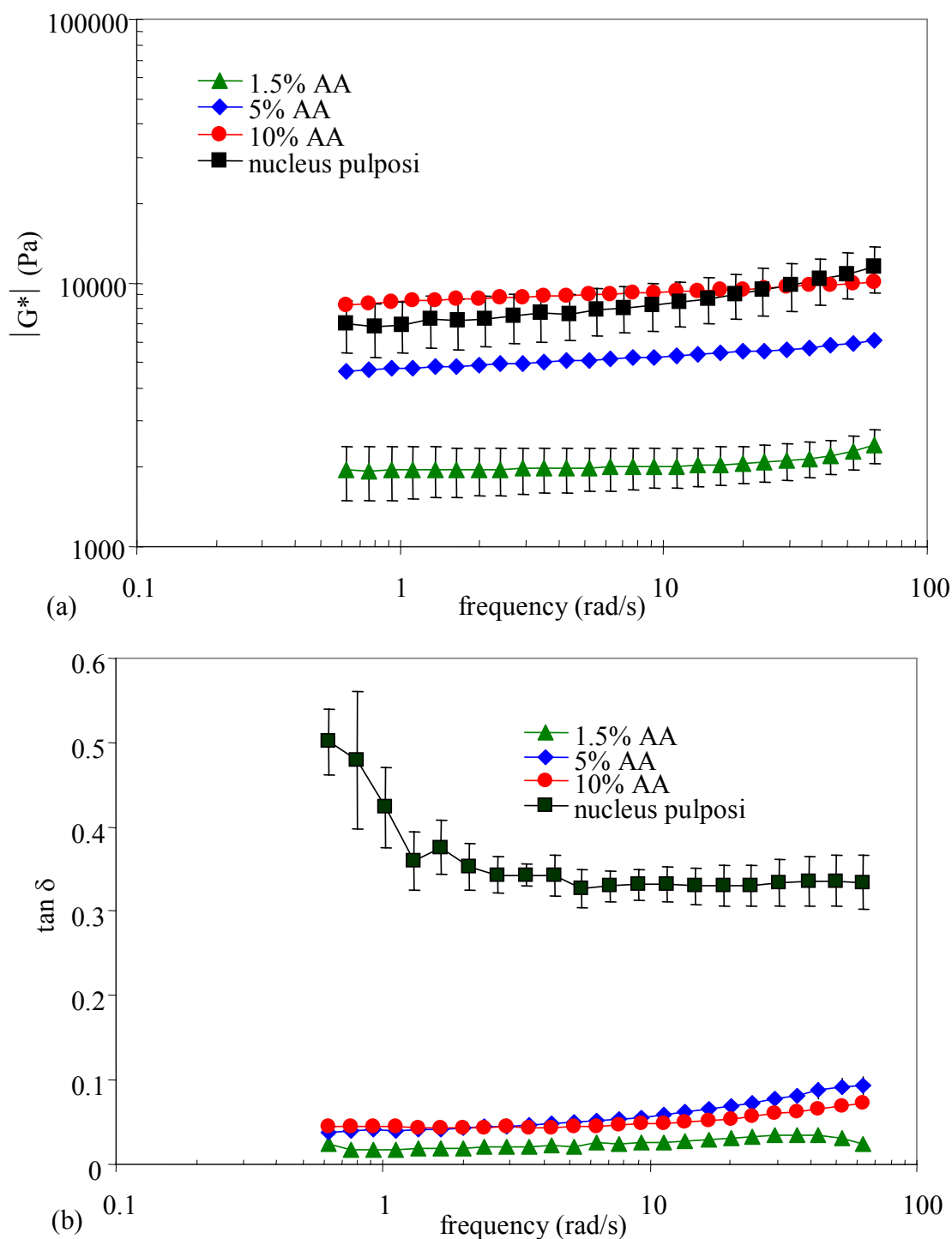


Figure 18. Variation in complex shear moduli (a) and phase shift angles (b) with percentage (w/w) of acrylic acid (AA) for 1,2-epoxy-5-hexene-PVA hydrogels. For visual clarity, only representative sets of error bars are shown for data obtained from the hydrogels.

Table 9. Variation in viscoelastic parameters of 1,2-epoxy-5-hexene-PVA hydrogels with monomer type at 10 rad/s (1.6 Hz)

Monomer	G'	G''	G*	tan δ	δ
DMAA	350	33.4	350	0.0960	5.48
NVP	520 \pm 22	110 \pm 70	30 \pm 230	0.208 \pm 0.222	11.74 \pm 12.51
HEA	920 \pm 100	130 \pm 100	930 \pm 120	0.145 \pm 0.122	8.23 \pm 6.93
AA	5260 \pm 1940	280 \pm 60	5270 \pm 1940	0.052 \pm 0.310	3.00 \pm 1.77
Nucleus Pulposi	7920 \pm 1550	2670 \pm 580	8350 \pm 1660	0.336 \pm 0.139	18.56 \pm 7.94

Monomers were included at a concentration of 5 wt. %.

Table 10. Variation in viscoelastic parameters of 1,2-epoxy-5-hexene-PVA hydrogels with percentage (w/w) of hydroxyethyl acrylate (HEA) at 10 rad/s (1.6 Hz)

HEA Concentration (wt. %)	G'	G''	G*	tan δ	δ
1.5%	960 350	90 40	960 350	0.096 0.073	5.50 4.14
5%	920 \pm 100	130 \pm 100	930 \pm 120	0.145 \pm 0.122	8.23 \pm 6.93
10%	1570 \pm 360	250 \pm 120	1590 \pm 380	0.160 \pm 0.111	9.08 \pm 6.36
Nucleus Pulposi	7920 \pm 1550	2670 \pm 580	8350 \pm 1660	0.336 \pm 0.139	18.56 \pm 7.94

Table 11. Variation in viscoelastic parameters of 1,2-epoxy-5-hexene-PVA hydrogels with percentage (w/w) of acrylic acid (AA) at 10 rad/s (1.6 Hz)

AA Concentration (wt. %)	G'	G''	G*	tan δ	δ
1.5%	2020	520	2080	0.258	14.49
5%	5260 \pm 1940	280 \pm 60	5270 \pm 1940	0.052 \pm 0.0310	3.00 \pm 1.77
10%	11100 \pm 2000	560 \pm 130	11100 \pm 2000	0.051 \pm 0.0212	2.91 \pm 1.22
Nucleus Pulposi	7920 \pm 1550	2670 \pm 580	8350 \pm 1660	0.336 \pm 0.139	18.56 \pm 7.94

Table 12. Variation in crosslink density with type of monomer added to initiate photopolymerization of 1,2-epoxy-5-hexene modified PVA

Monomer	Water Content (wt. %)	M_e (kg/mol)	Junction points/ molecule	v (mol/cm ³)
DMAA	96.3	8.0	17.9	4.83
NVP	93.0 \pm 0.6	17.7 \pm 4.2	7.81 \pm 1.93	4.55 \pm 0.46
HEA	88.8 \pm 1.2	36.0 \pm 8.1	3.32 \pm 1.05	3.58 \pm 0.71
AA	85.3 \pm 9.4	11.4 \pm 8.4	13.0 \pm 10.1	15.2 \pm 0.4

Monomers were included at a concentration of 5 wt. %.

Table 13. Variation in crosslink density with percentage of hydroxyethyl acrylate (HEA) added to initiate photopolymerization of 1,2-epoxy-5-hexene modified PVA

HEA Concentration (wt. %)	Water Content (wt. %)	M_e (kg/mol)	Junction points/ molecule	v (mol/cm ³)
1.5%	91.5 \pm 1.3	23.0 \pm 4.8	5.71 \pm 1.26	4.11 \pm 0.81
5%	88.8 \pm 1.2	36.0 \pm 8.1	3.32 \pm 1.05	3.58 \pm 0.71
10%	88.0 \pm 1.7	26.0 \pm 12.9	6.54 \pm 4.13	6.03 \pm 2.55

Table 14. Variation in crosslink density with percentage of acrylic acid (AA) added to initiate photopolymerization of 1,2-epoxy-5-hexene modified PVA

AA Concentration (wt. %)	Water Content (wt. %)	M_e (kg/mol)	Junction points/ molecule	v (mol/cm ³)
1.5%	91.0	9.21	15.4	10.8
5%	85.3 \pm 9.4	11.4 \pm 8.4	13.0 \pm 10.1	15.2 \pm 0.4
10%	85.0 \pm 2.2	4.99 \pm 0.82	30.4 \pm 6.0	34.6 \pm 0.9

Cytotoxicity Studies on 1,2-Epoxy-5-hexene-PVA Hydrogels

In accord with previous studies,⁷⁷ visual examination through an inverted light microscope demonstrated that cells proliferated normally when placed in direct contact with hydrogels formed from photopolymerization of glycidyl methacrylate modified PVA for 24 hours [Figure 19(A)]. Therefore, the latter materials were used as controls for cytotoxicity evaluation of hydrogels formed from photopolymerization of PVA modified with 1,2-epoxy-5-hexene in the presence of acrylic acid. The medium in wells containing the experimental samples was yellow, indicative of a $\text{pH} \leq 6.5$.⁸² One hydrogel sample had no affect on viability and proliferation of cells relative to the control [Figure 19(B)]. Another trial showed a moderate cellular response with a zone of dead and dying cells directly underneath and surrounding the periphery of the sample [Figure 19(C)]. Dying cells were rounded-up relative to viable cells and were detached from the culture plate. A final sample elicited a severe response and only cell debris and some detached dead cells were visible [Figure 19(D)].

Cells were exposed to fluid extracts obtained from media used to submerge the hydrogel samples for 72 hours. As expected, extracts taken from media surrounding hydrogels prepared via photopolymerization of glycidyl methacrylate modified PVA elicited no cellular responses that were visible under the inverted light microscope after 24 hours [Figure 20(A)]. Consequently, the glycidyl methacrylate-PVA hydrogels were again used as control materials. All experiments performed with extracts from solutions containing hydrogels prepared via photopolymerization of 1,2-epoxy-5-hexene modified PVA showed evidence of a fungal contamination.^{82,83} Although some fibroblast cells

remained visible, the culture was dominated by filamentous hyphae that moved in and out of focus [Figure 20(B)]. The extracts obtained from the media used for submersion of the experimental samples were yellow and turbid; however, whether this change in appearance was from the presence of hydrogel derived solutes or fungal contamination is not clear.

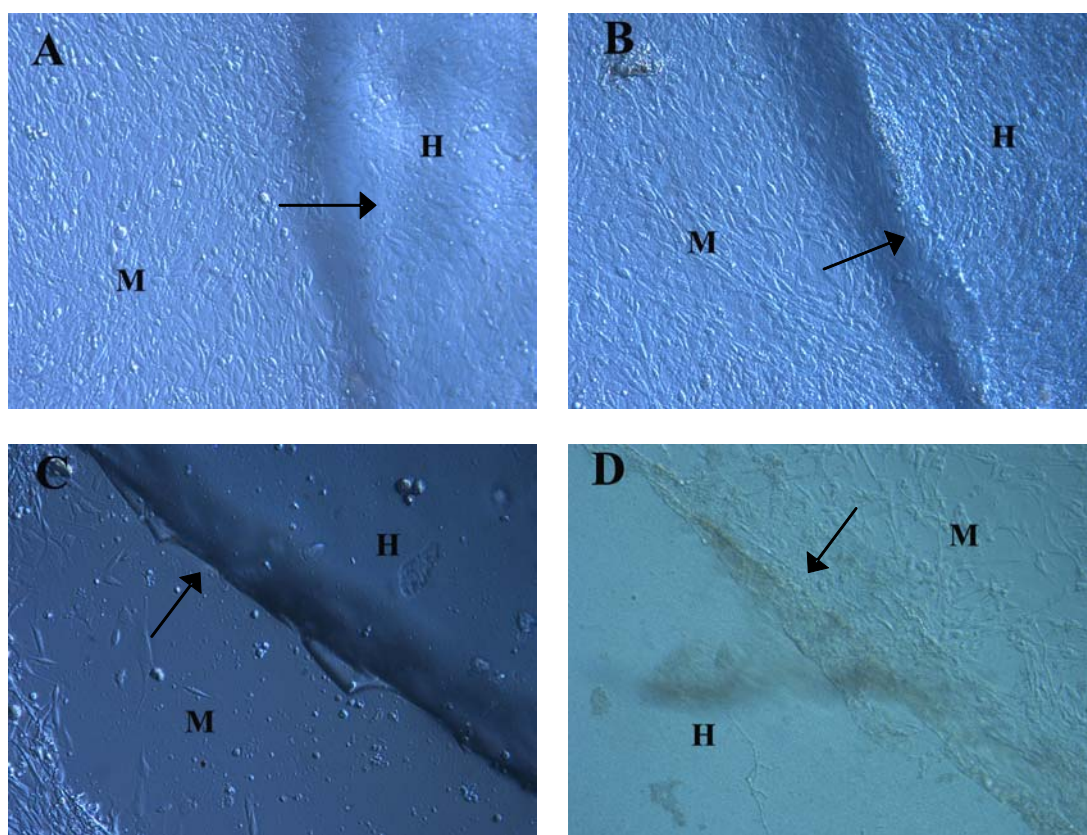


Figure 19. Light micrographs (100x) taken from an inverted light microscope showing the response of mouse fibroblasts to direct contact with hydrogels. An arrow has been used for identification of the boundary between hydrogel (H) and media (M). Hydrogels generated from photopolymerization of glycidyl methacrylate modified PVA served as the control (A). Cells directly underneath the hydrogel and in the surrounding media were unaffected. Hydrogels generated from photopolymerization of 1,2-epoxy-5-hexene modified PVA in the presence of acrylic acid gave various responses. One sample did not have any impact upon cell growth relative to the control (B), another sample showed regions of cell death (C), and a final sample showed complete cell death (D).

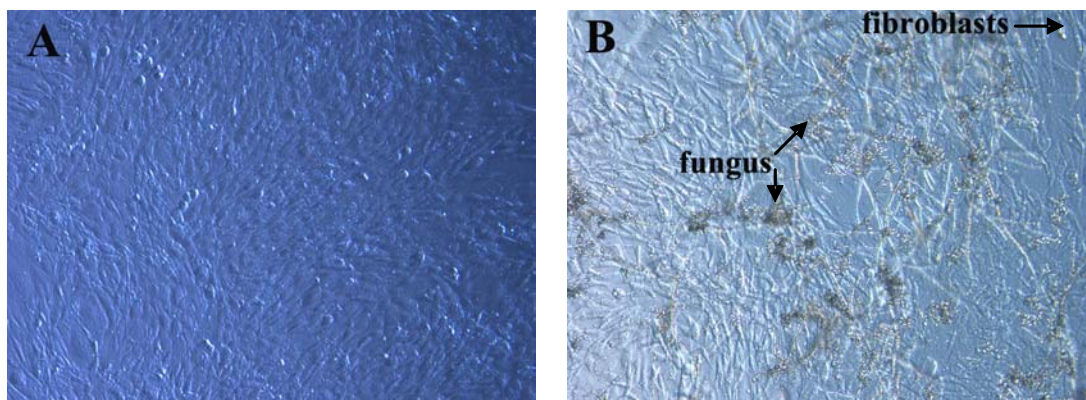


Figure 20. Representative light micrographs (100x) taken from an inverted light microscope showing the response of mouse fibroblasts to fluid extracts taken from media surrounding hydrogel samples. Extracts taken from hydrogels generated via photopolymerization of glycidyl methacrylate modified PVA served as the control (A) and the confluent monolayer was indicative of a non-cytotoxic response. Extracts obtained from 1,2-epoxy-5-hexene-PVA hydrogels led to some cell death (B); however, fungal contamination was evident and may have had a significant impact upon the results.

Dynamic Compression Testing

As shown in Figure 21, both the complex compressive dynamic moduli and phase shift angles for hydrogels obtained from glycidyl methacrylate modified poly(vinyl alcohol) were independent of the molecular weight of the PVA. Data obtained for PVA of $M_w = 50\text{-}85\text{k}$ was nonsensical and, consequently, excluded due to a problem with the starting material. $|K^*|$ ranged from 27 kPa to 76 kPa, while δ was between 11 and 23 degrees at high frequencies and 2.3 and 4.8 degrees at low frequencies. For all molecular weight ranges examined, the phase shift angle decreased as the frequency increased.

For hydrogels generated from 1,2-epoxy-5-hexene modified PVA, complex dynamic moduli obtained under compression (Figure 22) did not show the same dependence on the type of monomer added to induce photopolymerization as the equivalent parameter found in torsional shear. Hydrogels prepared with acrylic acid (AA), which possessed

the highest $|G^*|$, gave $|K^*|$ that were intermediate to those obtained with hydroxyethyl acrylate (HEA) and dimethylacrylamide (DMAA) (22 – 24 kPa). The phase shift angles for hydrogels prepared with AA decreased as the frequency increased (27 – 1.1 degrees), while δ obtained for hydrogels photopolymerized with HEA and DMAA showed no frequency dependence. Consequently, phase shift angles for hydrogels with AA were greater than those obtained for hydrogels with HEA and DMAA at low frequencies, while at high frequencies the opposite phenomenon occurred. A significant difference in the δ values found for hydrogels created with HEA and DMAA could not be identified due to the large amount of error.

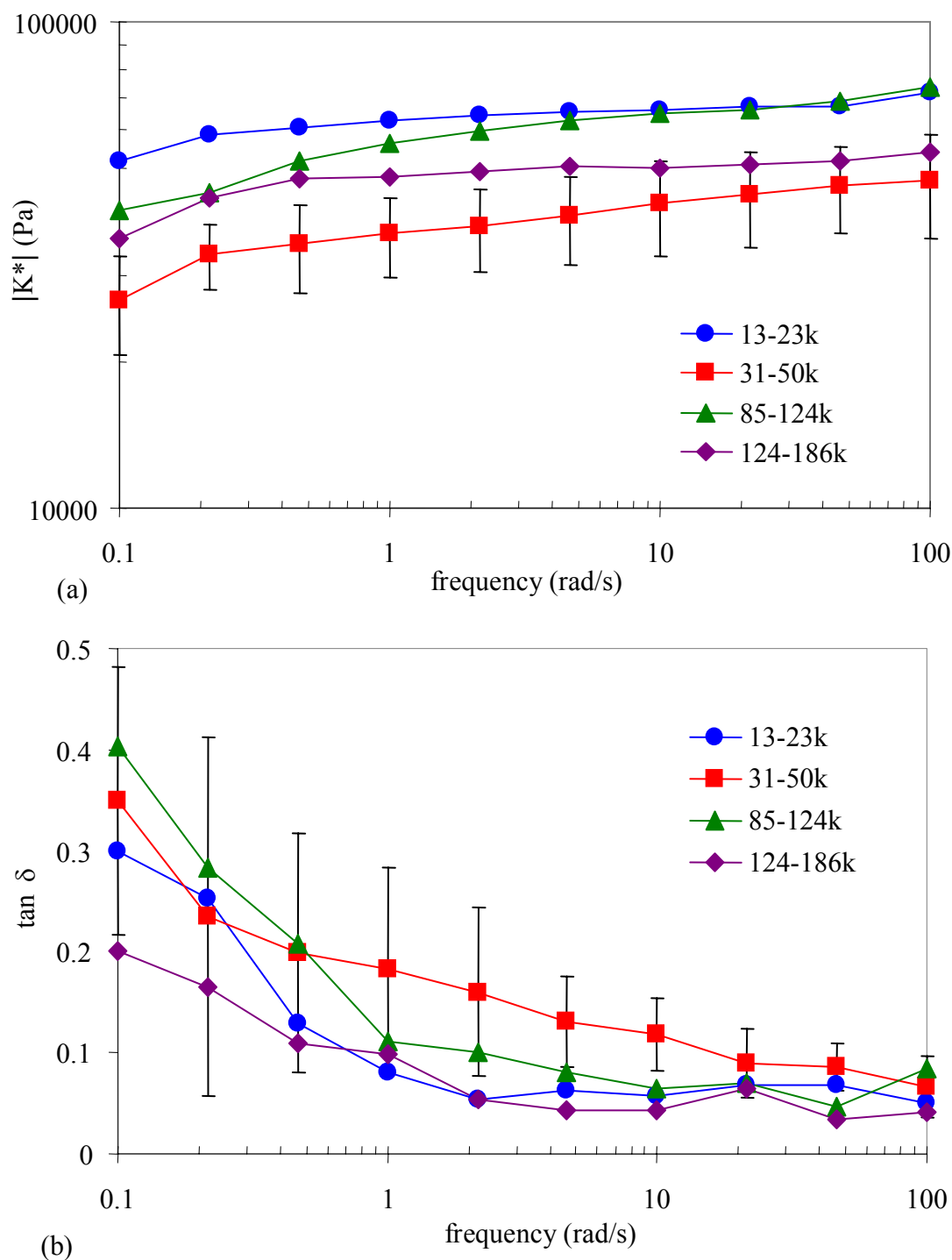


Figure 21. Variation in the complex compressive dynamic moduli (a) and phase shift angles (b) of glycidyl methacrylate-PVA hydrogels with molecular weight of PVA. The sample sets were too small to allow for statistical analysis of the data obtained for PVA of $M_w = 13\text{-}23\text{k}$, $85\text{-}124\text{k}$, and $124\text{-}186\text{k}$.

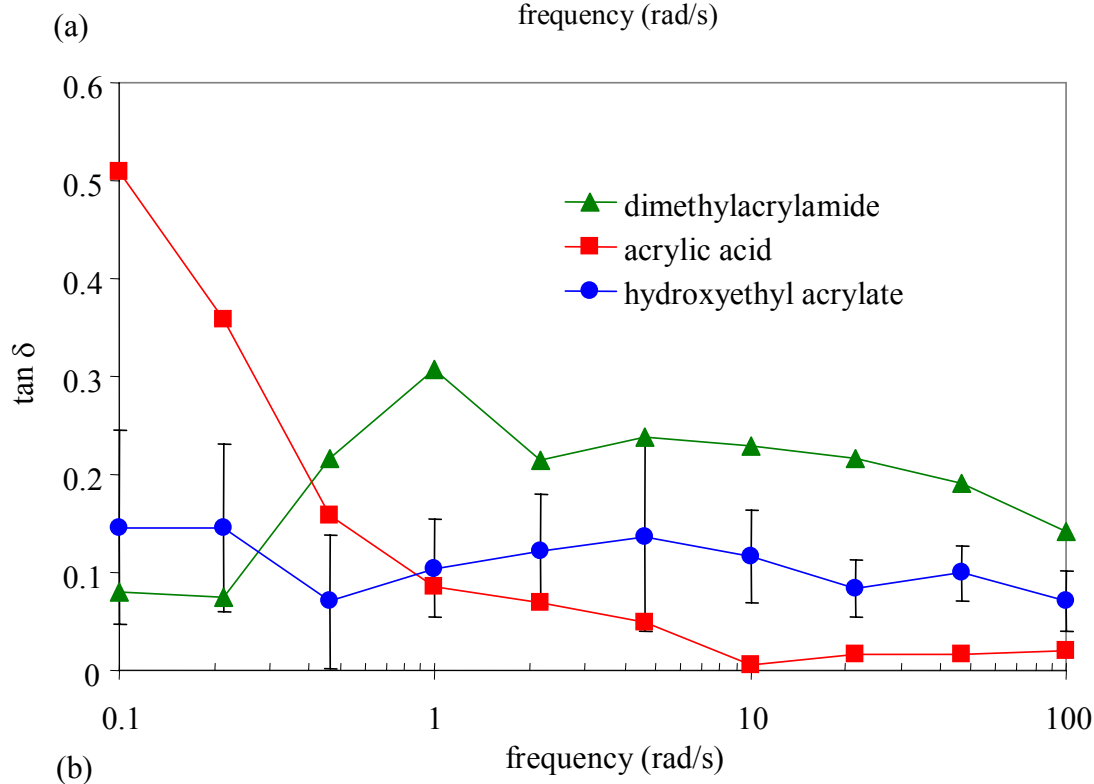
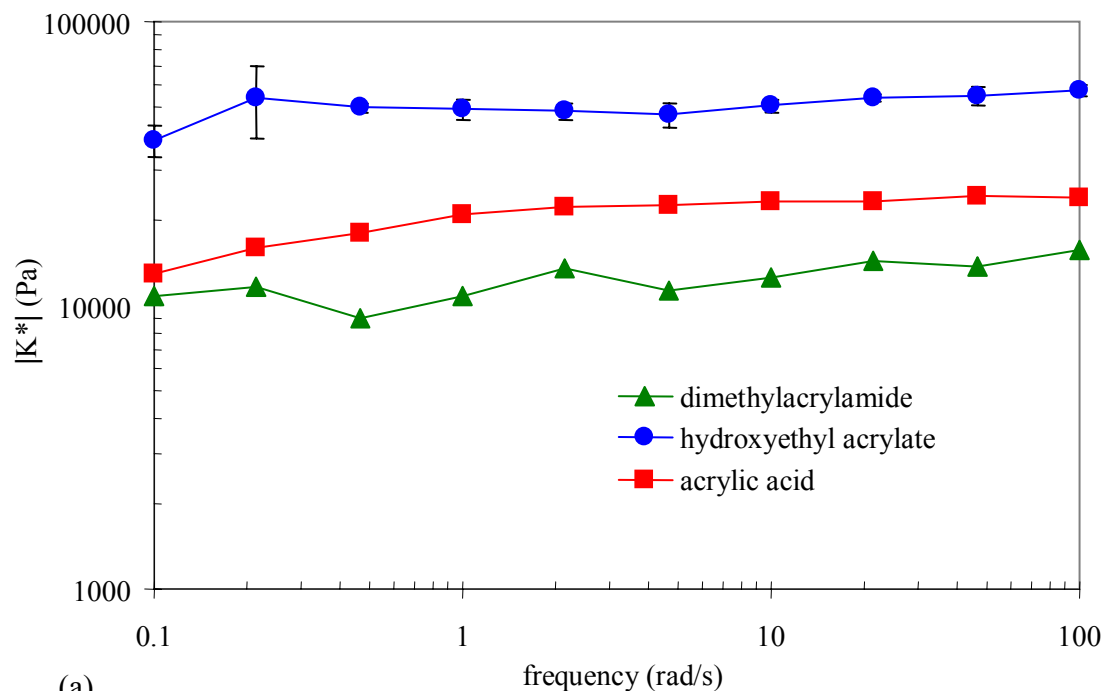


Figure 22. Variation in complex compressive dynamic moduli (a) and phase shift angles (b) with monomer type for 1,2-epoxy-5-hexene-PVA hydrogels. Monomers were included at a concentration of 5 wt. %. The sample sets were too small to allow for statistical analysis of the data obtained for dimethylacrylamide and acrylic acid.

Degradation Studies

As shown in Figure 23, no substantial change in moduli was observed for hydrogels prepared from glycidyl methacrylate modified PVA following submersion in Hank's solution, over the time frame of the experiment. During a 10 week period, $|G^*|$ remained close to 6 kPa at lower frequencies and 8 kPa at higher frequencies.

For hydrogels prepared via photopolymerization of 1,2-epoxy-5-hexene modified PVA in the presences of 1.5 wt.% hydroxyethyl acrylate, the moduli did not differ significantly over a 12 week period (Figure 24). $|G^*|$ ranged from 1.3 kPa to 1.9 kPa over the series of frequencies tested.

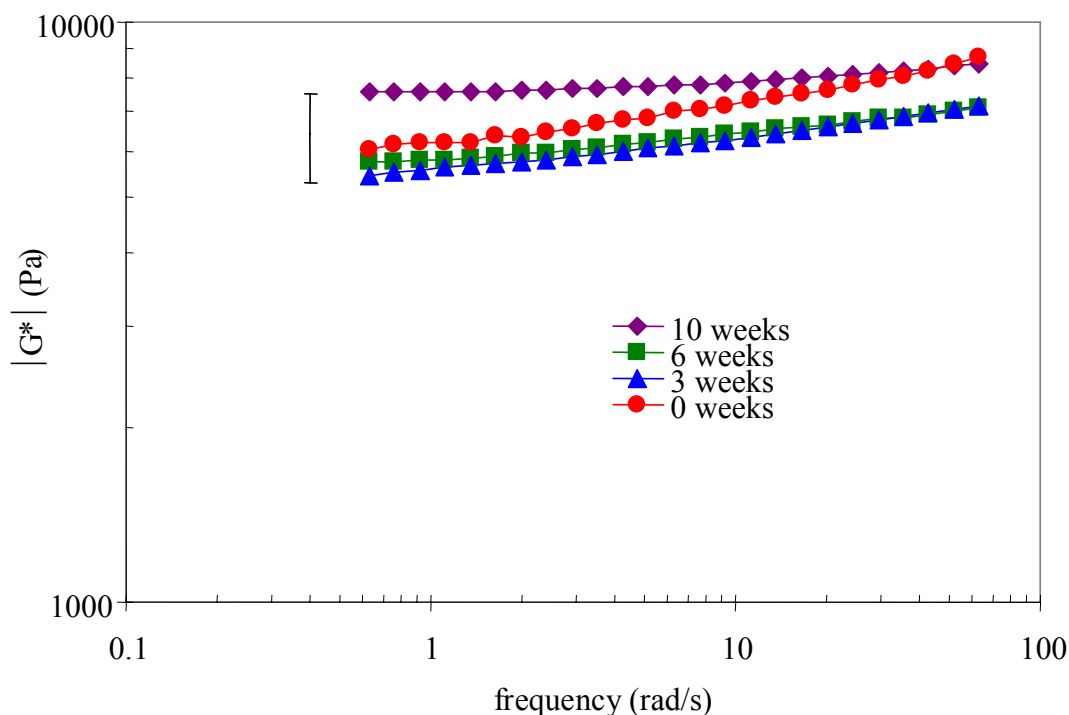


Figure 23. Variation in complex shear moduli of glycidyl methacrylate-PVA hydrogels (M_w of PVA = 50-85k) with time following immersion in Hank's solution. For visual clarity, only a representative error bar is shown

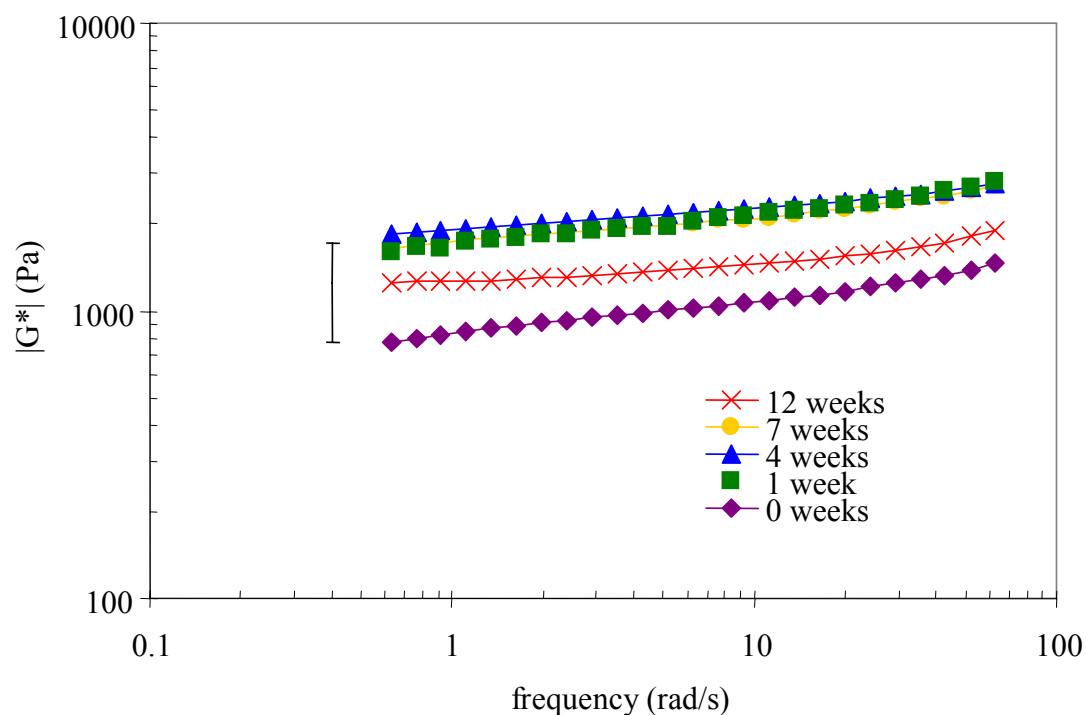


Figure 24. Variation in complex shear moduli of hydrogels generated from photopolymerization of 1,2-epoxy-5-hexene modified PVA in the presence of 1.5% (w/w) hydroxyethyl acrylate with time following immersion in Hank's solution. For visual clarity, only a representative error bar is shown.

DISCUSSION



"To be a cyclist is to be a student of pain....at cycling's core lies pain, hard and bitter as the pit inside a juicy peach. It doesn't matter if you're sprinting for an Olympic medal, a town sign, a trailhead, or the rest stop with the homemade brownies. If you never confront pain, you're missing the essence of the sport. Without pain, there's no adversity. Without adversity, no challenge. Without challenge, no improvement. No improvement, no sense of accomplishment and no deep-down joy. Might as well be playing Tiddly-Winks."

-Scott Martin

As discussed above, most studies on biomaterials, particularly those designed for use in nucleus pulposus replacement, have focused upon matching the behavior of the engineered tissue to that of the native tissues under static or transient loading. However, no studies thus far have identified a material that mimics the mechanical properties of the natural tissue when subjected to a physiological range of frequencies. An activity as simple as breathing imposes a vibrational frequency of 0.1 Hz upon the body.⁸⁴ Walking and driving are typically associated with frequency ranges of 1-3 Hz⁸⁵ and 4-6 Hz⁸⁶ respectively. Due to the viscoelastic nature of most biological tissues, particularly the

nucleus pulposus, comparative studies under dynamic loading are crucial. Viscoelastic characteristics are most evident in shear;²¹ therefore, rheology can be used as a benchmark method for the evaluation of biomaterials. The study presented herein aimed to identify synthetic hydrogels whose viscoelastic behavior mimics that of the nucleus pulposus for potential use in tissue replacement.

Photopolymerization of glycidyl methacrylate modified poly(vinyl alcohol) (PVA) yielded hydrogels whose complex shear moduli could be adjusted towards those of the nucleus pulposus by changing either the PVA molecular weight or the initial concentration of polymer in water. As a result of primary and secondary cyclization, in addition to crosslinking, the complex shear moduli generally increased with both increasing PVA molecular weight and polymer concentration prior to photopolymerization. Primary cyclization, whereby a pendant olefin reacts intramolecularly with a neighboring group, does not lead to an alteration in the network characteristics. Intramolecular cyclization is favored at low concentrations; therefore, the effective crosslink densities of hydrogels generated under dilute conditions, in addition to the resultant complex shear moduli, were lower than those observed in hydrogels formed from concentrated solutions. In contrast, secondary cyclization, or the reaction of double bonds on polymer chains that have already been crosslinked has a significant impact upon network properties.⁸⁷ Consequently, an increase in polymer molecular weight and, therefore, polymer chain length, led to higher crosslink densities and complex shear moduli. Although statistically significant differences ($p < 0.05$) in the network

characteristics were not found between all groups, this can readily be attributed to some overlap of the molecular weight and concentration ranges.

The critical concentration for entanglement was below the concentration of polymer prior to crosslinking for all experiments performed; however, entanglements had an additional impact upon the network characteristics as the molecular weight of PVA and initial polymer concentrations were varied. Trapped entanglements, or permanent loops within the macromolecular structure, can serve as physical crosslinks.⁸⁸ The crosslink densities calculated for hydrogels formed with higher molecular weight PVA and from more concentrated solutions of polymer are higher than anticipated based upon chemical crosslinking alone. As the molecular weight, and consequently polymer chain length, is raised, the propensity to form trapped entanglements, as well as the occurrence of secondary cyclization, is increased. In a similar manner, as the polymer solution becomes more concentrated, primary cyclization is reduced and the number of entanglements is increased. Therefore, the hydrogels are composed of mixtures of physical and chemical crosslinks that both contribute to the network characteristics.⁸⁸

The alterations in the network characteristics as polymer molecular weight and concentration were varied were reflected in the water contents of the glycidyl methacrylate-PVA hydrogels. Water will be absorbed until the swelling force is offset by the retractive force of the crosslinked network.⁵⁹ As the concentration of polymer in solution prior to polymerization was increased, the amount of primary cyclization decreased, the number of crosslinks increased, and the network became more resistant towards expansion. Consequently, more concentrated polymer solutions gave rise to

hydrogels with lower water contents. An increase in polymer molecular weight did not have a significant effect on the water content. Presumably, the occurrence of secondary cyclization does not have as much of an impact on the retractive force of the network as the formation of crosslinks.

The glycidyl methacrylate-PVA hydrogels did not show any signs of degradation over the time frame of study, as indicated by relatively constant complex shear moduli. Although hydrolysis of ester linkages has been shown to occur with a half life of 3.3 years under normal physiological conditions,²⁴ the lifetime of polyesters within the nucleus pulposus cavity may be reduced due to the lower pH (6.9-7.1) of the disc. As discussed above, the avascular intervertebral disc transports nutrients and metabolic byproducts through diffusion. At the center of the disc, the concentration of lactic acid is significantly greater than that of the blood plasma as a result of anaerobic metabolism, and a gradient in pH, which follows that of lactate, is developed.⁸⁹ Acid catalysis has been shown to significantly increase the degradation rate of esters.²⁴ If the susceptibility of esters towards hydrolysis does become problematic, the hydrogels may still find use as temporary scaffolds for tissue regeneration of the nucleus pulposus with mesenchymal stem cells.⁹⁰

In order to circumvent concerns over the potential degradability of the glycidyl methacrylate-PVA hydrogel system, a similar network with increased physiological stability was sought for long term tissue replacement. 1,2-epoxy-5-hexene was a logical candidate for addition to PVA. Although structurally akin to glycidyl methacrylate, the monomer lacks the labile ester group. As depicted in Figure 10, 1,2-epoxy-5-hexene was

coupled with PVA in the presence of a weak acid ($\text{CH}_3\text{CO}_2\text{H}$) over the course of 48 hours at 40°C . Unfortunately, review of the literature revealed that 1,2-epoxy-5-hexene is classified as a “nonpolymerizable” monomer, i.e a monomer for which homopolymerization is not possible.⁹¹⁻⁹³ Without the presence of an adjacent functional group that can stabilize the radical through either resonance or inductive effects, the equilibrium constant ($K_{\text{eq}} = k_{\text{activation}}/k_{\text{deactivation}}$) for generation of active radical species is low.⁹⁴ In accord with the literature, crosslinking did not occur when photopolymerization was attempted in a manner identical to that of glycidyl methacrylate modified PVA.

Recent research has revealed that although nonpolymerizable monomers are unfavorable for use in polymerization reactions in and of themselves, they can be used in the generation of copolymers.⁹⁴⁻⁹⁶ For example, following copolymerization of 1,2-epoxy-5-hexene with L-lactide via epoxide ring opening, the olefin side chains were successfully subjected to radical polymerization with poly(ethylene glycol) methacrylate using an AIBN initiator.⁹⁶ Encouraged by the latter result, our group attempted to form crosslinks between polymer chains by photopolymerizing 1,2-epoxy-5-hexene modified PVA in the presence of an additional monomer, as illustrated in Figure 25 with acrylic acid. Based upon the stability of the resultant hydrogels when submerged in physiological solution and ^{13}C NMR, a nondegradable, three dimensional network was successfully created.

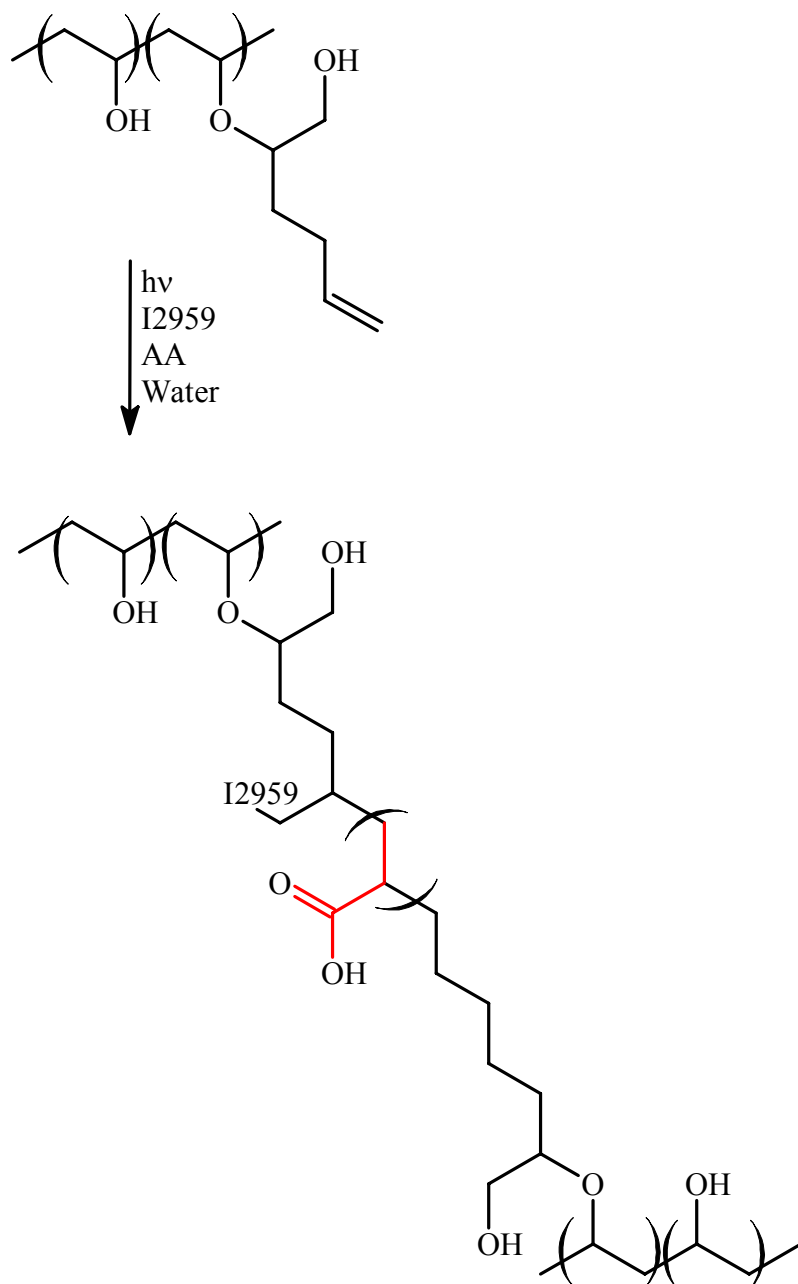


Figure 25. Proposed structure resultant from the photopolymerization of 1,2-epoxy-5-hexene modified poly(vinyl alcohol) in the presence of acrylic acid (AA). The AA monomers used to generate the crosslink are highlighted in red.

The complex shear moduli of 1,2-epoxy-5-hexene-PVA hydrogels could be controlled by varying the type of monomer used to promote crosslinking. The monomers chosen reflected hydrogels and other polymer based materials used in biomedical applications. For instance, networks partially composed of physically crosslinked poly(N-vinylpyrrolidone) are under consideration for nucleus pulposus replacement,⁹⁷ poly(hydroxyethyl acrylate) has been used in contact lenses since the 1960's,⁹⁸ and poly(acrylic acid)^{99,100} and poly(dimethylacrylamide)^{101,102} based hydrogels are being explored for use in targeted drug delivery. As indicated by the large differences in water contents, and consequently crosslink densities, photopolymerization of 1,2-epoxy-5-hexene modified PVA with various monomers led to alterations in the propensity of the resultant hydrogels to swell, or the retractive force of the network. In support of the latter notion, studies have shown that copolymers prepared with NVP will show a reduction in mechanical strength with increasing concentration as a result of an increased degree of swelling.¹⁰³

To a lesser extent, $|G^*|$ could be varied further by altering the percentage of monomer included in the 1,2-epoxy-5-hexene-PVA polymerization mixture. In general, an increase in the concentration of monomer led to an increase in the complex shear moduli. For hydrogels that incorporated acrylic acid, there was a corresponding increase in both the crosslink density and the number of junction points per molecule and a decrease in the molecular weight between crosslinks. As discussed above for glycidyl methacrylate-PVA hydrogels, the change in network characteristics was a result of secondary cyclization.

The phase shift angles of glycidyl methacrylate-PVA and 1,2-epoxy-5-hexene-PVA hydrogels were significantly less than those observed for the sheep nucleus pulposi over the entire range of frequencies tested. Additionally, while δ of the hydrogels showed no frequency dependence, δ of the natural tissue decreased as the frequency increased. The latter behavior suggests that some of the viscous nature of the nucleus pulposus is lost at higher frequencies. However, both the synthetic materials and the natural tissue possessed values of $\tan \delta$ between 0 and 1 ($\delta < 45^\circ$), indicative of viscoelastic solids. At frequencies lower than those examined in this study, the hydrogels presumably continue to exhibit “solid-like” behavior, while, as noted earlier, the nucleus pulposus begins to show a more “fluid-like” nature. Although the hydrogels do not completely mimic the viscoelastic behavior of the native tissue, a slightly more elastic characteristic may be beneficial in preventing extrusion through annular tears upon insertion into degenerative discs. Tests are currently under way to verify the latter hypothesis.

The hydrogels whose complex shear moduli were comparable to those of the sheep nucleus pulposi are summarized in Table 8. The known values of $|G^*|$ and δ for a number of other biological components, including an entire spinal motion segment and a proteoglycan-collagen solution, are also given to emphasize the large discrepancy in behavior between types of tissues and between the tissue and its individual parts. Of additional note, the water contents of the hydrogels were similar to those of sheep nucleus pulposi, as well as healthy human nucleus pulposi.³² A high level of hydration is a requisite for materials designed for nucleus pulposus replacement in order to ensure the

proper delivery of nutrients to the cells of the inner annulus fibrosus via diffusion from the endplate.

Table 15. Comparison of complex shear moduli and phase shift angles for biological tissues and hydrogels at 10 rad/s (1.6 Hz)

	$ G^* $ (kPa)	$\delta(^{\circ})$
Spinal Motion Segment ¹⁹	45000	5.5
Articular Cartilage ¹⁹	600-1000	13
Annulus Fibrosus ¹⁰⁴	125-175	-
Meniscus ¹⁹	100	22
Nucleus Pulposus (Iatridis et. al.) ¹⁹	11.3 ± 17.9	24 ± 5
Sheep Nucleus Pulposus	8.31 ± 2.4	18 ± 1.1
Glycidyl Methacrylate-PVA Hydrogel (25% initial concentration, M_w of PVA = 124-186k)	8.55 ± 0.024	7.5 ± 1.8
Glycidyl Methacrylate-PVA Hydrogel (25% initial concentration, M_w of PVA = 85-124k)	6.73 ± 2.5	8.4 ± 1.9
Glycidyl Methacrylate-PVA Hydrogel (35% initial concentration, M_w of PVA = 50-85k)	7.08 ± 5.0	9.9 ± 6.7
1,2-Epoxy-5-Hexene-PVA Hydrogel (10% AA)	9.20 ± 2.0	2.8 ± 0.26
1,2-Epoxy-5-Hexene-PVA Hydrogel (5% AA)	5.27 ± 2.5	3.3 ± 1.4
Collagen-Proteoglycan Mixture ¹⁹	0.04	60
Synovial Fluid ¹⁹	0.02	16
Proteoglycan Solution ²⁰	0.01	65

The tissue compatibility of 1,2-epoxy-5-hexene-PVA hydrogels was assessed *in vitro* through the direct contact assay and elution test. A large amount of cell death occurred in wells containing experiments samples; however, the results do not positively indicate that the cells were impacted directly by the release of toxic substances from the new materials. An outside fungal contamination was prevalent in experimental samples and made interpretation of the micrographs difficult. Presence of a fungus could only be detected during the elution tests; however, the signature hyphae may not yet have presented themselves during the short time period allotted for the direct contact assays.

Notably, the wells which contained control samples obtained from glycidyl methacrylate-PVA hydrogels did not show signs of contamination or cell death. Potentially, the 1,2-epoxy-5-modified PVA either contained a contaminant prior to photopolymerization or made the resultant hydrogels more susceptible towards outside contamination. The experimental sample that led to the greatest amount of cell death during the direct contact assay was allowed to equilibrate in Hank's solution for a shorter period of time than the others, indicating that proper extraction of unreacted materials may not have occurred. In the future, new purification processes may be necessary for 1,2-epoxy-5-hexene modified PVA and the hydrogel generated via photopolymerization of the latter. Despite the fungal contamination, viable cells were still present during the direct contact assay and elution test. Therefore, the cytotoxicity test results were encouraging, although not conclusive.

As emphasized throughout, although rheological testing can be viewed as a benchmark method for the comparison of synthetic and natural tissues, all materials should be analyzed in a variety of loading modes. To emphasize this point, some of the hydrogel samples were subjected to dynamic compressive loading. The results did not show the same trends observed in dynamic torsional shear, thereby adding to the notion that multiple mechanical tests are necessary.

Complex moduli obtained under compression did not show the same dependence on the molecular weight of PVA as moduli obtained in shear. The results are not surprising given that changes in the effective crosslink density are known to have the most significant impact upon the strength of the network in shear, rather than axial loading.⁹⁹

For direct comparison of the two results, $|G^*|$ and $|K^*|$ were related through Poisson's ratio, μ ,²¹ at a frequency of 10 rad/s.

$$\mu = \frac{3K - 2G}{2G + 6K}$$

Poisson's ratio showed a trend towards lower values with increasing molecular weight of PVA (Table 9). For comparison, $\mu = 0.30$ for bone,¹⁰⁵ 0.45 for ligaments,¹⁰⁵ and 0.44 – 0.49 for rubber.¹⁰⁶ Finite element studies have suggested that a Poisson's ratio similar to that of rubber is desirable to promote load transfer to the surrounding annular tissue.^{107,108} Currently, no information is available on the behavior of the nucleus pulposus under dynamic compression. Although a static compressive modulus of 310 kPa has been reported,¹⁰⁹ dynamic moduli are typically higher.^{21,110} Glycidyl methacrylate-PVA hydrogel prepared from PVA of $M_w = 85\text{-}125\text{k}$ appears to be suitable as a material for nucleus pulposus replacement based upon Poisson's ratio and the complex shear modulus.

Table 16. Comparison between complex dynamic compressive and shear moduli obtained for glycidyl methacrylate-PVA hydrogels with different molecular weights of PVA

MW (kg/mol)	Compressive Modulus (kPa)	Shear Modulus (kPa)	μ
13-23	66.0	2.45	0.482
31-50	42.2	2.74	0.468
85-124	64.7	5.48	0.459
124-86	50.2	8.56	0.419

For hydrogels prepared via photopolymerization of 1,2-epoxy-5-hexene modified PVA in the presence of different types of monomers, the complex dynamic compressive

moduli did not follow the same trend as the complex shear moduli. Although acrylic acid led to hydrogels with significantly higher $|G^*|$, the values for $|K^*|$ were intermediate to those obtained for dimethylacrylamide (DMAA) and hydroxyethyl acrylate (HEA). A significant difference in the complex dynamic compressive moduli for the different monomers could not be definitively identified due to the low sample number. However, calculation of Poisson's ratio with the equation given above showed a trend in Poisson's ratio that matched that of $|G^*|$ with DMAA leading to the highest Poisson's ratio and lowest complex shear moduli and AA giving rise to the lowest Poisson's ratio and highest complex shear moduli. μ for hydrogels containing AA may be too low to be suitable as a nucleus pulposus replacement; however, further tests will be necessary to determine which characteristics are crucial to the success of prostheses.

Table 17. Comparison between complex dynamic compressive and shear moduli obtained for 1,2-epoxy-5-hexene-PVA hydrogels with different types of monomers

Monomer	Compressive Modulus (kPa)	Shear Modulus (kPa)	μ
DMAA	12.5	0.350	0.486
HEA	50.7	0.928	0.491
AA	23.3	5.27	0.395

All monomers were included at a concentration of 5 wt. %.

In sum, two hydrogel systems have been successfully identified with viscoelastic behavior that mimics that observed for the nucleus pulposus. Degradation did not occur over the time frame examined. 1,2-epoxy-5-hexene-PVA hydrogels may be more appropriate for long term replacement if the hydrolytically labile ester linkages of glycidyl methacrylate-PVA hydrogels do become problematic. Results obtained under dynamic compression add to the notion that hydrogels resultant from

photopolymerization of glycidyl methacrylate modified PVA may be suitable for nucleus pulposus replacement based upon mechanical properties alone. Hydrogels from 1,2-epoxy-5-hexene modified PVA, with complex shear moduli that corresponded with those of the native tissue, possessed Poisson's ratios that may be too low to restore proper function to the intervertebral disc. Further research is necessary to determine which system is truly acceptable as a nucleus pulposus prosthetic.

CONCLUSIONS



"But to say that the race is the metaphor for the life is to miss the point. The race is everything. It obliterates whatever isn't racing. Life is the metaphor for the race."

-Donald Antrim

This study represents the first attempt to successfully mimic the more “solid-like” nature of the nucleus pulposus exhibited under dynamic torsional loading. Thus far, the materials intended for use in restoring function to degenerative intervertebral discs through tissue replacement have not undergone sufficient mechanical evaluation and have shown problems with wear, extrusion, and nutrient delivery. Two hydrogel systems based upon photopolymerization of chemically modified poly(vinyl alcohol) were successfully identified with viscoelastic behavior comparable to that of the natural tissue when the conditions of photopolymerization were properly modulated. Although the phase shift angles of the hydrogels were lower than those of the native tissue and did not show the same frequency dependence, a less viscous nature over all frequencies may be desirable in a replacement material to prevent extrusion out of the damaged annulus

fibrosus. Degradation did not occur over the time frame examined. 1,2-epoxy-5-hexene-PVA hydrogels may be more appropriate for long term replacement if the hydrolytically labile ester linkages of glycidyl methacrylate-PVA hydrogels do become problematic. More comprehensive mechanical testing is necessary to assess which hydrogel system is most suitable.

FUTURE WORK



"I'm a cyclist not simply in the sense that I ride a bike, but in the sense that some people are socialists or Christian fundamentalists or ethical realists - that is, cycling is my ideology, a system of thought based on purity and economy of motion, kindness to the environment and drop handlebars, and I want to convert others."

—**Robert Hanks**, *The Independent*, Aug. 15, 2005

The research presented herein represents only a single stage in obtaining a clear picture of how the viscoelastic behavior of synthetic hydrogels intended for nucleus pulposus replacement should match that of the native tissue. For a more comprehensive study, future research will focus upon dynamic mechanical testing of glycidyl methacrylate-PVA and 1,2-epoxy-5-hexene-PVA hydrogels in compression and tension. Despite the anisotropic, viscoelastic behavior exhibited by all soft biological tissues, the latter tests have not yet been performed on the nucleus pulposus. Therefore, further studies on the mechanical properties of the native tissue will also be conducted.

To ensure that materials intended for implantation can withstand typical physiological pressures, a rough model of a degenerative intervertebral disc has recently been created

from polyacrylate with a hollowed center ($d = 15\text{mm}$) that is representative of enucleated disc space. Gaps of various widths will be introduced into the exterior portion of the model to imitate tears and fissures of the annulus. Studies will be performed to determine how much load can be applied to hydrogels placed within the center of the model before extrusion through the simulated annular defects occurs. Our hope is that the less lossy synthetic material will be more resistant to extrusion than the native tissue.

Cytotoxicity studies of 1,2-epoxy-5-hexene-PVA hydrogels will be repeated to obtain a better understanding of what led to cell death during the course of our investigation. Purification procedures will be altered to ensure that all traces of unreacted monomer are removed prior to evaluation. The hydrogels will either be submerged in boiling water for long periods of time or will be dialyzed. Poly(vinyl alcohol) will be washed and 1,2-epoxy-5-hexene will be millipore filtered prior to reaction to minimize the likelihood of future contamination. The starting materials will also be stored in a more sterile environment. The elution test and direct contact assay will be conducted over the same period of time for better comparison between the two sets of results. Properly conducted cytotoxicity studies will be the first step towards establishing the efficacy of a novel non-biodegradable hydrogel system for tissue replacement.

In order to determine whether the glycidyl methacrylate-PVA hydrogels will be more appropriate for tissue replacement or regeneration, degradation studies will be conducted for longer periods of time and at a more physiologically relevant temperature. Given the labile nature of the ester linkages, some degradation is likely to occur if the time scale of

the experiment is extended past that used in the present study or if the temperature is increased.

BIBLIOGRAPHY



“Bike racing is art. Art is driven by passion, by emotions, by unknown thoughts. The blood that pumps through my veins is stirred by emotion. It’s the same for every athlete. And that’s why we do this.”

-Chris Carmichael

1. Hanley EN, Shapiro DE. The development of low-back pain after excision of a lumbar disc. *J. Bone Joint Surg. (Am.)* 1989; 71: 719-721
2. Lee CK, Langrana NA. Lumbosacral fusion. A biomechanical study. *Spine* 1984; 9: 574-581.
3. Bao QB. Artificial disc technology. *Neurosurg. Focus* 2000; 9: 1-7.
4. Bao QB, Higham PA. Hydrogel intervertebral disc nucleus. U.S. Pat. #5,047,055 (1991).
5. Bao QB, Higham PA. Hydrogel bead intervertebral nucleus. U.S. Pat. #5,192,326 (1993).
6. Ray CD, Dickhudt EA Assell RL. Prosthetic spinal disc nucleus. U.S Pat. #5,824,093 (1998).
7. Ray CD, Dickhudt EA, Ledoux PJ, Frutiger BA. Prosthetic spinal disc nucleus. U.S. Pat. #5,674,295 (1997).

8. Ray CD. The PDN prosthetic disc-nucleus device. *Eur. Spine J.* 2002; 11 (Suppl. 2): S137-S142.
9. Di Martino A, Vaccaro AR, Lee JY, Denaro V, Lim MR. Nucleus pulposus replacement. Basic science and indications for clinical use. *Spine* 2005; 30 (Suppl. 16): S16-S22.
10. Allen MF, Schoonmaker JE, Bauer TW, Williams PF, Higham PA, Yuan HA. Preclinical evaluation of a poly(vinyl alcohol) hydrogel implant as a replacement for the nucleus pulposus. *Spine* 2004; 29: 515-523.
11. Thomas J, Lowman A, Marcolongo M. Novel associated hydrogels for nucleus pulposus replacement. *J. Biomed. Mater. Res. A* 2003; 67: 1329-1337.
12. Thomas J, Gomes K, Lowman A, Marcolongo M. The effect of dehydration history on PVA/PVP hydrogels for nucleus pulposus replacement. *J. Biomed. Mater. Res. B Appl. Biomater.* 2004; 69: 135-140.
13. Boelen EJH, van Hooy-Corstjens CSJ, Bulstra SK, van Ooij A, van Rhijn LW, Koole LH. Intrinsically radiopaque hydrogels for nucleus pulposus replacement. *Biomaterials* 2005; 26: 6674-6683.
14. Boelen EJH, van Hooy-Corstjens, CSJ, Gijbels MJJ, Bulstra SK, van Ooij A, van Rhijn LW, Koole LH. Preliminary evaluation of new intrinsically radiopaque hydrogels for replacing the nucleus pulposus. *J. Mater. Chem.* 2006; 16: 824-828.
15. Horner HA, Phil M, Urban JPG. Effect of nutrient supply on the viability of cells from the nucleus pulposus of the intervertebral disc. *Spine* 2001; 26: 2543-2549.
16. Temenoff JS, Mikos AG. Injectable biodegradable materials for orthopedic tissue engineering. *Biomaterials* 2000; 21, 2405-2412.
17. Drury JL, Mooney DJ. Hydrogels for tissue engineering: scaffold design variables and applications. *Biomaterials* 2003; 24, 4337-4351.
18. Ashton-Miller JA. Biomechanics of the human spine. In: Mow VC, Hayes WC, ed. *Basic Orthopaedic Biomechanics*. New York: Raven Press, 1991: 337-374.
19. Iatridis JC, Weidenbaum, M, Setton, LA, Mow, VC. Is the nucleus pulposus a solid or a fluid? Mechanical behaviors of the nucleus pulposus of the human intervertebral disc. *Spine* 1996; 21: 1174-1184.
20. Zhu W, Iatridis JC, Hlibczuk V, Ratcliffe A, Mow VC. Determination of collagen-proteoglycan interactions in vitro. *J. Biomechanics* 1996; 29: 773-783.

21. Ferry JD. *Viscoelastic Properties of Polymers*. New York: John Wiley & Sons, Inc., 1970.
22. Hassan CM, Peppas NA. Structure and applications of poly(vinyl alcohol) hydrogels produced by conventional crosslinking or by freezing/thawing methods. *Adv. Polym. Sci.* 2000; 153: 37-65.
23. Oka M, Noguchi T, Kumar P, Ikeuchi K, Yamamuro T, Hyon SH, Ikada Y. Development of an artificial articular cartilage. *Clinical Materials* 1990; 6: 361-381
24. Gopferich A. Mechanisms of polymer degradation and erosion. *Biomaterials* 1996; 17: 103-114.
25. Nordin M, Frankel VH. *Basic Biomechanics of the Musculoskeletal System*. 3rd ed. Baltimore: Lippincott Williams & Wilkins, 2001.
26. Roughley PJ. Biology of intervertebral disc aging and degeneration: involvement of the extracellular matrix. *Spine* 2004; 29: 2691-2699.
27. Mow VC, Hayes WC. *Basic Orthopaedic Biomechanics*. 2nd ed. Philadelphia: Lippincott Williams & Wilkins, 1997.
28. Urban JPG, Holm S, Maroudas A, Nachemson A. Nutrition of the intervertebral disc: Effect of fluid flow on solute transport. *Clin. Orthop.* 1982; 170: 296-302.
29. Katz MM, Hargens AR, Garfin SR. Intervertebral disc nutrition: Diffusion versus convection. *Clin. Orthop.* 1986; 210: 243-245.
30. Ogata K, Whiteside, LA. Nutritional pathways of the intervertebral disc: An experimental study using the hydrogen washout technique. *Spine* 1981; 6: 211-216.
31. Ohshima H, Urban JPG. The effect of lactate and pH on proteoglycan and protein synthesis rates in the intervertebral disc. *Spine* 1992; 17: 1079-1082.
32. Buckwalter JA. Aging and degeneration of the human intervertebral disc. *Spine* 1995; 11: 1307-1314.
33. Ferguson SJ. Biomechanics of the aging spine. *Eur. Spine J.* 2003; 12 (Suppl. 2): S97-S103.
34. Walker HW, Walker BS, Anderson DG. Molecular basis of intervertebral disc degeneration. *The Spine Journal* 2004; 4: 158S-166S.

35. Roberts S, Urban JPG, Evans H, Eisenstein SM. Transport properties of the human cartilage endplate in relation to its composition and classification. *Spine* 1996; 21: 415-420.
36. Bibby SRS, Jones DA, Ripley RM, Urban JPG. Metabolism of the intervertebral disc: Effects of low levels of oxygen, glucose, and pH on rates of energy metabolism of bovine nucleus pulposus cells. *Spine* 2005; 30: 487-496.
37. Ohshima H, Urban JPG. The effect of lactate and pH on proteoglycan and protein synthesis rates in the intervertebral disc. *Spine* 1992; 17: 1079-1082.
38. Ray CD. The artificial disc: Introduction, history, socioeconomics. In: Weinstein JN (ed.) *Clinical Efficacy and Outcome in the Diagnosis and Treatment of Low Back Pain*. New York: Raven Press Ltd., 1992.
39. Urban JPG, Roberts S. Degeneration of the intervertebral disc. *Arthritis Research & Therapy* 2003; 5: 120-130.
40. Freemont TJ, LeMaitre C, Watkins A, Hoyland JA. Degeneration of intervertebral discs: current understanding of cellular and molecular events, and implications for novel therapies. *Expert Reviews in Molecular Medicine* 2001; 3: 1-10.
41. Adams MA. Biomechanics of back pain. *Acupuncture in Medicine* 2004; 22: 178-188.
42. Klara PM, Ray CD. Artificial Nucleus Replacement. *Spine* 2002; 27: 1374-1377.
43. Wilke H, Kavanagh S, Neller S, Haid C, Lutz EC. Effect of a prosthetic disc nucleus on the mobility and sic height of the L4-5 intervertebral disc postnucleotomy. *J. Neurosurg. (Spine 2)* 2001; 95: 208-214.
44. Panjabi MM. The stabilizing system of the spine. Part II. Neutral zone and instability hypothesis. *J. Spinal Disord.* 1992; 5: 390-396.
45. Hassan CM, Peppas NA. Structure and applications of poly(vinyl alcohol) hydrogels produced by conventional crosslinking or by freezing/thawing methods. *Adv. Polym. Sci.* 2000; 153: 37-65.
46. Oka M, Noguchi T, Kumar P, Ikeuchi K, Yamamuro T, Hyon SH, Ikada Y. Development of an artificial articular cartilage. *Clinical Materials* 1990, 6: 361-381.

47. Stoy VA, Stehliceck P, Kozlova Z, Drunecky T. Hydrogel-based prosthetic device for replacing at least a part of the nucleus of a spinal disc. U.S. Pat. App. #20,050,171,611 (2005).
48. Bertagnoli R, Sabatino CT, Edwards T, Gontarz GA, Prewett A, Parsons JR. Mechanical testing of a novel hydrogel nucleus replacement implant. *The Spine Journal* 2005; 5: 672-681.
49. Meakin JR, Hukins DW. Effect of removing the nucleus pulposus on the deformation of the annulus fibrosus during compression of the intervertebral disc. *J. Biomech.* 2000; 33:575-580.
50. Korge A, Nydegger T, Polard JL, Mayer HM, Husson JL. A spiral implant as nucleus prosthesis in the lumbar spine. *Eur. Spine J.* 2002; 11 (Suppl. 2): S149-S153.
51. Husson JL, Korge A, Polard JL, Nudegger, Kneubühler S, Mayer HM. A memory coiling spiral as nucleus pulposus prosthesis: concept, specifications, bench testing, and first clinical results. *J. Spinal Disord. & Techniques* 2003; 16: 405-411.
52. Frei HP, Rathonyi G, Orr TE, Nolte LP, Oxland T. Effect of a nucleus prosthetic device on the biomechanical behavior of the functional spinal unit. *Eur. Spine J.* 1999; 8: S36-S37.
53. Bao Q, Hudgins RG, Felt JC, Arsenyev A, Yuan HA. Method of making an intervertebral disc prosthesis. U.S. Pat. #7,077,865 (2006).
54. Singhal V, MacEachern CF, Craig NJA, Wardlaw D. Early clinical results of an in situ polymerizing protein hydrogel nuclear repair system. *Biospine*, 2006.
55. Yuksel KU, Walsh SP, Black KS. In situ bioprosthetic filler and methods, particularly for the in situ formation of vertebral disc bioprosthetics. U.S. Pat. App. #20,050,102,030 (2005).
56. Scotchford CA, Cascone MG, Downes S, Giusti P. Osteoblast responses to collagen-PVA bioartificial polymers in vitro: the effects of cross-linking method and collagen content. *Biomaterials* 1998; 19: 1-11.
57. Peppas NA. Hydrogels. In: Ratner BD, Hoffman AS, Schoen FJ, Lemons JE (ed.) *Biomaterials Science: An Introduction to Materials in Medicine*. San Diego: Academic Press, 1996.
58. Hennink WE, van Nostrum CF. Novel crosslinking methods to design hydrogels. *Adv. Drug Deliv. Rev.* 2002; 54: 13-36.

59. Hoffman AS. Hydrogels for biomedical applications. *Ann. NY Acad. Sci.* 2001; 944: 62-73.
60. Drury JL, Mooney DJ. Hydrogels for tissue engineering: scaffold design variables and applications. *Biomaterials* 2003; 24: 4337-4351.
61. Peppas NA, Stauffer SA. Reinforced uncrosslinked poly(vinyl alcohol) gels produced by cyclic freezing-thawing processes: a short review. *J. Control. Release* 1991; 16: 305-310.
62. Nuttelman CR, Henry SM, Anseth KS. Synthesis and characterization of photocrosslinkable, degradable poly(vinyl alcohol)-based tissue engineering scaffolds. *Biomaterials* 2002; 23: 3617-3626.
63. Martens P, Anseth KS. Characterization of hydrogels formed from acrylate modified poly(vinyl alcohol) macromers. *Polymer* 2000; 41: 7715-7722.
64. Mascini M, Mateescu MA, Pilloton R. Polyvinyl alcohol-collagen membranes for enzyme immobilization. *Bioelectrochemistry and Bioenergetics* 1986; 16: 149-157.
65. Barbani N, Cascone MG, Giusti P, Lazzeri L, Polacco G, Pizzirani G. Bioartificial materials based on collagen: 2. Mixtures of soluble collagen and poly(vinylalcohol) cross-linked with gaseous glutaraldehyde. *J. Biomater. Sci. Polimer Edn.* 1995; 6: 471-484.
66. Lozinsky VI, Zubov AL, Kulakova AL, Titova EF, Rogozhin SV. Study of cryostructurization of polymer systems. IX. Poly(vinyl alcohol) cryogels filled with particles of crosslinked dextran gel. *J. Appl. Polymer Sci.* 1992; 44: 1423-1435.
67. Cascone MG, Maltinti S. Hydrogels based on chitosan and dextran as potential drug delivery systems. *J. Mater. Sci. Mater. Med.* 1999; 10:301-307.
68. Ramires PA, Milella E. Biocompatibility of poly(vinyl alcohol)-hyaluronic acid and poly(vinyl alcohol)-gellan membranes crosslinked by glutaraldehyde vapors. *J. Mater. Sci. Mater. Med.* 2002; 13: 119-123.
69. Kim SJ, Yoon SG, Lee YM, Kim HC, Kim SI. Electrical behavior of polymer hydrogel composed of poly(vinyl alcohol)-hyaluronic acid in solution. *Biosens. Bioelectron.* 2004; 19: 531-536.
70. Orienti I, Trere R, Zecchi V. Hydrogels formed by cross-linked polyvinylalcohol as colon-specific drug delivery systems. *Drug Dev. Ind. Pharm.* 2001; 27: 877-884.

71. Bo Jiang. Study on PVA hydrogel crosslinked by epichlorohydrin. *J. Appl. Polymer Sci.* 1992; 46: 783-786.
72. Zhuang Y, Zhu Z, Chen L. Investigation of gelation behavior of polyvinyl alcohol-glutaraldehyde system. *J. Appl. Polymer Sci.* 1997; 63: 267-272.
73. Vidal MMB, Gil MH, Delgadillo I, Alonso Chamarro J. Swelling and thermal properties of poly(vinyl alcohol) containing hemoglobin membranes. *Journal of Bioactive and Compatible Polymers* 1999; 14: 243-257.
74. Stauffer SR, Peppas NA. Poly(vinyl alcohol) hydrogels prepared by freezing-thawing cyclic processing. *Polymer* 1992; 33: 3932-3936.
75. Hassan CM, Peppas NA. Structure and morphology of freeze/thawed PVA hydrogels. *Macromolecules* 2000; 33: 2472-2479.
76. Nguyen KT, West JL. Photopolymerizable hydrogels for tissue engineering applications. *Biomaterials* 2002; 23: 4307-4314.
77. Bryant SJ, Nuttelman CR, Anseth KS. The effects of crosslinking density of cartilage formation in photocrosslinkable hydrogels. *Biomed. Sci. Instrum.* 1999; 35: 309-14.
78. Tremenoff JS, Antonios GM. Injectable biodegradable materials for orthopedic tissue engineering. *Biomaterials* 2000; 21: 2405-2412.
79. Hou Q, De Bank PA, Shakesheff KM. Injectable scaffolds for tissue regeneration. *J. Mater. Chem.* 2004; 24: 1915-1923.
80. Graessley, WW. *The Entanglement Concept in Polymer Rheology*. Cambridge: Springer, 1974.
81. Misra GS, Mukherjee PK. The relation between the molecular weight and intrinsic viscosity of polyvinyl alcohol. *Colloid & Polymer Sci.* 1980; 258: 152-155.
82. Freshney RI. *Culture of Animal Cells: A Manual of Basic Techniques*. 4th ed. New York: Wiley-Liss, Inc., 2000.
83. Morgan SJ, Darling DC. *Animal Cell Culture*. Oxford, UK: BIOS Scientific Publishers Limited, 1993.
84. Frederiks J, Swenne CA, TenVoorde BJ, Honzikova N, Levert JV, Maan AC, Schalijs MJ, Bruschke AV. The importance of high-frequency paced breathing in spectral baroreflex sensitivity assessment. *J. Hypertens.* 2000; 18: 1635-1644.

85. Jahn K, Strupp M, Schneider E, Dieterich M, Brandt T. Differential effects of vestibular stimulation on walking and running. *Neuroreport* 2000; 11: 1745-1748.
86. Hassan R, McManus K. Perception of low frequency vibrations by heavy vehicle drivers. *J. Low Freq. Noise Vib. Active Cont.* 2002; 21: 65-75.
87. Elliot JE, Bowman, CN. Kinetics of primary cyclization reactions in cross-linked polymers: an analytical and numerical approach to heterogeneity in network formation. *Macromolecules* 1999; 32: 8621-8628.
88. Sperling LH. Introduction to Physical Polymer Science. 3rd ed. New York: John Wiley & Sons, 2001.
89. Ohshima H, Urban JPG. The effect of lactate and pH on proteoglycan and protein synthesis rates in the intervertebral disc. *Spine* 1992; 17: 1079-1082.
90. Crevensen G, Walsh AJL, Ananthakrishnan D, Page P, Wahba GM, Lotz JC, Berven S. Intervertebral disc cell therapy for regeneration: mesenchymal stem cell implantation in rat intervertebral discs. *Annals of Biomed. Engr.* 2004; 32: 430-434.
91. Marvel CS. *An Introduction to the Organic Chemistry of High Polymers*. New York: Johny Wiley & Sons, 1959.
92. Coessens V, Pyun J, Miller PJ, Gaynor SG, Matyjaszewski K. Functionalization of polymers prepared by ATRP using radical addition reactions. *Macromol. Rapid Commun.* 2000; 21: 103-109.
93. Debuigne A, Caille JR, Jerome, R. Synthesis and end-functional poly(vinyl acetate) by cobalt-mediated radical polymerization. *Macromolecules* 2005; 38: 5452-5458.
94. Matyjaszewski K, Xia J. Atom transfer radical polymerization. *Chem. Rev.* 2001; 101: 2921-2990.
95. Xia J, Paik HJ, Matyjaszewski K. Polymerization of vinyl acetate promoted by iron complexes. *Macromolecules* 1999; 32: 8310-8314.
96. Lee S, Cho KY, Seol WH, Park JK. Novel synthesis of reactive poly(ethylene glycol) grafted poly(L-lactide) via two step polymerizations. *Polymer Bulletin* 2004; 52: 393-400.
97. Thomas J, Lowman A, Marcolongo M. Novel associated hydrogels for nucleus pulposus replacement. *J. Biomed. Mater. Res. A* 2003; 67: 1329-1337.

98. Wichterle O, Lim D. Hydrophilic gels in biologic use. *Nature* 1960; 185: 117-118.
99. Liu YY, Shao YH, Lu J. Preparation, properties, and controlled release behaviors of pH-induced thermosensitive amphiphilic gels. *Biomaterials* 2006; 27: 4016-4024.
100. Ranjha NM. Swelling behaviour of pH-sensitive crosslinked poly(vinyl acetate co-acrylic acid) hydrogels for site specific drug delivery. *Pak. J. Pharm. Sci.* 1999; 12: 33-41.
101. Hiratani H, Mizutani Y, Alvarez-Lorenzo C. Controlling drug release from imprinted hydrogels by modifying the characteristics of the imprinted cavities. *Macromol. Biosci.* 2005; 5: 728-733.
102. Pitaressi G, Pierro P, Giammona G, Muzzalupo R, Trombino S, Picci N. Beads of acryloylated polyaminoacidic matrices containing 5-Fluorouracil for drug delivery. *Drug Deliv.* 2002; 9: 97-104.
103. Anseth KS, Bowman CN, Brannon-Peppas L. Mechanical properties of hydrogels and their experimental determination. *Biomaterials* 1996; 17: 1647-1657.
104. Iatridis JC, Kumar S, Foster RJ, Mow VC. Shear mechanical properties of human lumbar annulus fibrosus. *J. Orthop. Res.* 1999; 17: 732-737.
105. Farah JW, Craig RG, Meroueh KA. Finite element analysis of three- and four-unit bridges. *J. Oral Rehabil.* 1989; 16: 603-611.
106. Bedford A, Liechti KM. *Mechanics of Materials*. Upper Saddle River, NJ: Prentice-Hall, Inc., 2000.
107. Meakin JR, Reid JE, Hukins DW. Replacing the nucleus pulposus of the intervertebral disc. *Clin. Biomech.* 2001; 16: 560-565.
108. Meaking JR. Replacing the nucleus pulposus of the intervertebral disk: prediction of suitable properties of a replacement material using finite element analysis. *J. Mater. Sci. Mater. Med.* 2001; 12: 207-213.
109. Perie D, Korda D, Iatridis JC. Confined compression experiments on bovine nucleus pulposus and annulus fibrosus: sensitivity of the experiment in the determination of compressive modulus and hydraulic permeability. *J. Biomech.* 2005; 38: 2164-2171.
110. Tanaka E, van Eijden T. Biomechanical behavior of the temporomandibular joint disc. *Crit. Rev. Oral. Biol. Med.* 2003; 14: 138-148.

APPENDIX A: SPECTRA



“Few businesses match the marvelous choreography of a smooth-running bicycle store—the rubber smell, the incessant phones, hissing compressors and clamorous freewheeling bikes”

-Jim Langley

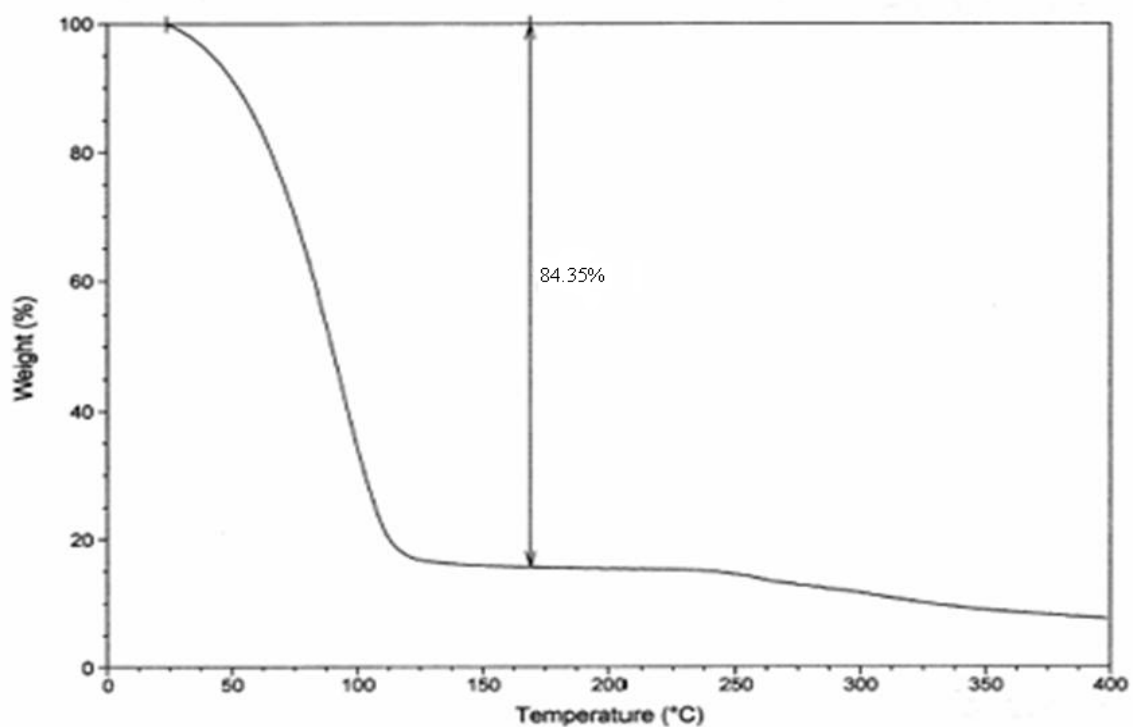


Figure A1. TGA of the sheep nucleus pulposus.

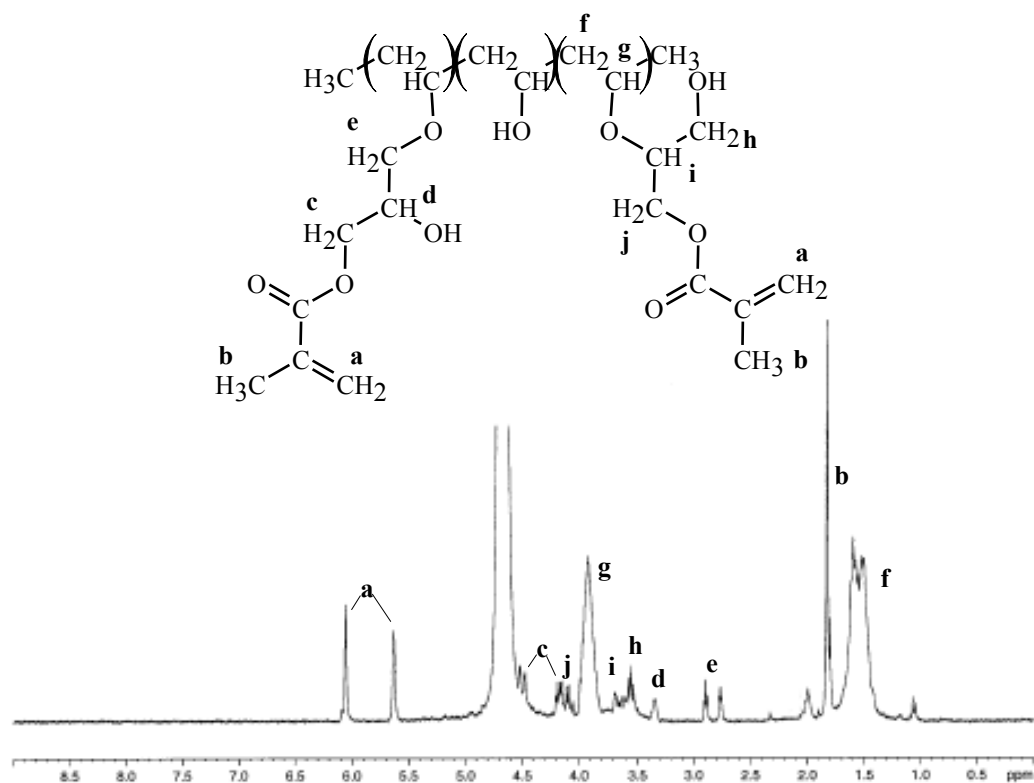


Figure A2. ^1H NMR of glycidyl methacrylate modified poly(vinyl alcohol).

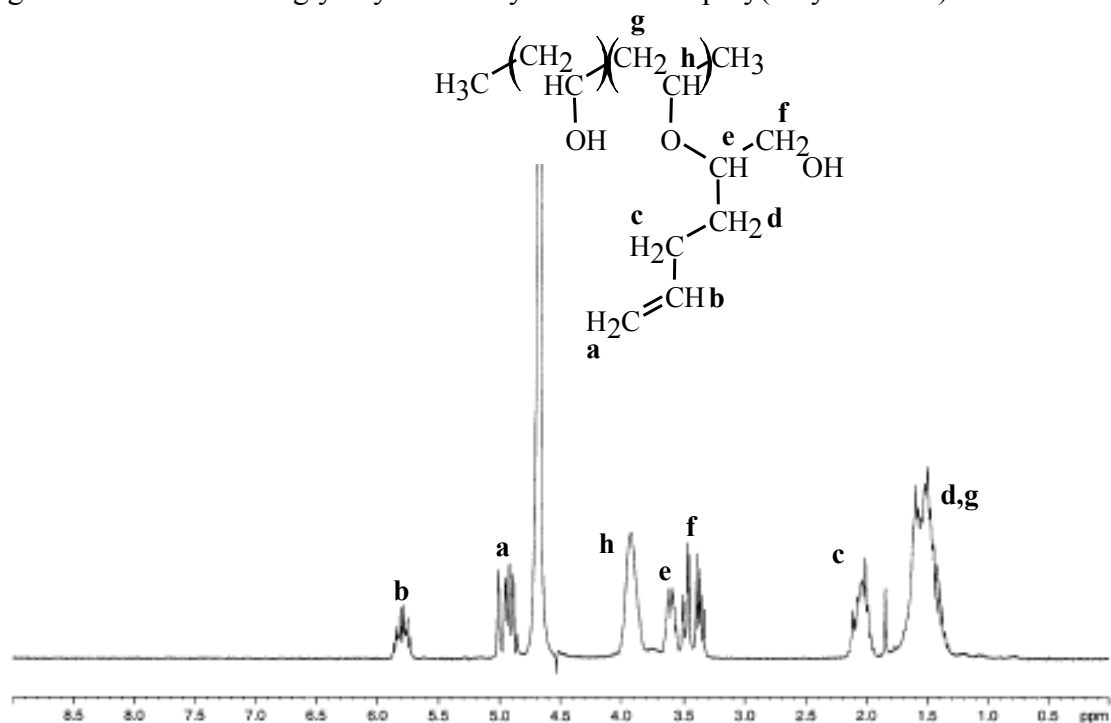


Figure A3. ^1H NMR of 1,2-epoxy-5-hexene modified poly(vinyl alcohol).

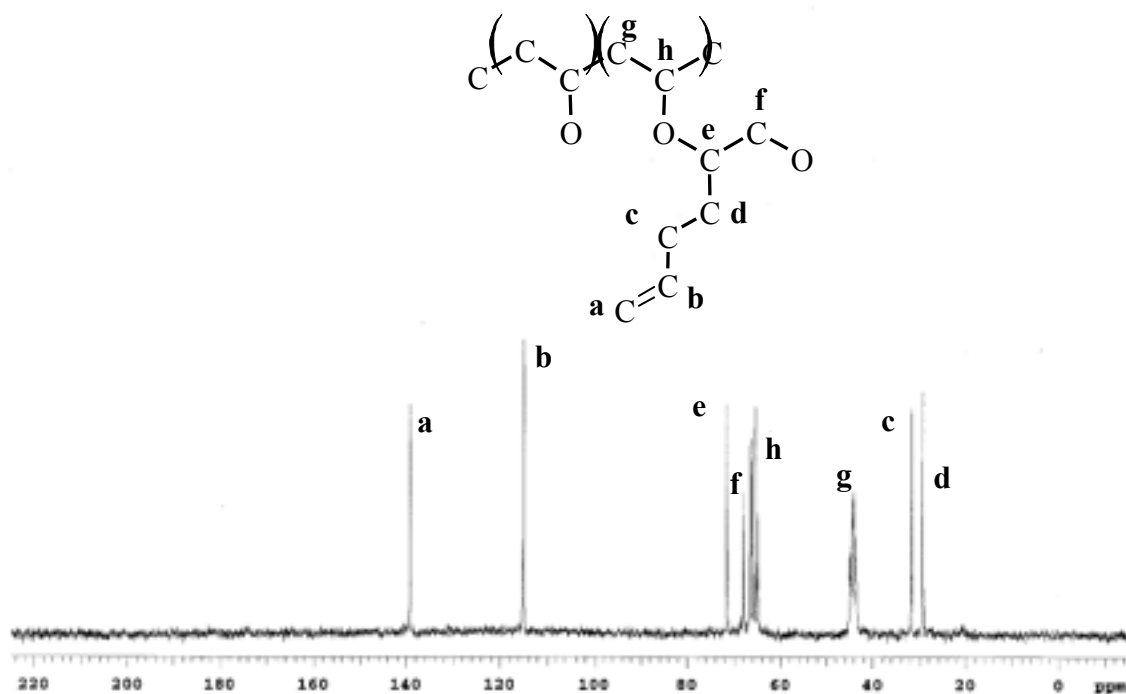


Figure A4. ^{13}C NMR of 1,2-epoxy-5-hexene modified poly(vinyl alcohol).

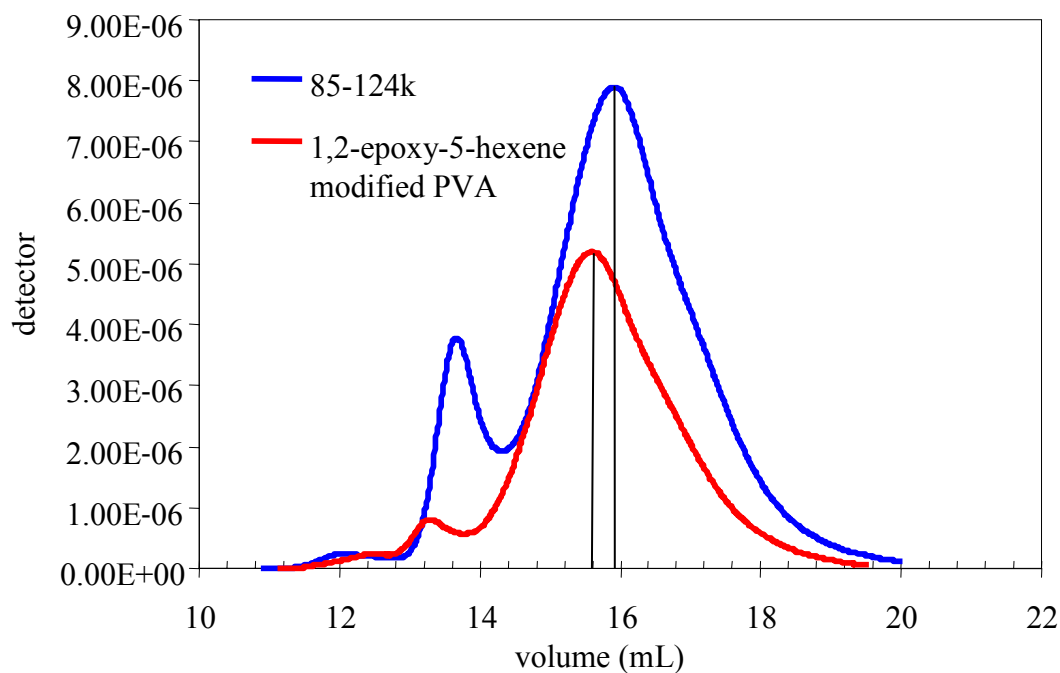


Figure A5. GPC of 1,2-epoxy-5-hexene modified poly(vinyl alcohol). Based upon elution volumes shown and comparison to PEO standards, the molecular weight of 1,2-epoxy-5-hexene modified PVA was determined to be ~ 20 kg/mol greater than that of unreacted PVA. The weight increase corresponds to reaction of approximately 18% of the hydroxyl side groups, a percentage comparable with that determined from NMR.

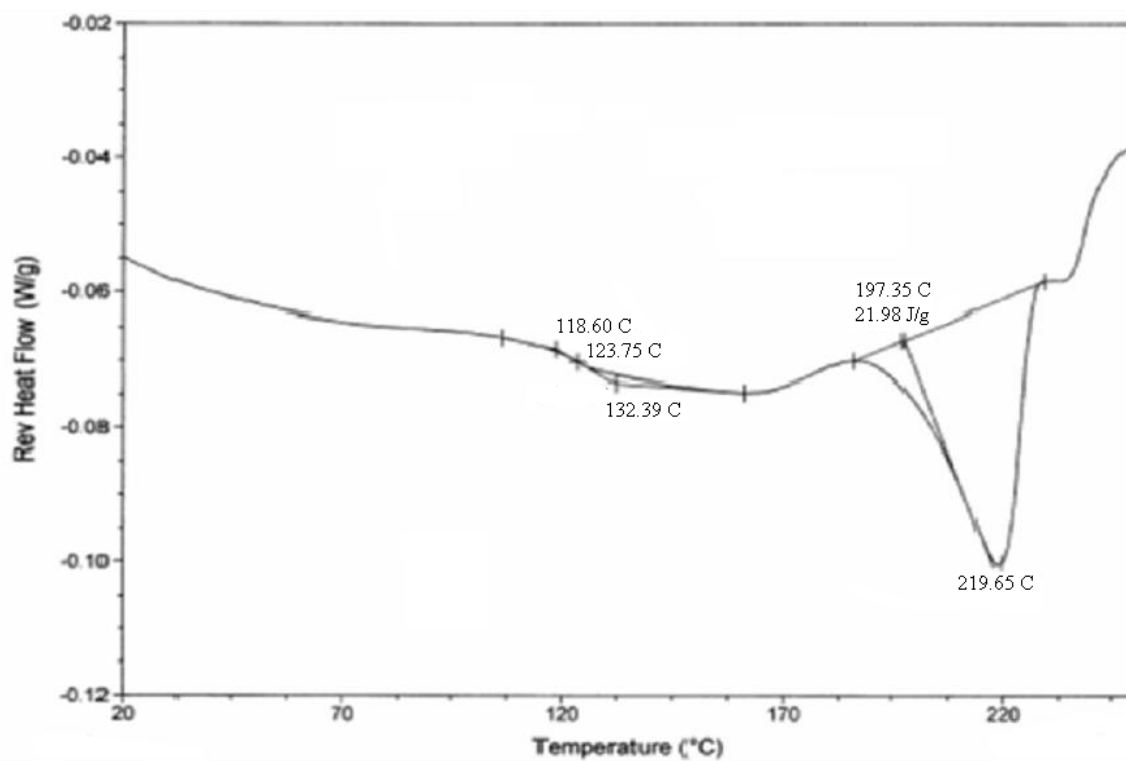


Figure A6. DSC of 1,2-epoxy-5-hexene modified poly(vinyl alcohol).

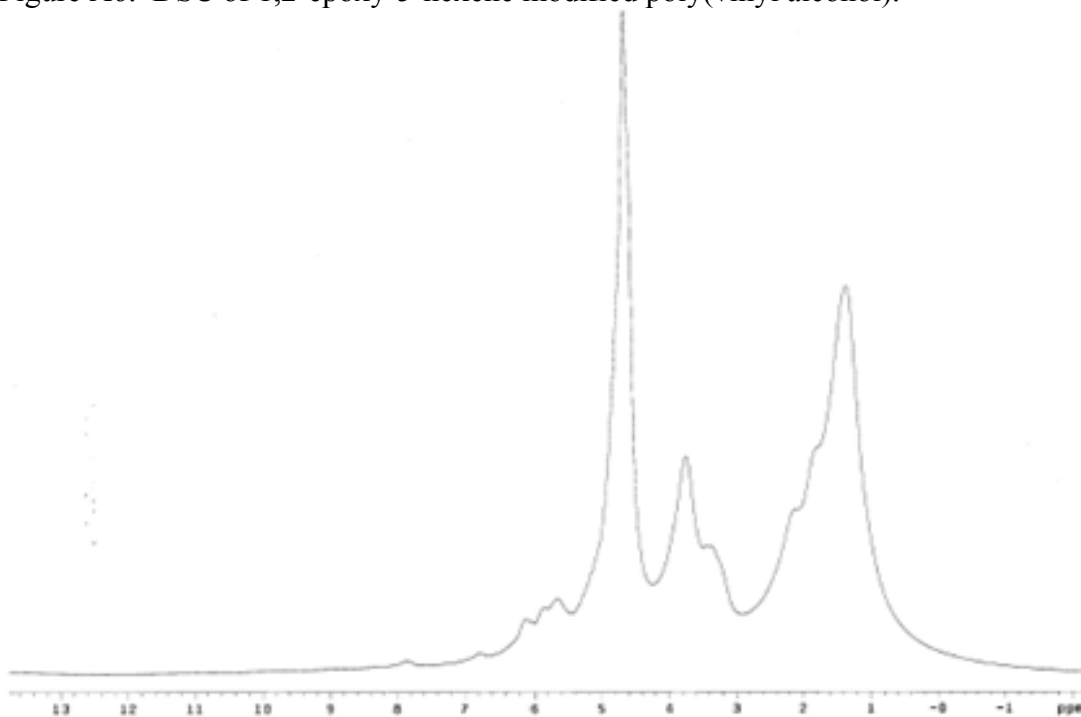


Figure A7. ¹H NMR of 1,2-epoxy-5-hexene-PVA hydrogel. Higher resolution of the peaks was not possible.

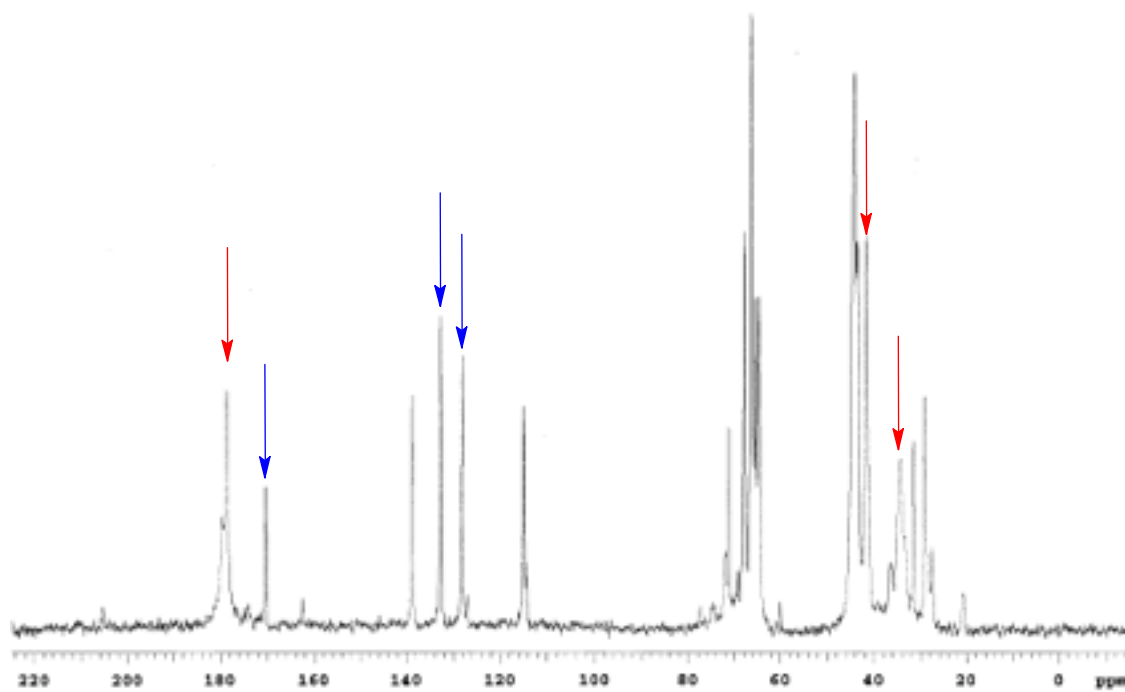


Figure A8. ^{13}C NMR of 1,2-epoxy-5-hexene-PVA hydrogel. Red arrows indicate polymerized acrylic acid, while blue arrows represent unreacted acrylic acid. All other peaks are identical to those given in Figure A3.

APPENDIX B: PLOTS OF STORAGE AND LOSS MODULI



When I go biking, I repeat a mantra of the day's sensations: bright sun, blue sky, warm breeze, blue jay's call, ice melting and so on. This helps me transcend the traffic, ignore the clamorings of work, leave all the mind theaters behind and focus on nature instead. I still must abide by the rules of the road, of biking, of gravity. But I am mentally far away from civilization. The world is breaking someone else's heart.

-Diane Ackerman

The data given as $|G^*|$ and δ in Figures 13, 14, and 16-18 is presented below in the form of the storage/elastic moduli, G' , and the loss/viscous moduli, G'' . The values can be related through the following equations:

$$|G^*| = \sqrt{G'^2 + G''^2} \quad \tan \delta = \left(\frac{G''}{G'} \right)$$

Under the sinusoidal application of stress, G'' is the ratio of stress 90° out of phase with the strain to the strain, and is equivalent to the amount of energy dissipated in the form of heat per cycle of deformation per unit volume. In contrast, G' is the ratio of the stress in phase with the strain to the strain, and is associated with the amount of energy stored and

released during each periodic deformation. Therefore, a material with a large G' relative to G'' possesses a significant amount of elastic characteristic.

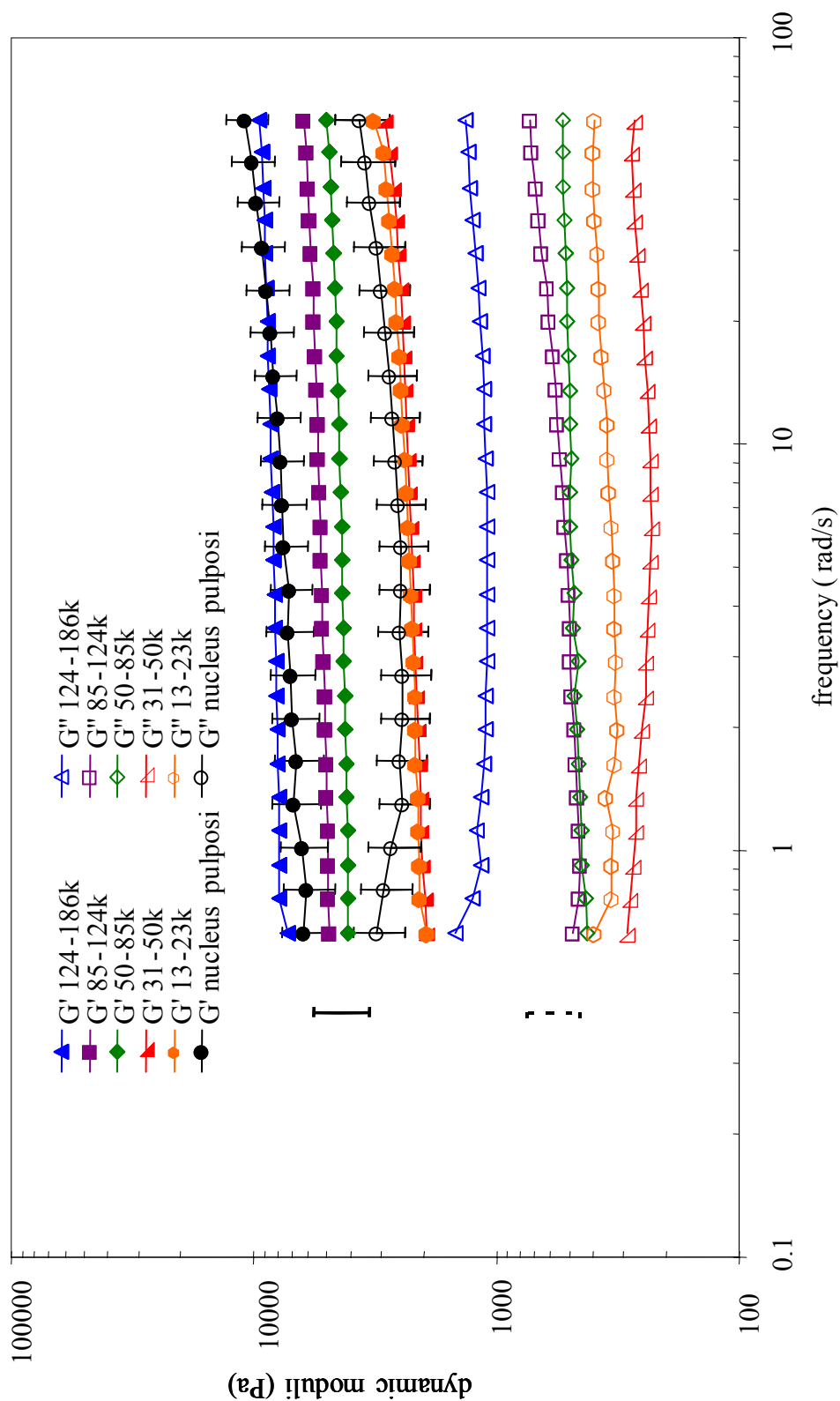


Figure B1. Variation in dynamic moduli, G' and G'' , of glycidyl methacrylate-PVA hydrogels with molecular weight of PVA. For visual clarity, only representative error bars are shown for G' (solid line) and G'' (dotted line). The plot correlates with those shown in Figure 13.

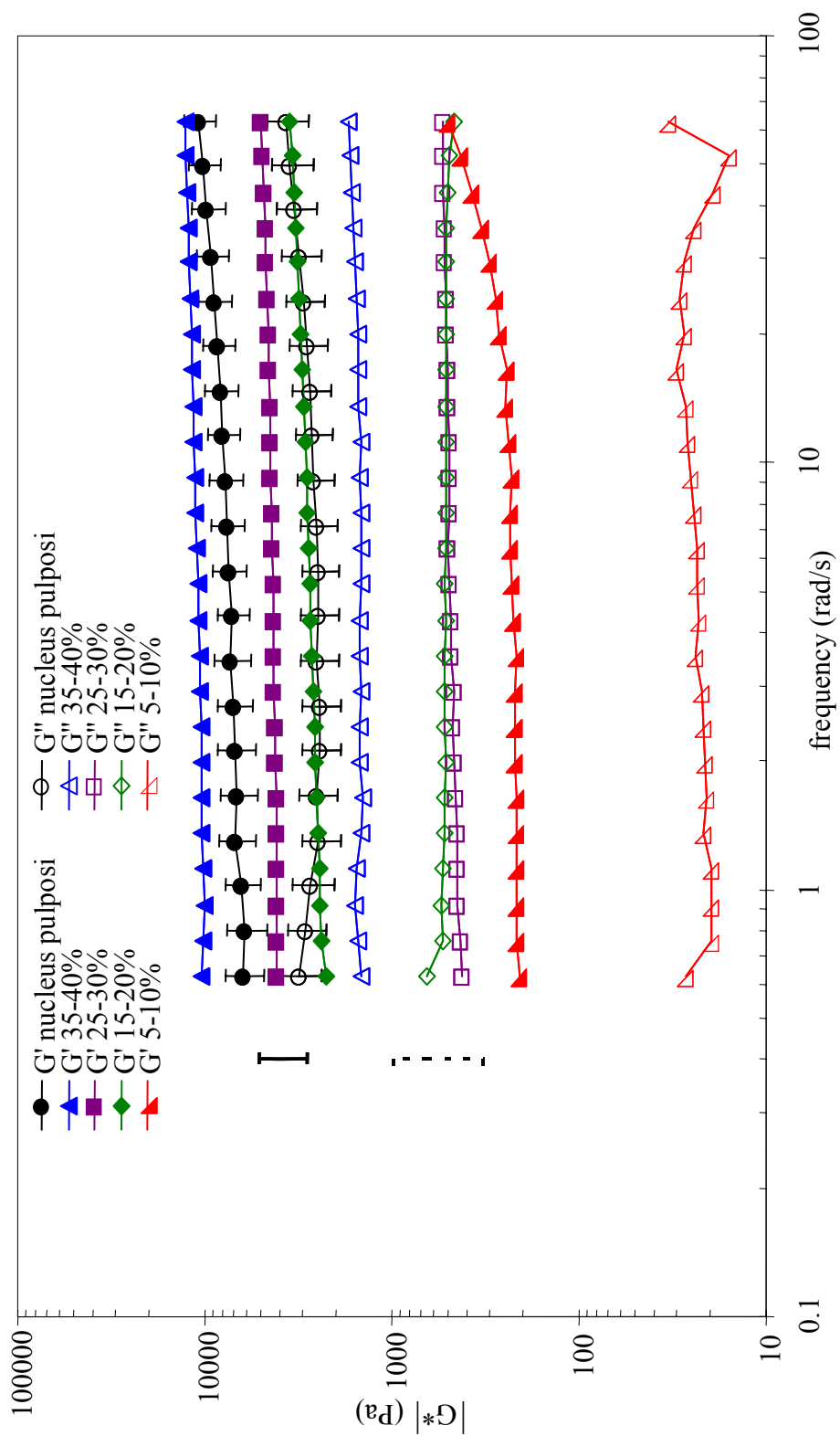


Figure B2. Variation in dynamic moduli, G' and G'' , of glycidyl methacrylate-PVA hydrogels with initial weight percent of polymer. For visual clarity, only representative error bars are shown for G' (solid line) and G'' (dotted line). The plot correlates with those shown in Figure 14.

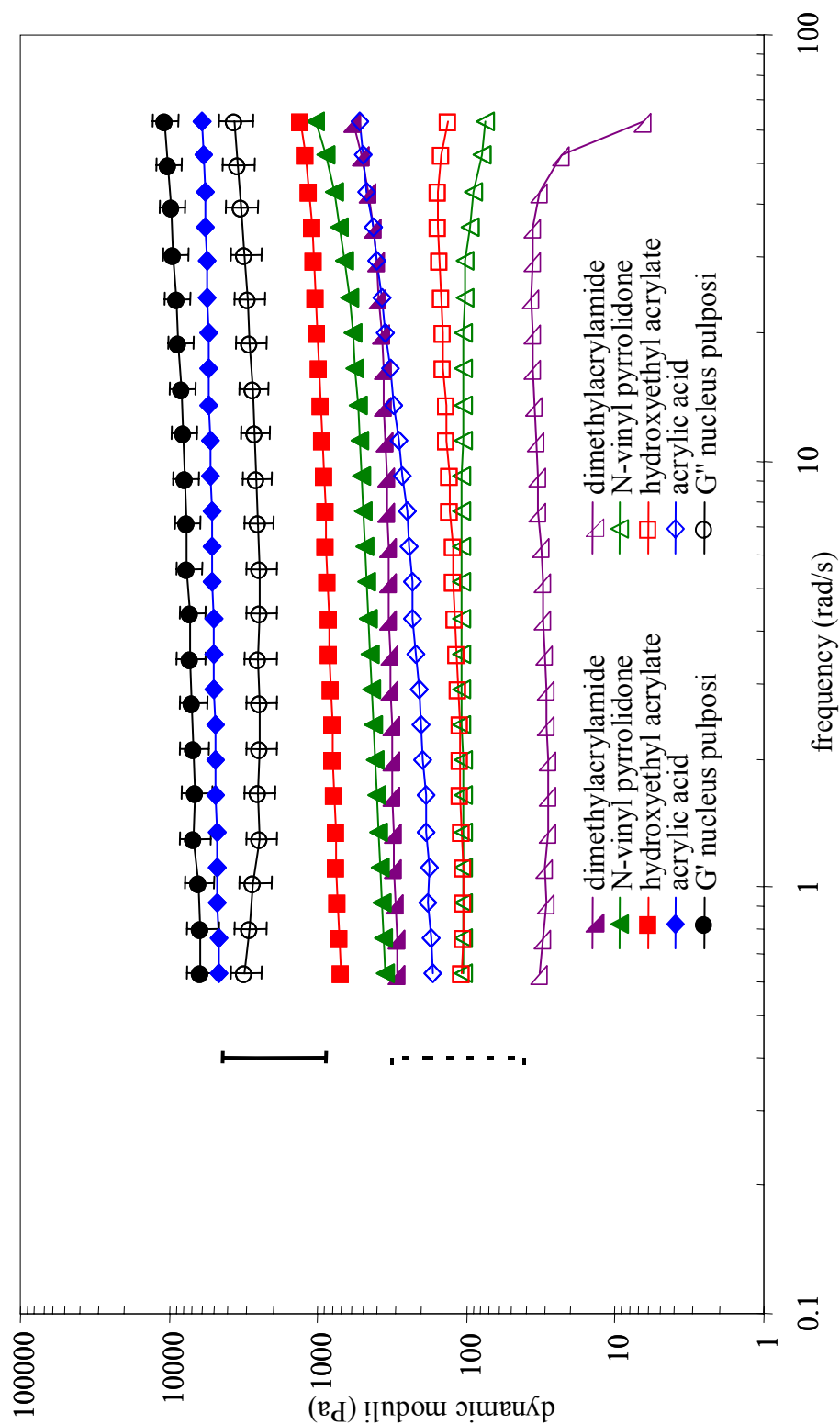


Figure B3. Variation in dynamic moduli, G' and G'' , with type of monomer for 1,2-epoxy-5-hexene-PVA hydrogels. Monomers were included at a concentration of 5 wt. %. For visual clarity, only representative error bars are shown for G' (solid line) and G'' (dotted line). The plot correlates with those shown in Figure 16.

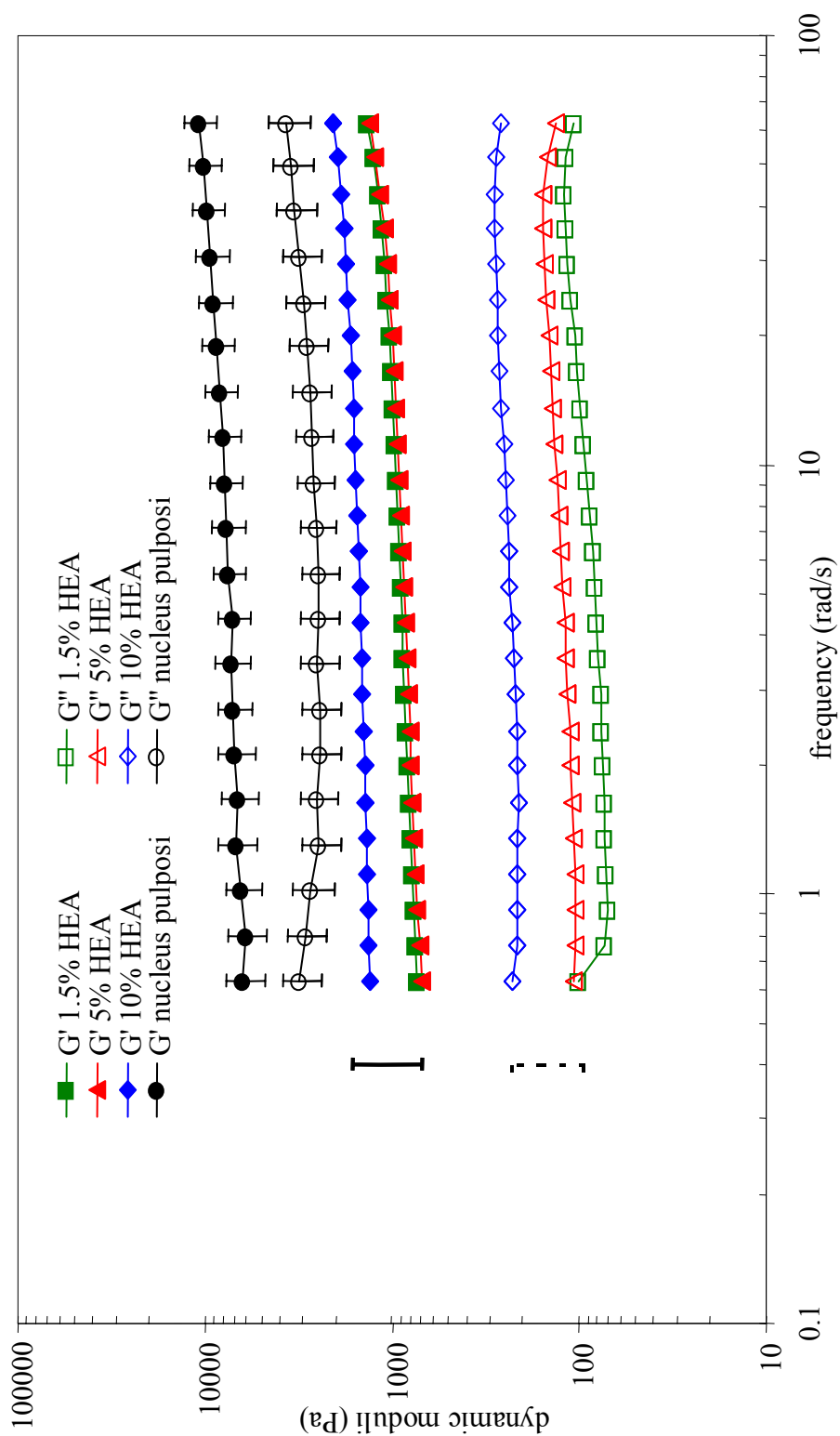


Figure B4. Variation in dynamic moduli, G' and G'' , with percentage (w/w) of hydroxyethyl acrylate (HEA) for 1,2-epoxy-5-hexene-PVA hydrogels. For visual clarity, only representative error bars are shown for G' (solid line) and G'' (dotted line). The plot correlates with those shown in Figure 17.

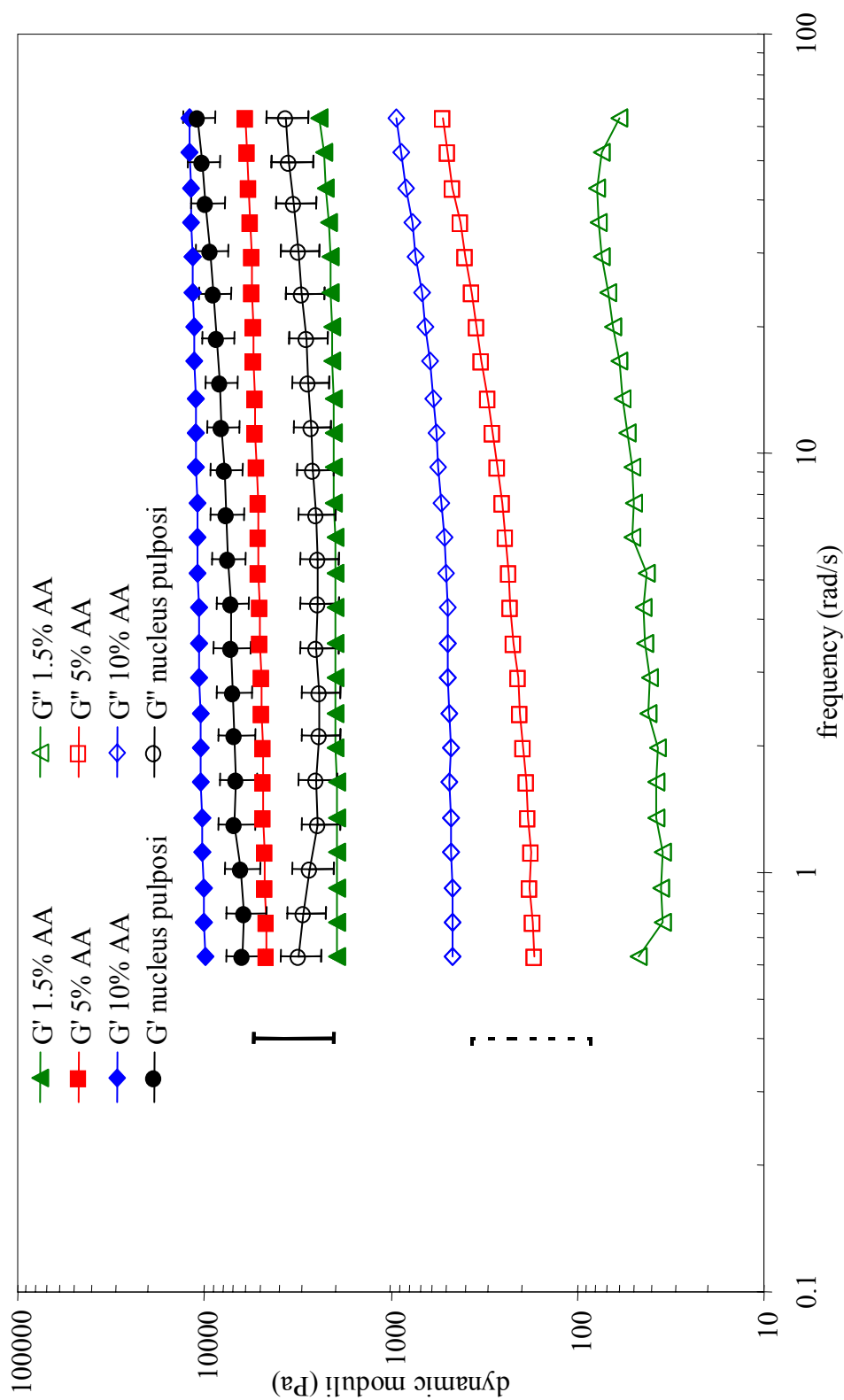


Figure B5. Variation in dynamic moduli, G' and G'' , with percentage (w/w) of acrylic acid (AA) for 1,2-epoxy-5-hexene-PVA hydrogels. For visual clarity, only representative error bars are shown for G' (solid line) and G'' (dotted line). The plot correlates with those shown in Figure 18.

